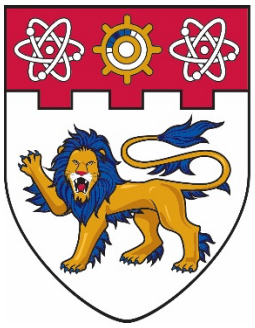

NANYANG TECHNOLOGICAL UNIVERSITY
SINGAPORE

UNDERSTANDING DRIVERS OF CHANGING FIRE ACTIVITIES: FROM THE PERSPECTIVE OF CAUSALITY

SIFENG WU
Interdisciplinary Graduate School
Complexity Institute

2022

UNDERSTANDING DRIVERS OF CHANGING FIRE ACTIVITIES: FROM THE PERSPECTIVE OF CAUSALITY

SIFENG WU

Interdisciplinary Graduate School
Complexity Institute

A thesis submitted to the Nanyang Technological University in partial fulfillment of the requirement for the degree of Doctor of Philosophy

2022

Statement of Originality

I hereby certify that the work embodied in this thesis is the result of original research, is free of plagiarised materials, and has not been submitted for a higher degree to any other University or Institution.

18/08/2022

.....

Date

.....

Sifeng Wu

Supervisor Declaration Statement

I have reviewed the content and presentation style of this thesis and declare it is free of plagiarism and of sufficient grammatical clarity to be examined. To the best of my knowledge, the research and writing are those of the candidate except as acknowledged in the Author Attribution Statement. I confirm that the investigations were conducted in accord with the ethics policies and integrity standards of Nanyang Technological University and that the research data are presented honestly and without prejudice.

18/08/ 2022

.....

Date

.....

Janice Ser Huay Lee

Authorship Attribution Statement

This thesis contains material from 2 published or submitted papers in which I am listed as an author.

Chapter 4 is submitted as Sifeng Wu, Stuart William Smith, and Janice Ser Huay Lee. "Geophysical and anthropogenic drivers for global and regional fire emission trends from 2001 to 2019." *under review*. preprint: https://doi.org/10.21203/rs.3.rs-1537229/v1

The contributions of the co-authors are as follows:

- I designed and conducted the analysis, interpreted the results and wrote the first draft.
- S.W.S. interpreted the results, revised the paper, and contributed to the writing.
- J.S.H.L. advised the analysis, interpreted the results, revised the paper and contributed to the writing

Chapter 6 is published as Sifeng Wu, Zhongyao Liang, and Yong Liu. "Quantifying the risk of irreversible degradation for ecosystems: A probabilistic method based on Bayesian inference." Ecological Indicators 107 (2019): 105621.

The contributions of the co-authors are as follows:

- I designed and conducted the analysis, interpreted the results and wrote the paper.
- Z.L. and Y.L. advised on the analysis and revised the paper.

18/08/2022

.....

Date

.....

Sifeng Wu

Acknowledgements

Sitting here trying to write the final words of this thesis, which I thought would be the easiest part, turned out to be quite challenging. I can't help but looking back on the past four years of my PhD, and keep thinking how different it actually have been than what I had envisioned before I actually started it. I've been through many ups and downs, like most of us have. And I can't deny that there have been times when I thought of giving up my PhD, many times. But I resisted the temptation, not because I am a strong-willed person, but because of all the help and support I received from so many kind people - my advisors, colleagues, family, and friends. I don't think I have expressed how grateful I am for everything often enough, and I'm very happy to have this opportunity to express it at the end of the thesis writing.

First and foremost, I appreciate my advisors, Steve, Janice, Lock Yue and Patrick. All of my advisors are terrific, and I am lucky to have them on my committee. I appreciate Steve for giving me the opportunity of pursuing my PhD at NTU, and the guidance he gave for starting my PhD research during the first year. I also appreciate Janice for taking on the hard work of having one more PhD student after Steve left and being a wonderful supervisor to me. It took a while for me to adjust to this change. I am so thankful to Janice and the whole CHNS lab for being so welcoming, which greatly helped my transition and the rest of my PhD. Lock Yue is such a patient and kind supervisor who is always ready to provide me with the feedback and resources I needed for my research. So is Patrick, always trying to provide invaluable feedback to my research, as well as other aspects of my PhD life. I won't be able to finish this thesis without the help and guidance from you all.

I also appreciate the three anonymous examiners whose comments significantly improved the quality of my thesis. Thank you for your hard work and being one of a small handful of people who have read my thesis carefully.

All the instructors of the courses I attended are greatly appreciated. I especially enjoyed the course *Nonlinear Dynamics* by Lock Yue, *Global Change Ecology* by Anna, and *Mathematical Statistics* by Ariel. These courses were both fun and useful, contributed to the fundamental knowledge without which I won't be able to finish this thesis. Some courses are less relevant or even boring (for sure I mean the TA course, sorry for being honest), but still are part of the compulsory requirement for my graduation. So, thank you all the same.

My colleagues and friends in CHNS lab and CI have been an important part along my PhD journey. They provided me the support and friendship that I will always remember. Guy has been a great mentor and collaborator to me during his time in CI as well as after he left for his new position. Ning Ning has also been a great help, especially when I started my first research project. Alex has been a good friend who generously shared his knowledge and ideas on math and beyond. All my colleagues in CHNS lab, Stuart, Yuti, Estya, Liz, Anushka, Lubis, Fan Yi, and some people who just stayed with us for a short time, it was such a pleasure to work with you all, and to share great memories of us hanging out in places in and outside of Singapore! Again, thank you for arranging these events, Janice!

I am also deeply appreciative of all the staff in CI and IGP. Bee Wee took care of everything even before I was admitted as a PhD student until CI was closed. Ellen, Kaylee, Victoria, and other people in IGP I don't know their names, I appreciate your effort for giving clear and specific instructions that guided me through every stage of my PhD, and being supportive all the time. Also, I appreciate NISTH for letting me share the space with them so that I can keep my desk for work at the final stage of my PhD.

A big thank you to my family, my parents, my grandparents, my uncles and aunts, and my cousins. I didn't spend enough time with you during the past few years, especially after the pandemic ruined our life. I am especially sorry for not being able to be there for so many important occasions that I should and so much want to be there. I feel sorry for the memories I lost for being away, and I hope I can make it up in the future.

I am not good at keeping close contact with my old friends. So, a big thank you to my old friends who haven't left me behind. A special thanks to Ge Zhi, who had the most conversations with me to share all our happiness and sorrows, and the sense

of disorientation on our way of becoming an independent and self-sufficient adult. Also a big thank you to the new friends I met in NTU. I am especially thankful to Ding Bangjie, a dear friend of mine who generously offered his companionship and praise, making my PhD life colorful. You are part of the reason I was able to withstand all the hard feelings and made it through.

I tried to be inclusive of al people I owe my appreciation, though it is quite possible that I still left out some of them. For those I fail to include your name here, my sincere apologies, and thank you.

Sifeng
July 2022

Abstract

Understanding the drivers of environmental changes is critical for predicting and managing this rapidly evolving world. One of the challenges commonly faced by existing studies of analyzing the drivers of an environmental change, be it at a small scale or a large one, is that the drivers presented are not necessarily the true causes that have causal relations with the target of their study. In this thesis, I used state-of-the-art techniques from causal inference to understand the drivers of changing fire activities at different scales. Fire is a fundamental process of the earth system, and the widely observed changing patterns of fire behavior is an important aspect of the global changes that can have profound impacts on ecosystems and human societies. Therefore, understanding the drivers of the changing fire behavior is of vital importance.

I first propose a causal framework that integrate models that can detect causality among variables, and intepretable machine learning models to select and quantify the impact of drivers on fire emissions. I tested this framework on 12 selected regions, and the results showed that the framework can effectively select the true causes as drivers of fire emissions, and also provide informative evaluations of their impacts on fire emissions. Then, I apply this causal framework to a global analysis for drivers of fire emission trend at a scale specific to biome and geological continents. Global fire-derived carbon emissions (fire emissions hereafter) are relatively stable over the period 2001-2019. This was mainly caused by the decrease in African savannas and the increase in Asian boreal forests. The main drivers for the decrease of fire emissions in African savannas are decreased vegetation caused by anthropogenic intervention, mainly through agricultural expansion. The increasing fire emissions in Asian boreal forests was mainly driven by agricultural activities and changing climates, especially drier climates in this region. For the other parts of the world, their drivers differ. In general, vegetation is the most widely observed driver which usually has a positive impact; climates is also widely observed as a fire emission driver, while the impact of the several aspects of climate, namely

temperature, humidity, water availability and wind, differ among areas; and anthropogenic interventions were relatively less important because it was identified as a driver for fewer locations.

I also apply scenario analysis to a theoretical grass-savanna-tree model to understand the role of climate change and anthropogenic interventions on the process of forest degradation where fire plays a critical role. I found that for scenarios with high level of climate change, the system displays bistability and hysteresis; while for scenarios with low level of climate change, the system responds to increasing anthropogenic interventions nonlinearly but does not display bistability. A tree dominated system will degrade into a grass dominated one under a high level of anthropogenic intervention, and the degradation process can be accelerated and worsened by higher level of climate change. At last, I proposed an indicator to evaluate the risk of irreversible degradation for a system with hysteresis using Bayesian inference for model parameterization. I apply this indicator to a real world case and found that the risk of irreversible degradation can indeed be high. The risk of irreversible degradation should be taking into account and measured in future management decisions due to the consequences and potential loss of irreversible degradation.

This thesis investigated the drivers of fire activities with emphasis on climate change and anthropogenic intervention as potential drivers. With the causal framework and its application to understanding drivers of fire-derived carbon emissions at the global scale from 2001 to 2019, climate change towards drier and warmer climates and anthropogenic intervention through deforestation are of vital importance in driving increasing carbon emissions in forest such as Asian boreal forests and Amazon forests. And the forest-savanna transition model showed the synergetic effects between the two drivers that can make the transitioning process from forest to savannas and grasslands in a shorter time and to a more degraded state. In the end, I proposed an indicator that can be adopted to measure the risk of irreversible degradation from forests to savannas, which is a promising research for my future plan.

Contents

List of Figures

List of Tables

Chapter 1

Introduction

1.1 Background and motivation

Environmental changes are widely observed across the world at different scales and often at an alarming rate over the past decades under the pressure of global climate change and human activities [1–3]. Understanding drivers that caused a particular environmental change is key to understanding the historical trajectories as well as predicting the future changes. The relationship between driver and system status is especially important for systems with potential thresholds for regime shifts. For such systems, when drivers approach the threshold, minor changes in the driver can lead to disproportionate and even irreversible change in system status [1, 4–6]. As such, a good understanding of the drivers associated with the environmental change is essential for rigorous decision-making in order to implement policies lead to optimal outcomes and prevent catastrophic degradation.

Understanding drivers of environmental change implicitly embed the requirement for causal understandings, because by definition if a claim is made that a variable is the driver of the change, that means the variable causes the change, and there should be causality between the variable and the environmental change. Therefore, part of the challenge lie in successfully detecting causality from the system where I observe the environmental change [7, 8].

"Correlation does not mean causality" is a well-known phrase to researchers [9–11]. Correlation between variables does not necessarily mean one can cause another.

Making conclusions or predictions based on correlation can be misleading. For example, Google developed a system called *Google Flu Trend* to predict the outbreak of flu based on the key words of people's search through the engine. However, the results were far from satisfying, especially over the time period 2011–2013. Part of the reason for their inaccurate predictions is that the words people search, like the typical flu symptom "fever", are not the cause of flu, but merely correlate with it. Therefore, using these keywords can not adequately predict the outbreak of flu [12, 13]. In statistical terms, it is also called "spurious correlation", meaning correlated variables that do not have causalities [14]. Getting to know the associations can be helpful in a way that observing one thing will give information on the ones associated with it. But its usefulness in boosting our understanding is oftentimes limited. It is vital to establish the causal relations beyond association in order to make sense of the world around us. We interpret the observations by understanding what causes the observed phenomenon, and what would be the consequences had we done differently [11, 15]. However, the tools that scientists developed over the centuries that are most widely used nowadays are mainly based on traditional statistical thinking, heavily reliant on correlation. When we conduct statistical analyses, the results are subject to a wide range of statistical fallacies that could undermine our judgement and lead to false conclusions [10, 16, 17].

"We are all victims of causality" is a quote from the movie *The Matrix Reloaded*. I reference it here out of context and interpret it as humans more than often fail to understand the causalities of a series of events properly and therefore make unjustified decisions. Reasons for this failure can be found on different levels and understood from different angles. Behavioral psychology studies pointed out it is hard to avoid such bias because of the way our brain functions. Human brains have the advantage of being capable of causal thinking. The downside of this advantage is that it tends to seek the causal links out of thin air, even if the evidence is far from being enough to support the speculated causes [15, 18]. A harmless example is the superstition some people hold to consider something as their lucky charm, because their experience seemed to show association between this "lucky charm" and good things happen to them. There is no reason that the two should have any causal relation if we think logically. Taking into account aspects that bear no causal relations to our judgement makes it susceptible to bias and noise, and this can lead to serious consequences under some circumstances. For example, race and crime are not causally related, but people make biased judgements against the minority all

the time, even without realizing it. Researchers proposed an operational framework called "decision hygiene" to fight against noise and error in human judgement. One principle of this "decision hygiene" is to offer only relevant information, meaning only aspects that bear causal relations with the outcome should be provided for decision making [19].

Besides the proposed "decision hygiene", models are also advocated in decision making because they are supposed to be "noise free", meaning they can make consistent decisions for a given instance, as opposed to human judgements that can be swayed by all kinds of irrelevant and random conditions [19]. This not only requires that the models are well-designed, but also that the inputs should be well-chosen, or else models can be just as biased as human judgements. It has drawn wide attention in the field of artificial intelligence that models can make biased decision against minorities because of the unbalanced data input to the models for training and/or the irrelevant factors (for instances, gender, race, and social security numbers) being included as a predictor [19–22]. Situations like this are more obvious and can be easily recognized. Others can be more subtle and thus passed as unnoticed to human eyes; but nonetheless undermines the credibility of the model. Operated without being noticed for a long time, it can reinforce the biased judgement and cause profound consequences considering the scale of using artificial intelligence for decision making nowadays. This calls for techniques to examine causal relations between variables instead of mere speculations before decision making, either by humans or by models.

Inspired by the "decision hygiene" proposed to improve human judgements, I incorporate causal thinking into our analysis to achieve "model hygiene" in some ways analogous to it. Our goal is to ensure the "drivers" we determined have causal relations with the target, which in this thesis refers to changes associated with fire activities. The recent and rapid advancement in causal inference provided the basis for the pursuit in this thesis. The concept of "causality" has long been vague, but has been clarified and formulated in a way that can be rigidly investigated and understood over the past decades. For example, in the book *The Extended Phenotype* by Richard Dawkins [23], a biologist and ecologist, and also the author of the well-known book *The Selfish Gene*, there was a brief discussion on genes being the *cause* of certain traits and physical behavior. Dawkins gave the example of sex chromosomes being the cause for females preferring knitting while males

prefering gun toys, and reached the conclusion that this differentiated preference among female and male is caused by the genes even though it is through social and cultural influence. I briefly quote his argument here, "It is also fully compatible with the view that the reason females enjoy knitting is that society brings them up to enjoy knitting. If society systematically trains children without penises to knit and play with dolls, and trains children with penises to play with guns and toy soldiers, any resulting differences in male and female preferences are strictly speaking genetically determined differences! They are determined, through the medium of societal custom, by the fact of possession or non-possession of a penis, and that is determined (in a normal environment and in the absence of ingenious plastic surgery or hormone therapy) by sex chromosomes." [23] About four decades have past since Dawkins wrote this argument. With the knowledge of modern causal inference, we can easily discern the flaw in this argument. If sex influenced the preference through societal custom, then sex should be a confounder rather than a direct cause for this difference [17].

With the knowledge and tools we can borrow from causal inference, I wish to investigate drivers of environmental change from the perspective of causality, and see what insights can be generated through the lens of causality. In this thesis, I specifically investigated the drivers of changing fire activities from the perspective of causality. Over the past decades, fire regimes have shifted due to climate change and anthropogenic intervention across the world [24–27]. Fire is an inherent and fundamental process that can impact ecosystems and human well-being [27, 28]. From the ecological point of view, fire can regulate ecosystems at multiple levels such as organism traits, population, species interactions, nutrient cycles especially carbon cycles, and many other ecosystem functions [3, 27, 29]. Changing fire activities also brings societal challenges, because increasingly destructive wildfires can cause significant loss of forests and biodiversity, and serious haze issues that received wide attention [30–32].

Systems with fire as an internal process have complex feedback among vegetation, climate, and social components of the system [33, 34]. Due to the complex feedback among these components, fire management can be extremely challenging in many regions, and the system often defy simple policy or management solutions, or even produce opposite consequences as opposed to the desired ones [35, 36]. For example, fire suppression as a fire management strategy brought unexpected and

undesirable outcomes in North America. Because a large number of small fires were suppressed over the past century, thus the fuel built up and the forest became increasingly well connected, losing the buffer zones that should have been created by small fires. As such, the forests became dangerously susceptible to mega-fires, which already resulted in severe consequences such as the 2020 record-breaking fire season in America [37, 38]. Additionally, the solution implemented to solve certain issues associated with fires can lead to adverse effect on others due to the interacting components within the system. For instance, scientists proposed to shift the human-induced fire activities to early dry seasons in African savannas to reduce the greenhouse gas emissions. While its usefulness in reducing emissions is still questionable, this can also cause social conflicts with the indigenous fire practices and affect human livelihoods [39, 40]. Therefore, understanding drivers that caused the changes of fire activities is critical for such systems with complex feedback if we wish to better understand and manage it [5, 8, 41, 42].

1.2 Outline of the Thesis

The structure and main content of this thesis is summarized in Figure 1.1. In this thesis, I try to understand the changing fire activities through the lens of causality. The chapters in this thesis are centered around this topic. This chapter provides a big picture of this field and the motivation for me to pursue this topic. Chapter 2 is a literature review that summarized relevant findings and advancements in this area. The main body of this thesis which presented the research findings of my own included Chapters 3 - 6. Chapter 3 and Chapter 4 are based on statistical models; and Chapter 5 and Chapter 6 are based on mechanism models, to be specific simple mechanism models used to describe complex nonlinear systems. The last chapter is a summary of the findings and prospects for future work based on this thesis. The content of the chapters following this one are summarized as follows:

- Chapter 2 summarized why causality is necessary for detecting and understanding drivers of environmental changes; the progress and current techniques available for understanding drivers; and then narrow down to our current understanding regarding drivers for fire activities at global and regional scales, as well as their limitations.

- Chapter 3 proposed a causal framework that unifies several state-of-the-art causal model and machine learning techniques in order to identify drivers and quantify their impact. I also apply the proposed framework to regions that experienced most frequent fires to test the validity of the framework.

- Chapter 4 first identified the overall temporal trend of fire emissions from 2001 to 2019 at global, regional, and pixel scales; then applied the causal framework proposed and tested in Chapter 3 to understand drivers for fire emission trends specific to geographical regions and biomes.

- Chapter 5 employed a mechanism model that describes the transition from grasslands and forests, and applied the model to simulate the degradation of forests and changing fire regimes under anthropogenic interventions.

- Chapter 6 proposed an indicator to measure the risk of irreversible degradation of ecosystems that can be incorporated with the model used in Chapter 5 to estimated the risk of irreversible degradation of forests to grasslands.

- Chapter 7 summarized the findings of the previous chapters and identified future opportunities. There are plenty of promising future work that can be derived from this thesis, such as applying the causal framework to other relevant context, and incorporating the model presented in Chapter 5 and the indicator described in Chapter 6.

There is a famous theorem in the field of machine learning called *No Free Lunch* theorem, which suggests that there is no single algorithm universally being the best-performing algorithm for all problems [9, 43]. Likewise, as complex as the social-ecological systems are, there is no single model that can best answer the question we are interested in [44, 45]. Therefore, I tried to answer the question from at least two perspectives with two different techniques, statistical model (Chapters 3 and 4) and process-based model (Chapters 5 and 6). In this way, I gave a more comprehensive picture of how fire activities are modified by different environmental stressors and how different systems might respond.

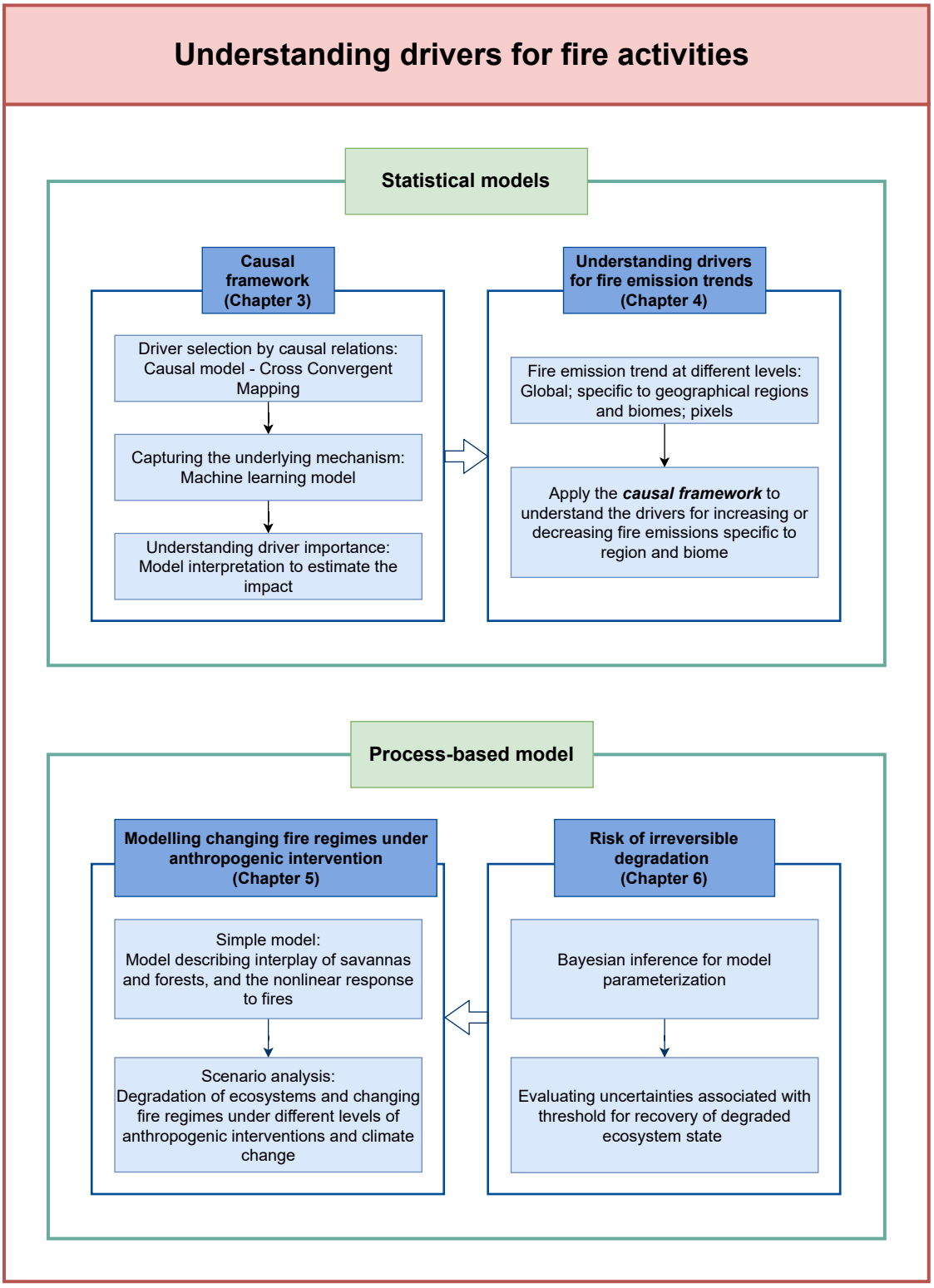

FIGURE 1.1: An overview of the thesis structure and content.

Chapter 2

Literature Review

This chapter is a literature review begins with a description of why causality is needed for understanding drivers of environmental changes and why detecting causality is difficult, especially for complex nonlinear systems. Next, it outlines the development of techniques for detecting and understanding causality that are divided into two categories: causal inference which is more data-driven, and using process-based models which are more reliant on prior knowledge for model design. Lastly, the review focuses on our current understanding on drivers for changing fire activities, which forms the bulk of the work in this thesis, and the updated perspective and techniques used to determine causality.

2.1 Understanding drivers for environmental changes

Typically, drivers for environmental changes are identified by 1) control-treatment experiments; and 2) statistical analyses. Control-treatment experiments are usually more straightforward and therefore better perceived by researchers. One of the classic examples of using control-treatment experiments to identify drivers for environmental change is the experiment in Lake 227 in Canada that identified phosphorous as the driver for lake eutrophication by controlling the nutrient input to the neighboring lakes and comparing their primary production [46]. Lake eutrophication is a typical phenomenon of ecosystem regime shift that can have a profound impact on freshwater ecosystems [47]. The driver of eutrophication

underwent a major debate for various reasons. This experiment conclusively testified that the driver for eutrophication is the external phosphorous input other than other plausible ones like nitrate inputs [46]. However, control-treatment experiments are only applicable to small scale ecosystems that are relatively isolated with clear boundaries. Large scale control-treatment experiments are usually unfeasible for technical and possible ethical reasons. For example, there has been a long debate over whether it is legitimate to make the claim "smoking causes lung cancer" back in the 1960s. Because it is unethical to conduct a control-treatment experiment when the researchers are aware of the health concerns of smoking; and there are limited tools to establish causal relationships between smoking and lung cancer from the epidemic data back then [11, 48].

Data-driven methods to understand the drivers for ecological changes are often employed through statistical models. These include conventional statistical models or more recently developed machine learning models. Either way, the studies often attempt to make causal claims [8, 49, 50]. The word "driver" suggests a causal relationship implicitly, being the driver for an observed environmental change means being the cause. When trying to identify drivers for the phenomenon of interest, the research inherently encapsulate the need for causal understandings. Ideally, the methods employed by such studies should be able to answer the question of cause and effect; while in reality, a large number of current studies in the field of ecology still use conventional statistical analysis which is based on correlation. This can be problematic because the focal systems, either ecosystems or coupled social-ecological systems, are often complex systems that can display chaotic behavior [51, 52]. Chaotic behavior of complex systems can obscure the correlation between variables that have causal relations [7]. This can happen even for a simple deterministic nonlinear system. For example, a system with two coupled state variables X and Y governed by system dynamics described as (2.1) [7], if observed at different time periods, X and Y can be correlated or uncorrelated (Figure 2.1). The relationship of X and Y defined by (2.1) clearly indicates Granger causality between the two variables. Granger causality posits that previous data points of Y and X provide information for predicting X and Y, respectively [53]. The values of X and Y depend on their values of the previous time steps ((2.1)), providing the information for forward predicting each other, thus Granger causality exist between X and Y. However, if one uses correlation to infer the causal relationship between X and Y, there is no guarantee that one can actually detect correlation between

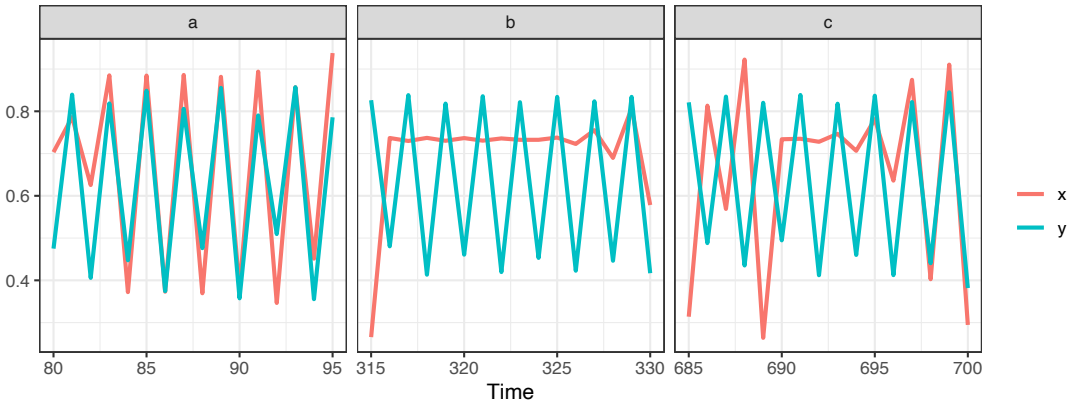

FIGURE 2.1: The two variables of a complex system that have causal relations can be correlated (a) or uncorrelated (b and c) depending on the window of observation. The three subfigures are obtained from a continuous series of simulation of a nonlinear system. Only three windows of observations were displayed as examples to show the systems can be correlated in some periods (such as a) and anticorrelated in other periods (such as b and c). Mathmatical models for simulation to generate the figures followed Sugihara et al. [7]

the two variables to support the causal link, likely leading to the false conclusion that there exits no causal relation between the two variables .

$$\begin{aligned} X_{t+1} &= X_t \times (a - aX_t - bY_t) \\ Y_{t+1} &= Y_t \times (c - cY_t - dX_t) \end{aligned} \tag{2.1}$$

From this simple example, we can see that correlation is either necessary nor sufficient to establish the causal relations between variables for a complex system. Therefore, using correlation to infer causality is not reliable for such complex systems. This is especially true for a system that undergoes a regime shift, which is characterized by abrupt changes in the system state [47]. After the external driver reaches a certain threshold, small disturbances within the system can trigger such regime shifts and lead to sudden degradation that are often difficult or even impossible to reverse [4, 44]. Judging from the data, the external driver can stay relatively stable throughout the whole process of regime shift while the system state changes significantly, leading to the false conclusion that the external driver is not the cause of the shift. In order to better answer the question of cause and effect, techniques to resolve the challenge of uncorrelated cause and effect in complex systems are required [7, 50].

2.2 Statistical models

2.2.1 A historical overview

How to define causality has been discussed from a philosophical point of view for thousands of years with little consensus on what constitutes causality [11]. As mentioned above, back in 1960s, there is a hot debate on the relationship between lung cancer and smoking, whether it is a mere correlation or we can actually say that smoking *causes* lung cancer. The core issue of this problem was the lack of tools to draw concrete conclusions on cause and effect.

Historically, correlation was discovered as a result of Galton and Pearson's pursuit of understanding how the height of fathers affect that of their sons' starting from 1880s [54, 55]. Their studies led to a series of important discoveries in statistics including correlation coefficient and regression to the mean. Ironically, they started from understanding causality while end up being skeptical about it. Pearson (after whom *Pearson correlation* is named) then declared that correlation is all there is. He thought that causality is merely a special case of correlation, where the absolute value of correlation coefficient is 1 [11, 56].

The skepticism against causality lasted for a long time. An important research that changed this perspective later was conducted by Sewall Wright [57] who was originally a geneticist and proposed a new method to decouple the influence of genetic factors and others like environmental factors. Though it was not immediately acknowledged and appreciated by the wider scientific community, it has become one of the most important methods today for causal analysis which is often known as Structural Equation Models.

Nowadays, scientists have gone a long way in the pursuit of causality. There are a handful of techniques to approach the question of cause and effect. Each may have different definitions of 'causality' and the underlying assumptions for these techniques could be subtle and different from one another. Here, I gave a brief introduction to the most common techniques for causal inference. These techniques have their advantages and disadvantages, and I only employed some of these techniques in my thesis. The reasons for the chosen techniques are explained in detail in each chapter.

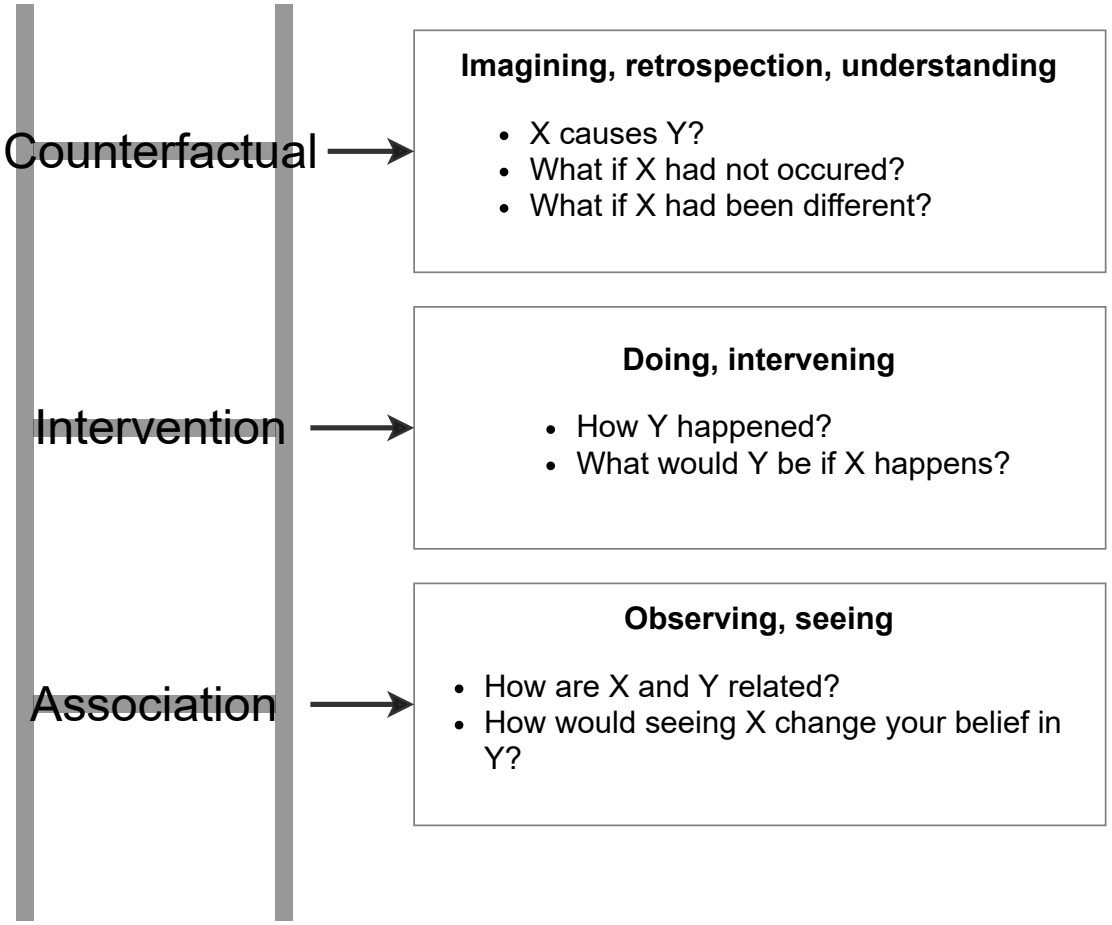

FIGURE 2.2: An illustration of the ladder of causation. (Modified from *The book of Why*[11])

2.2.2 Granger causality test

Granger causality test is proposed by Granger [58] to cope with spurious correlation, and has become a widely-accepted method for causality detection in scientific studies. Causality detected by Granger causality test is specifically named Granger causality in order to distinguish it from other definitions of causality. It has deep roots in linear regression, time series analysis and stochastic process [53]. The premise of Granger causality is predictability instead of correlation. Supposed we have two variables X and Y, and time series data for both. If the inclusion of previous data points of X $(x_{t-1}, x_{t-2}, ...)$ improves the predictability of y_t, compared to using only autocorrelation of Y, then X Granger-causes Y, and vice versa [53, 58]. For example, the mathematical formula for a bivariate linear model is as follows:

$$y_t = \sum_{i=1}^{p} \alpha_i y_{t-i} + \eta_t \tag{2.2}$$

$$y_t = \sum_{i=1}^{p} \beta_{1i} x_{t-i} + \sum_{i=1}^{p} \beta_{2i} y_{t-i} + \epsilon_t \tag{2.3}$$

where X and Y are the variables, x_t and y_t are the data points for time t; p is the time lag used for the regression, meaning how many previous time points are included; α and β are the coefficients for the regression; η and ϵ are the error terms. Suppose inclusion of the term $\sum_{i=1}^{p} \beta_{1i} x_{t-i}$ could significantly reduce the variance of η, aka $\sigma_\epsilon^2 < \sigma_\eta^2$ is statistically significant, then it can be concluded that X Granger-causes Y. It is also required that coefficients β_{1i} are significantly different from 0. This means the inclusion of X are actually contributing to the model outcome, and has a positive effect in improving the accuracy [53, 58]. It is obvious that Granger causality encapsulates two basic assumptions for causality: the causes should happen prior to effects; and causes should contain information for effects thus inclusion of causes could improve the predictability of outcome.

The example is an simple illustration to explain the meaning of Granger causality. In terms of its application, Granger causality test has been expanded to fit the requirements of more complex problems. The example I gave here is for two variables, while in practice multiple variables are often involved. Instead of conducting the same test in a naive pairwise way, a more sophisticated method called conditional Granger causality for multivariate is proposed by Chen et al. [59]. Another advantage of the conditional Granger causality is that it can distinguish the direct Granger causes from the indirect ones that influence the effect through other variables, thereby avoiding the issue of confounders [59]. Also, the model (2.2) is a linear model, which assumed a linear relationship between the variables. This requirement can be relaxed by using nonlinear models instead [60]. But implementation of nonlinear models are much more difficult than a linear model. Therefore, the nonlinear models are often substituted by other approximation methods when the relationships are nonlinear[61, 62]. And some researchers even argue that linear Granger causality test can be valid even if nonlinearity is expected under some circumstances [63].

Granger causality test has been widely applied in the fields of economics, neural science, as well as ecology [59, 63, 64]. However, it has some serious limitations. One limitation of Granger causality test is that it is sensitive to noise and its validity for a nonlinear complex system is often limited [65]. Moreover, Granger causality test is designed for a stochastic system, which means its application to deterministic systems could be problematic [7, 58].

2.2.3 Bayesian causal inference

Bayesian methods claim to be capable of explaining causality, and this has been considered one of the major advantages of Bayesian methods over frequentist approaches. The rational of Bayesian inference being capable of explaining causality comes from the Bayesian equation (2.4), which implies that the probability of event A will increase given that we know B happened. This aligned with the early-days' philosophical view of causality. One of the most powerful tools in Bayesian methods for causal inference is Bayesian network, which combines Bayesian thinking and graph theory.

$$P(A|B) = \frac{P(A\&B)}{P(B)} \tag{2.4}$$

A major reason that had prevented the subscription to Bayesian method is that instead of giving a binary conclusion like hypothesis test given by frequentist approach, it gives the probability of the hypothesis being true, which doesn't fit the expectation that a scientific research should be able to give a solid and conclusive outcome. However, this has in turn become the advantage of Bayesian methods. On the one hand, our view has evolved and come to accept that every conclusion comes with a degree of uncertainty, therefore a probabilistic representation of the probability of a hypothesis being true might be better from a scientific point of view.

2.2.4 Structural Equation Model

Another way to address the difficulty in causal inference are structural equation models (SEM). SEM originated from the path analysis proposed by Wright [66].

It was later rediscovered by social scientists and renamed SEM [67, 68]. When applying SEM, we have to start with hypothesizing the causal model, and then estimate the model parameters by fitting the model to the data. It has been and still is one of the major tools for effect analysis in many areas like economy, social sciences, and so on. The advantage of SEM is that the model functions are invariant to possible changes of other variables, making it possible to investigate and quantify the effects of certain interventions at the system level [67], which fits the second level of the causality ladder, aka intervention (Figure 2.2). Though the mathematical formula for SEM looks identical to that of ordinary regression, it nonetheless could answer the question, what is the relative importance of various causes, which is beyond the capability of regression and correlation [11, 57, 66, 69].

SEM gained its popularity because it is efficient to perform. However, its efficiency is achieved at the expanse of eliminating possible causal descriptions among the variables [53]. When using SEM, one has to specify the structure of the model prior to the subsequent analysis. This gives SEM the advantage of providing quantitative descriptions of the cause and effect relations by incorporating qualitative understanding into the model as prior knowledge. However, we need to make sure the given prior knowledge is correct to ensure the validity of the subsequent conclusion.

Graphical models are quite similar to SEM. They adopt different representations of the causal model. Graphical models use a graphical representation, while SEM is represented by mathematical equations [68]. However, the fundamental ideas are the same, and it is oftentimes a matter of preferred terminology in different fields. Social scientists prefer to use the word SEM; while computer scientists prefer graphical models, sometimes termed as network analysis. It is less commonly mentioned in the literature of SEM, but in studies of graphical models, it is also possible to first specify several plausible models as hypothesis, and then test each by fitting the model to the data. The fitness of each model can give hints on which is the best causal model. This methodology enlarged the usefulness of SEM / graphical model. Not only can they be used for quantifying contributions of causes, but to investigate the causal relations between variables [10, 11, 68].

2.2.5 Machine Learning

Machine learning has deep roots in statistical learning, and is boosted by the most recent advancement in computational capacities and availability of large amounts of data [9]. One significant distinction between machine learning methods and traditional statistical analysis, though the former has deep roots in the latter, is the extensive application of nonparametric models. This means the distribution that can be reduced and fully described by a few parameters, which is fundamental to traditional statistical inference and hypothesis testing, becomes less significant. This allows for more flexibility in machine learning models, and greatly enables its application in ecological studies [70, 71].

Machine learning approaches are usually good at making precise predictions, but known to produce an inscrutable 'black box', which do not fit into the inference framework where we care more about the model structure rather than its precise prediction [9, 70, 71]. Under most scenarios of simulating social-ecological systems, prediction accuracy is more of a justification for the validity of the model, a way to convince people that the model does capture the underlying processes and mechanisms. But the main purpose is often times not the prediction accuracy itself, but using the model to advance our understanding of the system. Therefore, a black box model will be less beneficial since the model structure is not open for interpretation [72]. However, models built by machine learning approaches are not completely unknown in a sense that the model structure as well as the parameters are all transparent and accessible. For example, a neural network, which is a typical example of a 'black box' model, usually has a structure specified manually by the modeller, and all the parameters for the linear transformations and nonlinear activation functions could be accessed. We call these 'black box' models mainly because they are too complex for human brains to comprehend [73–75].

Traditionally, there is often a tradeoff between model performance and interpretability. But this tradeoff is not inevitable with the rise of model interpretation methods, especially the ones that are model agnostic, compatible with most models ranging from statistical models to machine learning models [73, 76, 77]. Although there are some concerns associated with interpreting 'black box' models [75], as long as they are used properly, it is still possible to leverage the powerful performance of machine learning approaches without comprising the interpretability at the same time.

2.3 Process-based Models

Apart from the above-mentioned methods that are data-driven and based on statistical thinking, another line of thinking would be using the process-based models. Process-based models describe systems with a set of governing equations that represent the underlying processes of the system [78, 79]. It can be simple or complex, ranging from the minimal models that only contain a few equations and variables[78] to highly complex models consisting of hundreds of equations that can simulate the whole earth system [80]. However, having more complex models does not necessarily mean we can answer more complex questions. It has been widely recognized that minimal models can give rise to very complex behavior. For instance, the well-know "butterfly effect" originated from three deterministic equations; yet chaotic behavior can emerge from this simple set of equations [81]. Later on ecologists such as May and Oster [82] also reported similar observations that simple equations can be used to describe complex ecosystem dynamics. To decide on the complexity of the model, it often depends on the research question we want to answer and the scale of the focal system such as an ecosystem scale or a regional scale [83, 84]. In this part, I focused on simple models because it has been a prominent tool for advancing our understanding of drivers for environmental changes, especially for regime shifts widely-observed in ecosystems and social-ecological systems [5, 44, 85].

External drivers are an inseparable part of the simple models used to describe the ecosystem, especially the ones used for modelling regime shifts in ecosystems [5]. Therefore, using simple models requires a good understanding of the mechanisms that drive the shift.

It is quite typical that a scenario analysis be conducted for a process-based model. The most familiar example to us all might be the different scenarios for global warming based on model predictions. Scenario analysis is not generally associated with causal analysis. However, the association between the two could be quite obvious once we see the underlying linkage. Depending on the way the scenario analysis is conducted, a retrospective or prospective scenario analysis fits the definition of counterfactual (third level of causality ladder) or intervention (second level of causality ladder), respectively (see Figure 2.2 for the causality ladder)

[11, 86, 87]. Scenario analysis tries to estimate the expected outcome under different configurations of the environment, aka, the outcome under different settings of some key aspects of the system. This gives an opportunity for looking into the alternatives. For a prospective scenario analysis, a range of plausible future pathways considering the uncertainty and complexity of social and environmental systems are examined to predict how the future unfolds with each pathway[88, 89]. This aligns with the definition of intervention, which tries to answer what will the future be like if current behavior were to be altered. While for a retrospective scenario analysis, it looks into the past on how different aspects and components of the system contributed to the existing system [87]. Although it is more often that only decomposition analysis are included, it is feasible to change past settings to investigates how those changes will modify existing ones, which fits the definition of a counterfactual.

Although researchers usually categorize the model into statistical or process-based models, boundaries between the two are becoming increasingly vague, and in practice, they are almost inseparable. For example, the parameterization of a process-based model usually involves statistical methods, like maximal likelihood estimation or Bayesian inference [90, 91]. And some statistical models incorporate our understanding of the underlying mechanism, like the network analysis I discussed beforehand. Since the two methods could benefit from one another and have mutual enhancements in their performances, more and more studies try to combine the two to obtain better results [91, 92].

2.4 Drivers for changing fire activities

The last two decades have witnessed a few extreme fire events such as the 2015 extreme fire in Southeast Asia associated with the El Niño, the 2019 Australian fire [30], and the substantial area burned in the Arctic in 2019 and 2020 [93]. These extreme fires have drawn widespread public attention due to the consequences associated with them [32, 94]. The number of research on fire activities increased significantly over the years as well. The number of publication per year increased almost exponentially over the past 4 decades (Figure 2.3). A vast number of these studies seek to understand the causes of fires at different spatial and temporal

scales. The spatial scales vary from ecosystems to global, and the temporal scales vary from a single fire event to a time period of centuries [95–100].

Changing climate and anthropogenic interventions are major concerns for increases in fires across the world, with complex feedback between climate, vegetation, fire and human activities [27, 35]. Carbon emitted to the atmosphere through fires can have a positive feedback on climate, which can accelerate climate change, through interactions among fire, vegetation and climate [34, 97, 101, 102]. There are ongoing discussions on the causes of changing fire activities and the future projection of fire activities at the regional and global scales under different scenarios of climate change and human behavior [24, 28, 33, 96, 103, 104]. Climate change and anthropogenic interventions are major concerns for increases in fires in many regions across the world [30, 74, 93, 98, 105]. Climate conditions, such as rainfall, temperature, and moisture, control fire regimes at the global scale [24, 106]; and extreme climate events such as extended droughts are often associated with abnormally large fires and fire emissions [30, 99, 107]. Fire activities are also altered by anthropogenic intervention through ignition, land-use change, and fire suppression [108, 109]. Understanding the drivers behind changes in fire activities especially in fire emissions is key to understanding the historical fires and projecting into the future trend [33, 74, 101]. Capturing the important drivers that have major impacts on fire emissions is also critical for fire management because targeting the important drivers can optimize the expected outcome and reduce uncertainties associated with it [36, 110].

The overall trend for global fires when measured by burnt area is declining. And the main reason for this declining trend is the declined burnt area in South Africa, which is an dominant hot spot for global fire activities. The driver for this declining trend in South Africa is mostly human induced, specifically by land-use conversion to agricultural land [108, 111]. At the regional scale, different regions displayed highly differentiated trend and drivers associated with burnt area. For instance, another hot spot for fire is Southeast Asia. Although it is a relatively small area, its fire frequency and emissions are high due to the drainage and development of peatlands for agriculture [112, 113]. Studies showed that extreme fire events in this region are highly correlated with drought, as a consequence of El Niño [99]. Human interventions through deforestation and logging also contributed significantly to frequent fires in this regions [32, 94].

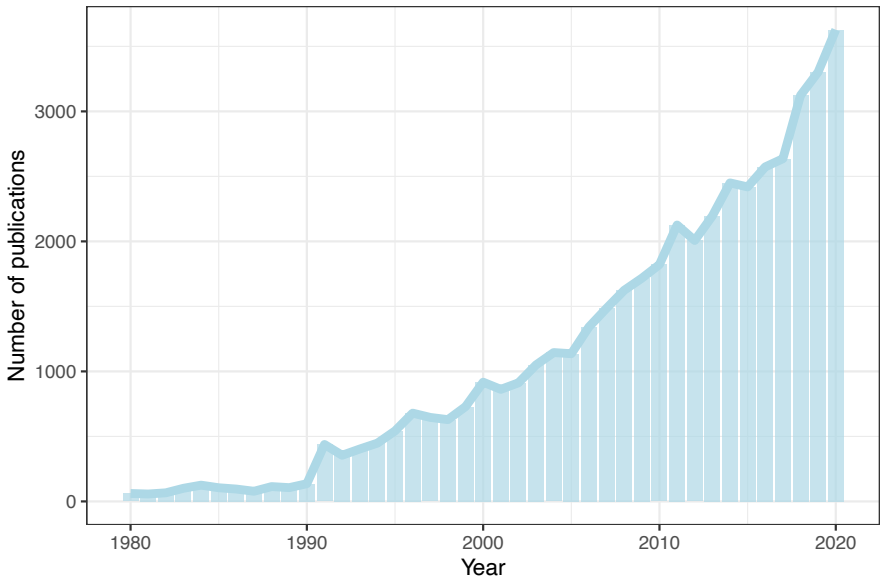

FIGURE 2.3: Number of publications under the topic *fire* from 1980 to 2020. Only articles in the field of environmental sciences, ecology and forestry were included. The data was obtained from *Web of Science* (access date: 7 June 2021).

Another concern associated with changing fire activities is the carbon emitted to the atmosphere during the processes. Therefore, establishing reliable fire emission products and understanding the corresponding drivers are as important as other aspects of fires [101, 107, 114]. Typically, existing fire emission data are based on satellite observations, combined with process-based model to estimate the emissions [114]. The emissions are often calculated from burnt area, which is directly monitored by satellites; and then multiplied with the fuel loads and combustion completeness according to the model equations and structures used to simulate fire emissions [107, 114]. An alternative approach to estimate fire emissions uses satellite observations of atmospheric carbon monoxide (CO), a key fire combustion tracer. Such models are called atmospheric inversion models which is also capable of providing observations for fire-derived CO and CO_2 emissions across the globe at a high temporal resolution for the past two decades [101]. Both approaches for fire emission estimation provide global coverage with spatial-temporal details that can be used for global and regional studies, although both suffer from their respective limitations [74, 101]. Fire emissions derived from burnt area underestimate fires due to undetected small fires, which is especially problematic in Africa where small fires contribute a large proportion of the fires [114, 115]. While fire emissions estimated by atmospheric inversion have limited spatial resolution and

higher uncertainties associated with atmospheric transport models and satellite measurement [101].

Fire products such as burnt area and fire emissions provide the basis for evaluating the spatial-temporal dynamics of fire emissions at different spatial and temporal scales [30, 101]. However, they do not provide a straightforward understanding of the drivers behind the changing fire emissions, which can identify opportunities and leverage points for fire management [101, 103, 116]. In order to understand the relationship between fire emissions and other variables associated with relevant geophysical and anthropogenic factors, data-driven statistical models are commonly used.

For example, multiple linear regression is a widely-used statistical model to quantify the relationships between fires and other factors [93, 94]. But such linear models often fail to capture the nonlinear response of fire emissions to other factors [74, 99]. Machine learning models on the contrary are powerful tools for advancing the prediction accuracy of fire emissions because they can learn from the data to simulate the complex mechanisms underlie the observed phenomenon [70, 74]. A number of studies successfully applied machine learning models to produce reliable estimation of fires at various temporal and spatial scales that outperform simple statistical models and certain process-based models [74, 117].

These standard statistical models and machine learning models can be used for analyzing the response between variables. However, no matter how accurate these models can predict the targeted output such as burnt area and fire emissions, there is no guarantee that we can conclude on the causality between model inputs and output [8, 11]. In order to guarantee that the drivers or causes we claimed have causal relations with the observed environmental changes, we must bring in new techniques from causal analysis. This point will be further discussed in the introduction part of Chapter 3, which closely followed this part. I skipped the discussion here to avoid repetition.

TABLE 2.1: Some terms used in the thesis that are interchangeable and their meanings.

Names	**Meaning**
input, predictors, independent variables, features, variables	variables used as model input to generate predictive results
output, response, dependent variable	predictions generated by the model

Notes on terminology

In this thesis, a number of modelling techniques ranging from traditional statistical models to a number of machine learning models were involved, and the terminologies may differ depending on the preferred terms in traditional statics or machine learning. In order to avoid confusion, I briefly listed some commonly used terminologies that basically refer to the the same thing and are used interchangeable along the thesis to avoid confusions (Table 2.1).

Part I

Statistical model

Chapter 3

A causal framework for understanding drivers of fire emissions

We start by proposing a framework that can be used for analyzing drivers of environmental changes, and apply it to understanding drivers of fire emissions. The framework is a unification of several state-of-the-art machine learning techniques. It provides a procedure that we can follow step by step in order to 1) select drivers for the observed phenomenon, which in our case is fire emissions; and 2) answer the question of cause and effect quantitatively. We tested the validity of the causal framework we proposed by testing that 1) the selected drivers are not merely a reflection of variables that have high correlation with fire emissions; 2) the selected drivers can effectively predict fire emissions, further testifying that the drivers have causal relations with fire emissions; and 3) present a quantitative measure of the impact of drivers on fire emissions. We applied this framework to 12 locations that experienced the most frequent fires covering 7 biomes across the world. This is to test how well this framework performs across these locations and its potential for generalization. We found that for most locations, the framework 1) can select drivers from a set of candidate variables and successfully distinguish correlation from causality; 2) selected drivers can effectively predict fire emissions, and often produce similar or better prediction accuracy compared to using equivalent number of input selected by correlation (highest r^2) for most of the 12 regions except 2; and 3) can provide an informative result for understanding the impact of drivers

on fire emissions. Therefore, we conclude the causal framework we proposed is valid and have several advantages in understanding drivers for fire emissions. More importantly, it is highly promising for future applications because it is flexible and can be applied to different research questions that seek causal understandings. In addition, it can be further extended to explore causal structure and causal feedback between multiple variables in order to generate new insights.

3.1 Introduction

Environmental changes are widely observed across the world at different scales and often at an alarming rate over the past decades under the pressure of global climate change and human activities [1–3]. Understanding drivers that caused a particular environmental change is key to understanding its historical trajectory as well as predicting future changes. The relationship between driver and system status is especially important for systems with potential thresholds of critical transitions, because with drivers approaching the threshold, minor changes in the driver can lead to disproportionate and even irreversible change in system status [1, 4–6]. As such, a good understanding of the drivers associated with the observed environmental change is also essential for rigorous decision-making in order to implement policies that intervene on the most important driver, resulting in optimal outcomes and preventing catastrophic degradation.

Understanding drivers of environmental change implicitly embed the requirement for causal understandings, because by definition X being a driver of event Y means X causes Y, suggesting the causality between X and Y. There are two basic components to this question, 1) identifying causality between variables, namely whether a particular variable is a cause/driver of the observed event; and 2) quantifying the response between cause and effect, meaning the magnitude of change in system status given certain amount of change in the cause/driver [8]. These two questions can usually be adequately answered by well-designed randomized control experiments, which is the primary tool for causal inference in ecological studies [8, 49]. However, for complex systems where such experiments are not feasible, which is often the case due to practical and/or ethical reasons, causal analysis can only rely on observational data and have to be analyzed with care in order to gain credible conclusions [49, 118].

A large number of existing data-driven ecological studies do attempt to make causal claims. However, a lot of these studies still employ standard statistical models such as multiple linear regression and generalized linear regression that are designed to infer correlations among variables rather than causality [10, 72, 119]. This could be problematic because correlation is an unreliable tool for inferring causality; as the famous quote "correlation does not imply causality". Moreover, correlation-based analysis that did not take into account the causal relationship between variables can lead to conflicting conclusions [8, 11, 49]. A typical and widely-observed example is the Simpson's paradox, where the relationship between variables observed at smaller scales can be reversed after aggregating to larger scales [11, 120]. This paradox is caused by the existence of confounders. Neglecting the causal relationship between confounders and the outcome can led to statistical fallacy [120].

Besides the standard statistical analysis, machine learning and deep learning models [1] have become increasingly popular over the past decade in the field of ecology due to their exceptional prediction performance [70]. These models do not rely on researcher's knowledge to specify the functional forms between the predictors and the output but can learn the functional forms and underlying patterns from the data. Therefore, they are much more flexible and better at simulating the nonlinear response between variables compared to traditional statistical models, which is often desirable for ecological studies [9, 70, 71]. However, most machine learning and deep learning models can not answer the question of cause and effect any better than the traditional statistical models. This is because despite their model complexity and ability to infer and optimize model structures from vast amount of data, at the very core they still almost exclusively operate on statistical mode, which is not designed for causal analysis [16, 121, 122].

There are some tools at our disposal to elucidate causal relationships among variables, and the most common ones in ecological studies include structural equation model, causal graph, and Bayesian network [8, 49, 50]. These methods can be used to quantify the response relationship between cause and effect, but inevitably involve assumptions regarding the causal structure reflected by their model equations or network structures. The credibility of the causal claims made through these methods largely depends on the credibility of their assumed causal structure

[1] Deep learning is in fact is a branch of machine learning, specifically refers to deep neural network with multiple hidden layers. However, deep learning often stands out as an independent topic in research and practice. Therefore, we keep both terms here to be more inclusive.

[68, 123]. However, examination of the assumed causal structure can be difficult especially in a non-experimental and data-driven setting [8]. On the other hand, there are ways to shed light on the credibility of the assumed causal structure by examining the causal relationship between variables through the data, such as Granger causality test and cross convergent mapping (CCM) [7, 58]. These methods are designed to test whether a certain variable causes another, and can detect causality instead of correlation. For instance, [42] revealed with CCM that, although insolation, temperature, and concentrations of greenhouse gases (GHGs) are all correlated, casual relations were only detected between temperature and GHGs, not between temperature and insolation, suggesting that GHGs are the direct driver of climate change rather than the orbital insolation. However, these models are designed to test causality without providing a quantitative measure of the response between cause and effect.

To resolve this gap, we propose a framework that takes into account the two aspects of causal analysis, namely detecting causality and quantifying response between cause and effect, such that we can present a comprehensive understanding of the drivers associated with the phenomenon. The framework includes two parts, 1) a causal model to select drivers from a set of candidate variables by identifying the causal relation between the variables and the system status; and 2) an interpretable machine learning model to estimate the impact of each driver on the system. By incorporating the causal model with an interpretable machine learning model, this framework provides theoretical grounds to identify and measure the causal relationship between the selected drivers and the environmental change. The flexible interpretable machine learning model can be a useful tool for inferring the quantitative response between drivers and the changing system status [73, 124].

In this chapter, we apply this framework to investigate the drivers of fire-derived carbon emissions as an example to test the validity of this framework. For the causal model, we used CCM. CCM is designed to detect causality between variables in complex systems where the causal relationships can be obscured by the chaotic behavior of the system [7]. Ecosystems with fire as an internal process are complex nonlinear systems characterized by chaotic behavior [27, 35]. Therefore, CCM is appropriate for our application. For the interpretable machine learning model, there are in fact a good number of machine learning models we can choose

from. We compared four most widely used machine learning models, namely 1) random forests (RF); 2) gradient boosting model (GBM); 3) support vector machine (SVM); and 4) neural network (NN). These models all have robust implementations that have been tested by a vast number of studies and can usually achieve satisfying model performance given proper training [9, 125]. For model interpretation, we used SHapley Additive exPlanations (SHAP) explainer because 1) it is model agnostic, meaning it can be applied to any statistical and machine learning models including the four models we selected; and 2) it can estimate the impact of the input, in our case the drivers, for the whole range of the values we observed, and therefore provide a more informative result on the driver impact [73, 76]. We applied this framework to 12 geographical units covering 7 biomes across the world to testify the validity of the causal framework we propose.

3.2 Methods and data

3.2.1 Overview of the framework

The whole framework includes two parts that can be further decomposed into four steps: 1) collecting a set of candidate variables that are relevant to the phenomenon of interest; 2) selecting drivers from the candidate variables based on their causal relationship with the outcome, which is the ecosystem status; 3) building and optimizing machine learning models to simulate the response between the drivers and the outcome; and 4) interpreting the optimized machine learning models to estimate the impact of drivers on ecosystems (Figure 3.1). The output of each step is the input for the next step, meaning the candidate variables collected in the first step will be the input of the causal model at the second step, then the drivers selected at the second step will be the input of the machine learning model at the third step, and finally the optimized machine learning model will be the input of the model explainer at the fourth step.

The two parts of the framework, namely the causal model and the interpretable machine learning model, are presented to answer the two components of a causal analysis respectively, namely 1) causality and 2) response between cause and effect. As discussed above, the causal model is only capable of detecting causality between variables without giving a quantitative measure of the response between cause

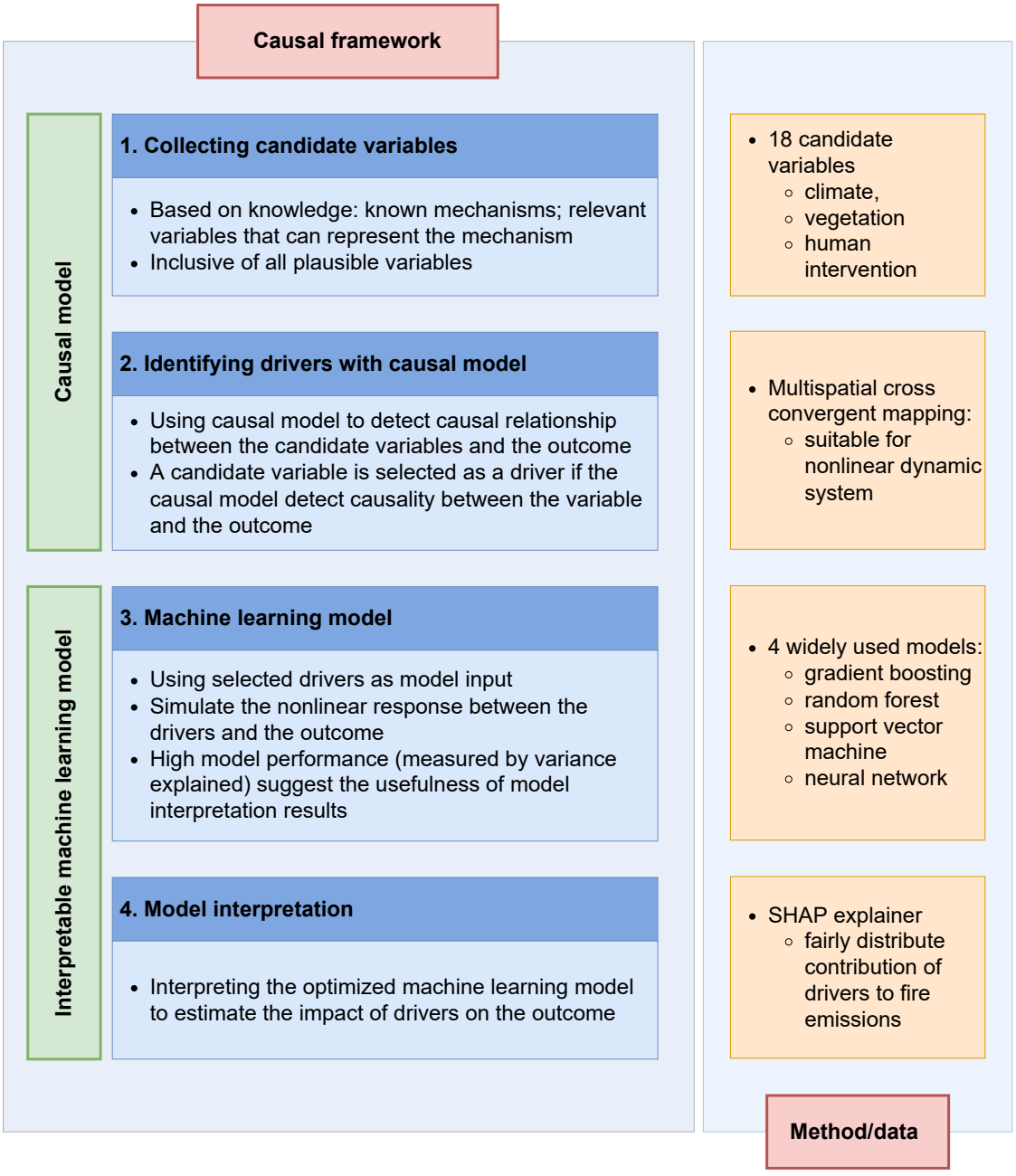

FIGURE 3.1: General steps of the causal framework, and techniques and data we used for applying this framework to understand drivers of fire-derived carbon emissions.

and effect. While interpretable machine learning models can be used to infer the response between input variables and output, it is unable to determine causality. The two parts complement each other in a way that the causal model guarantees the causal relationship between the input and output of the interpretable machine learning model, and the response estimated by the interpretable machine learning model is between cause and effect.

3.2.2 Data

We used total carbon emissions from Global Fire Emissions Database (GFED4s) to represent fire emissions. Hereafter the term "fire emissions" specifically refers to fire-derived total carbon emissions unless otherwise specified [107, 126, 127]. We included 18 variables covering different aspects of geophysical and anthropogenic conditions as potential drivers (Table 3.1). Any relevant variables that might influence fire emissions and available should be included at this stage. Although some variable can be a driver of fire emissions only for certain regions in a certain time period, whether this remains to be true for other regions will be tested by the causal model. This means we should be as inclusive as possible and leave the selection process to the casual model. Therefore, we collected all variables, to our best knowledge, that have been documented to have influence on fire emissions and available at the temporal and spatial scale and resolution of this analysis. We retained some correlated variables that describe the same environmental aspect, for instance *EVI* and *NDVI*, both measuring the vegetation cover and can complement each other in global vegetation studies [128]. We did not eliminate them for the following reasons: i) to avoid making assumptions on which is the better indicator; ii) different measurements could add additional information in prediction; and iii) the subsequent machine learning models will not be undermined by correlated features [129]. Without making assumptions, the 18 variables were then selected and reduced by the causal model.

We used a relatively coarse spatial resolution, $2^\circ \times 2^\circ$, because fires are inherently stochastic at fine scales, but its emergent behavior could be better predicted and explained at coarse-grained levels [27, 52, 130]. Therefore, a coarser resolution is better suited for predicting and interpreting fire emissions through models. In addition, the causal model CCM we used here is extremely time consuming because

TABLE 3.1: Potential drivers for fire emissions. The 18 drivers are divided into 6 categories. The relation to its category indicates the variable is positively (+) or negatively (-) related to the environmental condition of its category.

Variable	**Meaning**	**Category**	**Relation to its category**
def	climatic water deficit (mm)	water	−
pdsi	Palmer Drought Severity Index	water	−
pr	precipitation (mm)	water	+
ro	runoff (mm)	water	+
swe	snow water equivalent (mm)	water	+
soil	soil moisture (mm)	water	+
aet	actual evapotranspiration (mm)	humidity	+
pet	reference evapotranspiration (mm)	humidity	−
vap	vapor pressure (kPa)	humidity	+
vpd	vapor pressure deficit(kPa)	humidity	−
srad	downward surface shortwave radiation (W/m^2)	heat	+
tmmn	min temperature (℃)	heat	+
tmmx	max temperature (℃)	heat	+
vs	wind speed at 10m (m/s)	wind	+
EVI	Enhanced Vegetation Index	fuel	+
NDVI	Normalized Difference Vegetation Index	fuel	+
population	population density	anthropogenic	+
agriculture	percentage of agricultural land	anthropogenic	+

the algorithm for the model has exponential time complexity. Although smaller spatial resolution, though not too small as explained above, such as $1° \times 1°$, might be a possible choice, using this will have about 3 times more pixels, leading to about 10 times of the current computational time. Since the spatial resolution of $2° \times 2°$ already give us a decent amount of data point for the analysis we wish to conduct, we used this resolution with no further comparison. For future studies, a careful reconsideration of the spatial resolution based on their own spatial and temporal scales and other relevant factors are needed. We set our time scale to be from 2001 to 2019. Fire emission data before 2001 were prolonged with additional active fire observations instead of MODIS 500m data [107]. Therefore, we only included data after 2001 to avoid bias. To obtain a consistent spatial and temporal scale and resolution, all data were spatially aggregated to $2° \times 2°$, if needed, and were compiled on an annual basis. Details of data processing can be found in Appendix A.

3.2.3 Causal model for selecting drivers

We used the causal model, multispatial cross convergent mapping (multispatial CCM) [131], to test the causality between all candidate variables and the target variable. A candidate variable is selected as a driver only if there is a significant ($p <= 0.05$) causal relationship between this variable and the target. Multispatial CCM is based on the CCM technique, a method designed to detect causality in nonlinear systems from time series data. CCM assumes that if X causes Y, historical observations of Y can be used to predict X. Therefore, CCM test the causality between X and Y, specifically whether X causes Y, by the level of the convergence of the predictive power of Y for X [7, 42]. Originally, CCM requires long-term observations, which limited its application; whereas multispatial CCM resolved this challenge by leveraging spatial replications. Given time series data from multiple sites within a system, multispatial CCM can effectively detect causality between variables with much shorter time series compared to original CCM [7, 131]. Given time series data of two variables X and Y, multispatial CCM can simultaneously test whether X causes Y and whether Y causes X. In our analysis, we used multispatial CCM to test all 18 potential variables one by one against fire emissions. We are interested in whether the variable being tested caused fire emissions, and variables that are deemed to cause fire emissions ($p <= 0.05$) are selected as a driver of fire emissions.

As multispatial CCM makes use of the spatial replicates, it is required that all the sites come from a relatively homogeneous system for its implementation [132]. In order to satisfy this requirement and to limit the computational time, we only include large clusters of pixels that 1) are spatially contiguous, and 2) have the highest frequencies of fire emissions, namely pixels that experience fire emissions every year from 2001 to 2019. These clusters are also defined by their geographical location and biome in order to suffice the homogeneity within each cluster. We obtained 12 clusters that covered 8 biomes (defined by Olson et al. [133]) distributed in different continents (Figure 3.2). We used the 12 clusters to show the implementation of our framework and to test its validity across different systems. Pixels with high fire emission frequencies but do not form large clusters were not included (Figure A.1 in Appendix A).

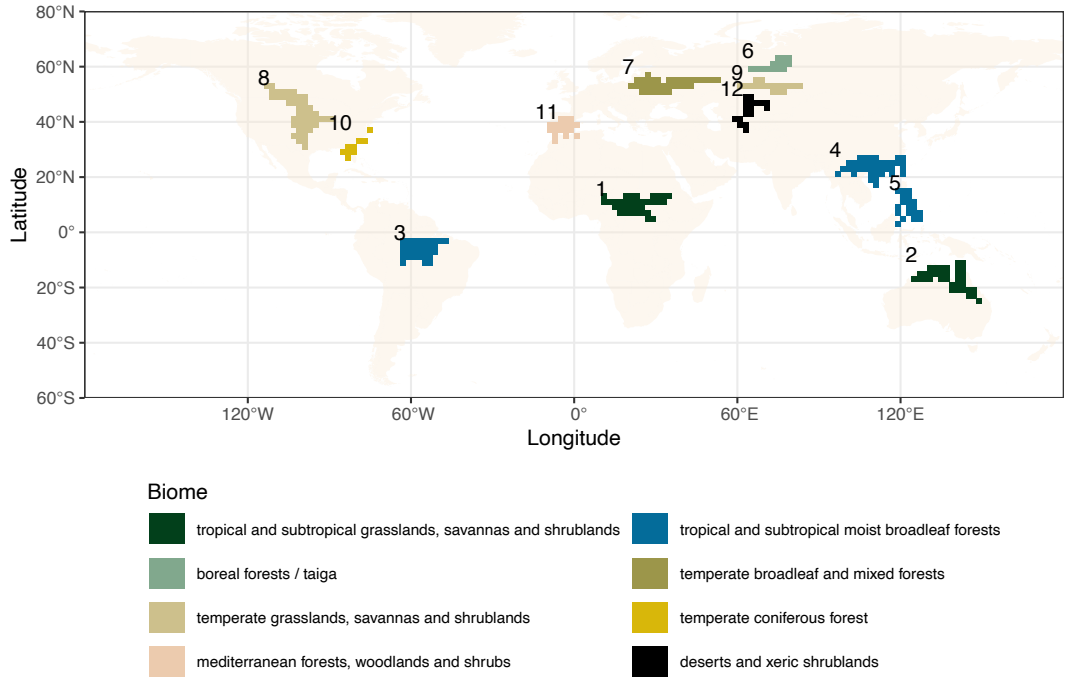

FIGURE 3.2: Areas selected as the unit to apply the causal model multispatial CCM. The color of the pixels denote the biome. All pixels experienced fire emissions every year from 2001 to 2019. And pixels within a particular selected area are contiguous.

3.2.4 Interpretable machine learning models

The first step of building an interpretable machine learning model is to build a machine learning model in the conventional way. In general, which machine learning model performs best depends on the question and data [9]. Therefore, we tried four most widely-used machine learning models to estimate the response between drivers and fire emissions, namely gradient boosting model (GBM), random forests (RF), support vector machine (SVM), and neural network (NN) [9]. Models were all used in a regression setting as their output were supposed to be fire emissions, a continuous variable. Optimization for these models were performed with randomized search in order to achieve better model performance. Model performance was measured by variance explained, which is a commonly used model performance score for regressions. Moreover, variance explained is dimensionless and can be compared across different data and models. Higher values of variance explained mean better performance, and the highest possible value is 1 [9]. Model performance scores were given by 5-fold nested cross-validations (CV). Nested CV is a

technique designed to avoid bias and overestimation of model performance compared to the traditional plain cross-validation [134]. Mean and variance of the performance score, variance explained, were given by nested CV. A high model performance score with small variance means the model can consistently predict fire emissions accurately, which requires that 1) the input variables contain useful information to predict and explain fire emissions; and/or 2) the machine learning model successfully simulate the response between the input and the output, and thus can be used for interpretation [9, 73].

Complex machine learning models, while good at simulating the nonlinear response and making accurate predictions, are less straightforward when interpreting the relationship between their input and output variables [9, 73]. Therefore, additional model interpretation technique are required in order to understand the contribution of each input to the output [122]. We used SHapley Additive exPlanations (SHAP) explainer to interpret the optimized models. SHAP explainer is designed to decouple the contribution of each input to the model output based on the response of the output to varying inputs simulated by the machine learning model [76, 77]. The impact of each input was estimated over the whole range of driver values, which is the direct output of SHAP explainer, SHAP values. Positive SHAP values indicate a positive impact of the driver on fire emissions, and vice versa. SHAP explainer has been successfully applied in many fields of studies to identify the most important factors including understanding the predictors of fire emissions [73, 74, 135].

3.2.5 Testing the validity of the causal framework

As mentioned above, "correlation does not imply causation". We first tested the validity of the causal framework by showing that the causal model can distinguish between correlation and causation. Since we do not have the ground truth for which variables are the true causes that have causal relations with fire emissions, we did this by comparing the variables that have highest correlations with fire emissions, and the ones being selected as drivers by the causal model. If the two groups do not entirely overlap, that means whether a candidate variable is selected as a driver of fire emissions is not dependent on their correlation. To elaborate on this process, we 1) selected drivers of fire emissions specific to each cluster from the candidate

variables, and 2) calculated the pairwise correlation between all candidate variables and fire emissions, indicated by the R^2 values. R^2 can take any value between 0 and 1, and the closer to 1, the more correlated are the two variables. If across the 12 clusters we experimented, the causal model can exclude variables that are highly correlated with fire emissions as drivers and/or include variables that have low correlations with fire emissions as drivers, it suggests that the causal model does distinguish between correlation and causality.

Secondly, we tested the validity of the framework by the predictive power of the selected drivers for fire emissions, which is the performance scores of the machine learning models. There is no ground truth for us to validate that the drivers we selected for fire emissions specific to each cluster are true drivers. As a work-around, we tested their ability to produce accurate predictions because if variable X causes Y then X should contain useful information for predicting Y [11, 64]. We also compared the performance of machine learning models by 1) using drivers selected by the causal model as input, 2) using the same number of variables that have the highest correlations with fire emissions for each cluster as input, and 3) using all 18 candidate variables as input. In the first two approaches, the number of input for the machine learning models were reduced either based on their causal relation with fire emissions or correlation. Both in effect can be considered as a step for feature reduction, a common step in a typical workflow to build machine learning models [9, 136]. Feature reduction techniques most commonly used in machine learning are based on correlation, such as the second approach we used here, or other matrices designed to measure the similarity between variables [136–138]. The advantages of using feature reduction technique to reduce the number of input variables include 1) to avoid excessive noise introduced by the additional data that might obscure the pattern and lead to lower performance [139]; and 2) to avoid "the curse of dimensionality", which refers to the phenomenon that with higher dimensional data, model parameterization becomes exponentially more difficult and computationally expensive [140]. In our framework, using causal model for feature reduction had the above advantages, but more importantly ensured that the variables selected as drivers have causal relations with the fire emissions.

Note that neither of the two steps described above can be used to test the causality. The first step is to show that the causality detrmined by CCM is different from correlation; and the second is to show that using variables selected by the causal

model can ensure the predictability of the target, which is the fire emisisons in our case. The causality is alredy tested through CCM before the two steps. The results of the two steps can help establish 1) the credibility of the causal relationship between the selected drivers; and 2) the framework can indeed help achieve one of the most important reason to seek causality, which is to predict and to better understand the phenomenon, through testing the machine learning model performance.

Multispatial CCM was implemented by `multispatialCCM` [132] in R [141]. GBM was implemented by `LightGBM` [129]; RF, SVM and NN were implemented through `scikit-learn` [142]. Randomized search for hyperparameterization was also done by `scikit-learn` [142]. SHAP explainer was implemented by `shap` [135]. All steps of interpretable machine learning models were implemented in Python [143].

3.3 Results

3.3.1 Driver selection by causal model

For the 12 units we included, the causal model was able to reduce 18 candidate variables to smaller numbers of drivers for fire emission. The numbers of drivers ranged from 5 to 16 among the 12 units (Figure 3.3). The result also showed that the causal model can distinguish between correlation and causality, because whether a candidate variable was selected as a driver did not depend on its correlation (R^2) with fire emissions. Candidate variables with high correlations with fire emissions were not necessarily selected as a driver by the causal model. For example, *def* had the highest correlation with fire emissions in region 3, which is the tropical forests in South America, whilst *def* was not selected as a driver for fire emissions in this region (Figure 3.3). On the other hand, variables that were selected as drivers can have low correlations with fire emissions. All 12 regions contained drivers that ranked among the lowest in terms of their correlation with fire emissions. And for regions 8 and 11, only variables with the lowest correlations with fire emissions were selected as fire emission drivers rather than highly correlated variables (Figure 3.3). The correlation between the selected drivers and

fire emissions showed that high correlation with fire emissions was neither necessary nor sufficient for being selected as its driver, suggesting the causal model did distinguish between correlation and causality.

3.3.2 Machine learning model performance

The 4 machine learning models we used, namely GBM, RF, SVM and NN, produced consistent results in terms of model performance scores for each region using 3 different sets of input (Figure 3.4, and Figure A.2, Figure A.3, Figure A.4 in Appendix A). The only exception was that NN had slightly higher performance scores in regions such as African savannas, while its standard deviation of performance scores were extremely high in regions with relatively lower performance scores such as Asian boreal forests. Since our main focus is the model performance using selected drivers as input, we only show results from GBM here as an example.

For all 12 regions we tested, GBM achieved similar or higher performance scores using drivers selected by the causal model as input compared to using variables with the highest correlations or all 18 candidate variables for most regions. The only exceptions were regions 8, temperate broadleaf and mixed forests in North America, and 11, Mediterranean forests, woodlands and shrubs in Middle East (Figure 3.4). For regions where variables with high correlations with fire emissions were selected as drivers, such as region 1 savannas-Africa and region 7 temperate forests-Europe, the machine learning models can achieved similar performance compared to using inputs selected by highest correlations and all 18 candidate variables. For regions where variables with the highest correlation with fire emissions were not selected as drivers, the machine learning performance using drivers as inputs can still be comparable with that using most correlated variables as input for some regions; but not for all regions. For example, regions 3 and 4 were both of the biome tropical forests and their candidate variable with the highest correlation with fire emissions were not selected as drivers (Figure 3.3), region 4 has almost the same machine learning performance score using drivers as input compared to the other two sets of inputs; while region 3 had lower performance scores using drivers as input (Figure 3.4).

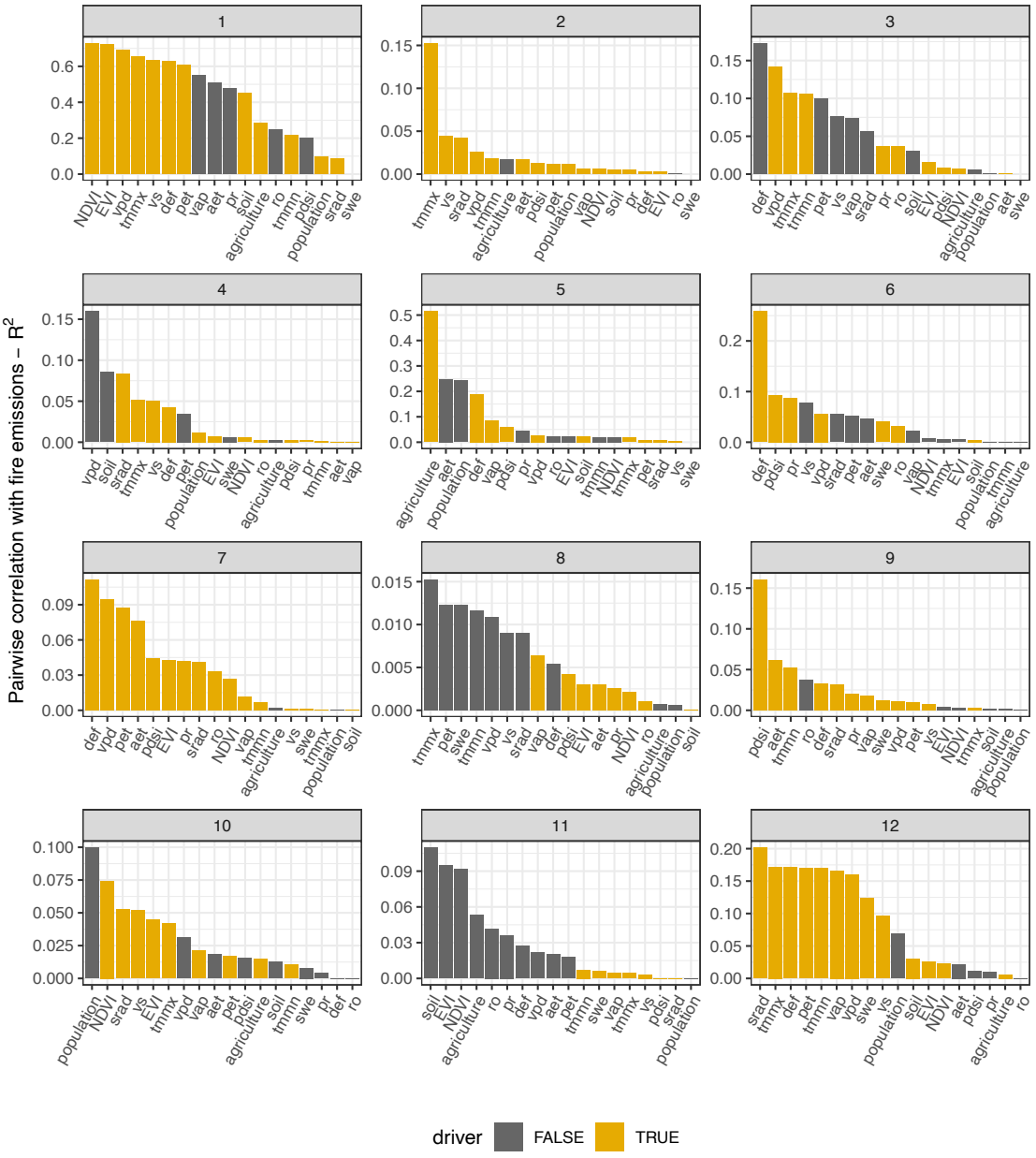

FIGURE 3.3: Correlation between all candidate variables and fire emissions and drivers selected by the causal model (full namaes of the variables included in this figure can be found in Table 3.1). Pairwise correlations between candidate variables and fire emissions, were measured by R^2. For each region, the variables were arranged in a decreasing order by their correlations with fire emissions. Yellow bars denoted the variables that were selected as a driver of fire emissions in the respective region by the causal model, and grey bars not.

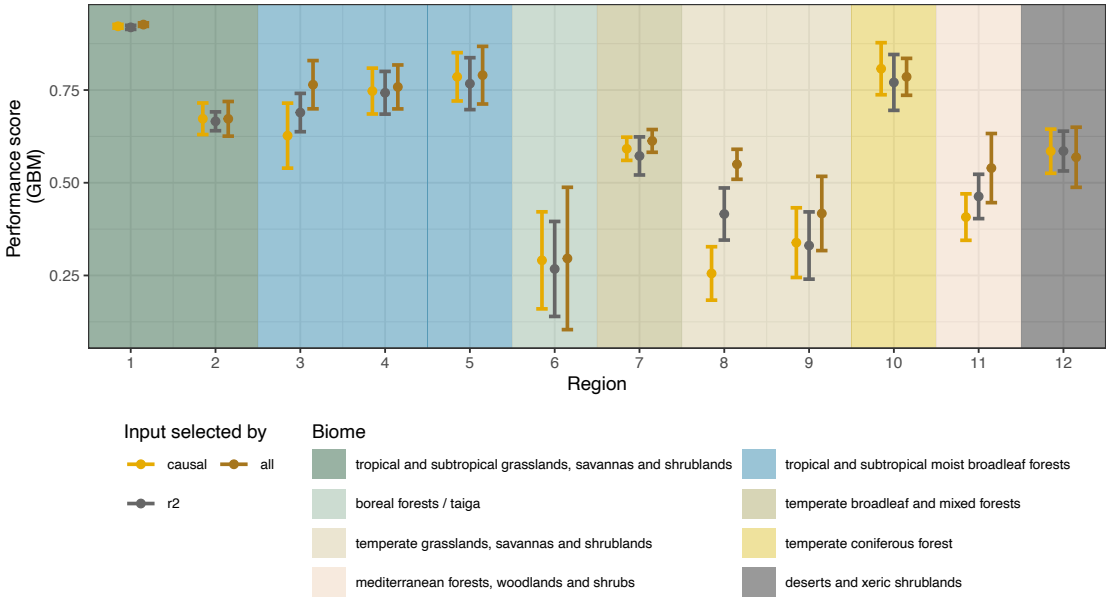

FIGURE 3.4: Gradient boosting model performance scores for all regions with input selected by i) causal model, ii) highest correlation (numbers equivalent to the number of drivers selected by causal model for each region), and iii) all 18 candidate variables. Dots and error bars represented the mean and standard deviation of the performance scores calculated by a 5-fold cross validation.

3.3.3 Driver importance by interpreting machine learning models

Here, we use tropical savannas-Africa as an example to show the results of drivers' impact on fire estimation through interpreting the machine learning models obtained for each region. To be consistent, we also used the model interpretation of GBM here as an example (Figure 3.5). The impact of each driver on fire emissions is estimated over the whole range of their respective values. Negative values of the impact represent negative impact, and vice versa. The impact of the two vegetation indices followed similar pattern, when *EVI* and *NDVI* were of low values, they had a negative impact on fire emissions; and with the increase of their values their impact became positive; while with continuing increase their impact saturated and plateaued (Figure 3.5). We also calculated the overall importance of each driver for ranking purposes, and the two vegetation indices were the most important drivers (Figure 3.5). The impact of the rest of the drivers were marginal compared to vegetation. Their impact were all highly nonlinear, some were more on the negative side, such as the two associated with anthropogenic intervention

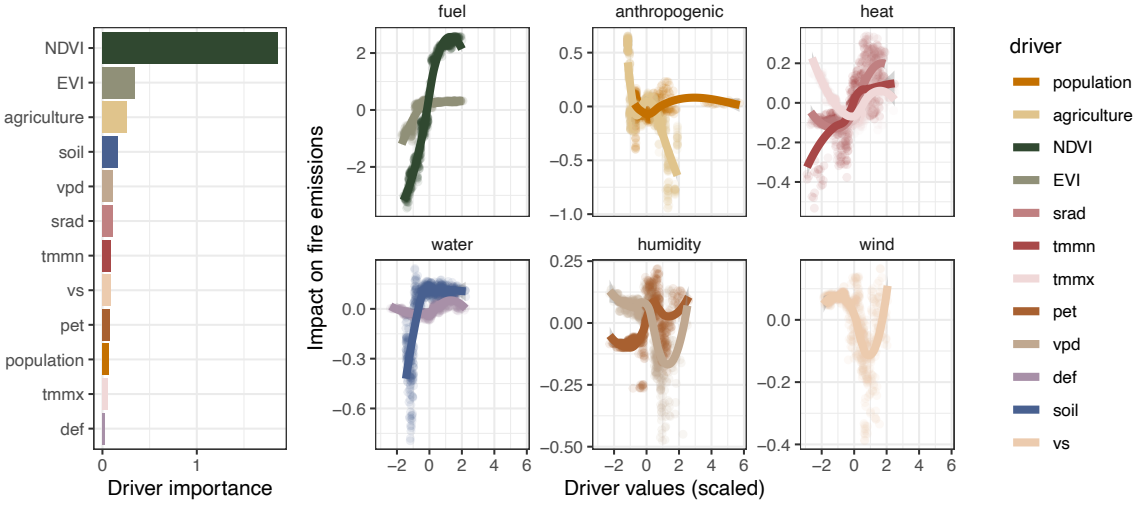

FIGURE 3.5: Impact of drivers on fire emissions estimated for region 1, tropical grasslands, savannas and shrublands in Africa (full namaes of the drivers shown on the y axis of the left-hand plot can be found in Table 3.1). Impact on fire emissions were estimated for the whole range of driver values individually by SHAP explainer (SHAP values). The importance of each driver is summarized by taking the mean absolute values of SHAP values.

agricultural and *population*; while some were more on the positive side, such as *vs* (Figure 3.5).

3.4 Discussion

In this chapter, we proposed a causal framework to investigate the drivers of environmental changes, and applied it to understand the drivers of fire-derived carbon emissions to test its validity. The causal framework we proposed included 1) selecting drivers based on its causal relation with the target (in our case is fire emissions), by a causal model, for which we chose multispatial CCM; and 2) using interpretable machine learning models to estimate the impact of selected drivers on fire emissions. We tested the validity of the framework we proposed by 1) calculating the correlation (R^2) between all variables and fire emissions to make sure that the causal model can be used to distinguish between correlation and causality; and 2) testing the machine learning model performance with the drivers as input to guarantee that the drivers selected by the causal model captured useful information to predict and explain fire emissions. The results showed that high correlation with fire emission is neither sufficient or necessary for a variable to be selected

as a driver, suggesting the causal model can distinguish between correlation and causality. When testing this causal framework, machine learning models for most regions with the drivers selected as input can achieve similar or better performance than the other two sets of input generated without using the causal model.

A clear advantage of this causal framework is that, through the addition of the causal model, we provide theoretical grounds for the causal relationship between the drivers and the output, fire emissions. Therefore, the relationship between input variables and output estimated by the subsequent interpretable machine learning model are justified to answer the question of cause and effect [11, 69]. This is the most important task to conduct a credible causal analysis. For a randomized controlled experiment designed to infer cause and effect, the credibility of its result is mainly judged by whether the experiment plausibly isolates the true causal relationship between the control and the response variables. While the variance of the response explained by the variations in the control variables is less important [8, 144].

It is worth mentioning that using this framework did not always improve the predictability of fire emissions, as shown in our results that regions 8 and 11 had slightly lower performance using drivers selected by the causal model. However, we argue that the slightly comporised model performance does not undermined the validity of the framwork for the following two reasons. Firstly, the performance of regions 8 and 11 using the causal framework were still quite sufficient compared to previous studies. Wang et al. [74] used more than 20 variables as their machine learning model input to predict fire emissions in North America, and their model performance achieved 26% - 70% variance explained. Our model performance for regions 8 and 11 with the causal model were 27% and 42% variance explained, reasonably within their range. Secondly and more importantly, the main purpose of this causal framework is to isolated the causal relationship through the causal model. This is also the reason that, although using variables with highest correlations or all candidate variables can sometimes achieve higher performance, they are not preferred if we desire a causal understanding.

This analysis is very much constraint by the data availability because it covered a dozen of ecosystems distributed around the world. For researcher who are interested in following this framework, we strongly recommend that they carefully

reconsider what variables can be included as potential drivers for their own researches. For instance, we did not include some important factors that can reflect anthropogenic interventions on fire activities, such as the proximity to human habitat, roads and traffic, and economic activities [94, 109, 145], because these data were not available at the spatial and temporal scale and resolution of this study. If future studies have access to these indicators, they will definitely benefit from including them. Likewise, the resolution we used in this analysis is partly limited by the computational resources we have. Future studies also needs to reconsider this according to the research question and data at hand.

We did not investigate the interactions between drivers in this study. Therefore, the causal structure remained unclear. But it is possible to extend this framework to explore the interactions and causal structures between the variables. For example, both anthropogenic intervention, indicated by *agriculture* and *population*, and vegetation (*EVI* and *NDVI*) were selected as fire emission drivers for region 1, which is the African savannas. According to previous studies for this area, anthropogenic intervention through conversion to agricultural land were the main reason for the decreased fire activities [108, 111]. Therefore, it is reasonable to further hypothesize that *agriculture* is the driver of *EVI* and *NDVI*. This hypothesis can be tested by the causal model multispatial CCM with the same data we used for identifying fire emission drivers as well. Previous studies that seek causal understandings often use structural equation models and network approaches, and have to make assumptions on the causal structure with their knowledge on the system [10, 68]. However, the validity of their assumptions on the causal structures often remain unexamined [8]. Disproportionate efforts to theorize about potential variables to include as model inputs rather than making sure the functional relationship between these variables is correct have been criticized [71]. Our framework serves as the first step towards resolving this gap by examining the causal relationship between the variables we collected and the outcome, i.e., fire emissions.

Similarly, the causal framework we proposed can also be used to investigate the feedback between variables by identifying whether the causal relationship is bidirectional or one-way. Although we only analyzed whether the included variables were causes for fire emissions, it is possible to also test whether fire emission is the cause for these variables. For example, van Nes et al. [42] investigated the feedback between greenhouse gases (GHG) and climate change with the same model used in

this chapter CCM by testing whether increasing GHGs causes climate change and whether climate change causes increasing GHGs. Likewise, we can investigate the feedback between fire emissions, climate and vegetation by this causal framework, such as the positive observed for some tropical and temperate forests [27, 98]. Identifying such causal feedback is crucial for ecosystem management because positive feedback are extremely risky as they could trigger regime shifts that have fundamental impacts on ecosystems [85, 146]. Although CCM has been successfully applied to detect directed and bidirectional causal relationships, it cannot infer all cases of hidden common causes, which is know as confounding, a phenomenon widely observed in complex systems [8, 11]. This issue can in theory solved by extensions of CCM such as techniques proposed by Benkő et al. [147] and De Brouwer et al. [148], but the more challenging work remained to be having the right data that can be used to detect the confounders [8, 10].

3.5 Conclusion

In this chapter, I proposed a causal framework to understand the drivers of changes in ecosystems. The framework can be divided into two steps, 1) selecting drivers from a set of potential drivers with a causal model; and 2) quantifying the contributions of each selected drivers with interpretable machine learning models. I applied this framework to understanding the geophysical and anthropogenic drivers of changing fire emissions. The findings showed that, 1) the framework can detect drivers based on the causal relations between the variables and fire emissions; 2) the selected drivers can predict fire emissions accurately, suggesting that these drivers can be used for interpretation to quantify their contributions to fire emissions; 3) by comparing the results produced for the 12 widely studied regions, I found the results aligned with current findings for these regions, therefore this framework can produce reasonable and reliable results. This framework provided a clear and repeatable working procedure for researchers investigating drivers of an observed phenomenon. It has the merits of guaranteeing causality instead of correlation between the drivers, which make the results more reliable and less prone to bias. Therefore, it has the potential to be applied to future relevant studies, and I believe adopting this framework can contribute to better understandings in environmental changes and the their underlie drivers in a broad context.

Chapter 4

Geophysical and anthropogenic drivers for global and regional fire emisison trends from 2001 to 2019

In this chapter, we applied the causal framework to understand the drivers for fire emisisons trends from 2001 to 2019. Fire plays an important role in the earth system. Carbon emissions from fires affect the global carbon budget and consequently climate change. Biome-specific qualities such as vegetation, climate and human land-use change are altering long-term trends in carbon emissions from fires. Whilst some biomes and continents have witnessed increasing fire-derived carbon emissions, others see decreasing trends. Yet, currently a biome-wide perspective on fire-derived carbon emission trends is lacking. We used total carbon emissions data from the Global Fire Emissions Database (version 4 with small fires) to investigate the spatial and temporal dynamics of fire emissions from 2001 to 2019 across the world. While the global trend for fire emissions stayed relatively unchanged (non-significant trend), this was due to contrasting trends in two geographical regions and biomes. Specifically, a decreasing trend in savannas and grasslands across the African continent and an increasing trend in boreal forests in Boreal Asia. The decrease in emissions in African savannas and grasslands was driven by a decline in vegetation, and thus fuel, and an increase in anthropogenic intervention, especially agricultural expansion. Increase in fire emissions from boreal forests in Boreal Asia was concentrated in a small area in east Siberia taiga, heavily driven by both

agricultural activities and climate change towards a drier climate (e.g., lower humidity). Although the total amount of emissions is a magnitude smaller for boreal forests, its contribution to global fire emission trend ($+7.4 \pm 2.2 \times 10^{12} gC/year$) is comparable to that of tropical savanna and grasslands ($-9.7 \pm 1.4 \times 10^{12} gC/year$). For many biomes, fire-derived carbon emissions are driven by several anthropogenic activities, vegetation and climate drivers, likely due to the complex feedback governing emissions. This global and biome-wide study highlights that anthropogenic activities in relatively small regions can shape global fire-derived carbon emission trends. Monitoring and management interventions are needed to address increasing fire-derived carbon emission areas, particularly the east Siberian taiga, and other forested biomes where deforestation contributes to rising emission trends.

4.1 Introduction

Carbon emissions from fires contribute around 2.2 gigatones of carbon per year globally during 1997–2016 [107]. Part of this carbon released by fires is reabsorbed by ecosystems through biochemical processes in the vegetation and soils [101, 103]. Long-term effects of fires and the emitted carbon vary depending on the region and biome. For example, in African savannas and grasslands, regular fires are part of the historical natural cycle of the ecosystem's regeneration process [149]. The emitted carbon from fires has been documented to be reabsorbed in roughly equivalent amounts through this regeneration process over a period of years to decades and such carbon emissions are considered as "fast respirations" [103, 107]. However, for ecosystems such as boreal forests and peatlands in Equatorial Asia, fires can alter the carbon mass balance and turn the ecosystem into a net carbon source, because the carbon stored in the soil and vegetation are emitted to the atmosphere. This alteration can last for decades to centuries because of the impaired ecosystem functions to support vegetation regrowth and accumulation of soil carbon. Thus, carbon emissions from fires can have long-term effects on the global carbon cycle [101, 103, 150].

Over the past decades, fire regimes have shifted due to climate change and anthropogenic intervention across the world [24–27]. The decline in global burnt area has been extensively studied and shown to be mainly driven by agricultural expansion and human suppression of fires [96, 108, 111]. However, global carbon

emissions from fires are relatively less studied and understood, especially in terms of the temporal trends and their distribution among regions and biomes, and for the drivers of these spatially differentiated trends. It is important to investigate the temporal trends of carbon emissions from fires and its spatial distribution due to its differentiated effects on the global carbon budget. Modelling approaches and satellite derived data for global fire emissions have existed since the 2010s and are constantly evolving with technological developments [101, 107, 114]. These datasets have been used in regional and global studies of fire emissions at a coarse spatial scale, often at the regional or ecosystem level [30], but have not been used to assess the spatial-temporal dynamics of global carbon emissions from fires at a higher resolution nor the drivers of these trends.

Fires and fire-derived carbon emissions are influenced by a wide range of geophysical and anthropogenic factors. Climate is a widely studied controlling factor for fires, and among all the climatic factors, rainfall and temperature are the most important factors for controlling fire regimes [24]. In addition, extreme climatic condition, such as extended periods of drought, increases the likelihood of extreme fire events in many regions [30, 99, 151]. For fire emissions, the availability of fuel and completeness of combustion have a large effect on the amount of carbon released from fires [107, 127]. Fuel is typically measured by vegetation cover or primary plant productivity, and in some ecosystems such as peatlands, soil carbon. Combustion completeness is a measure of the percentage of burnt material against all available fuel, and is also impacted by geophysical factors such as wind and humidity [107, 111, 152]. Besides geophysical factors, anthropogenic changes to ecosystem landscape can determine trends in fire emissions. Human induced fires could be used for clearing the forests, logging and agricultural purposes; and suppression can be done by removing vegetation, preventing accumulation of fuel, and intervening ongoing fires [27, 94, 108, 111, 153]. The impact of anthropogenic interventions on fires can be complex and differ depending on the intervention, ecosystem, and the interaction between ecosystems and human activity [35].

Here, we conduct a comprehensive spatial-temporal analysis for global carbon emissions from fires and evaluate the geophysical and anthropogenic drivers of these trends specific to the world regions and biomes. We ask the following questions: (1) What is the overall trend in fire emissions at the global scale? (2) How do these trends vary across subregions defined by biome and geographical region? (3)

What are the anthropogenic and geophysical drivers associated with fire emission trends in each subregion? (4) What are the most important drivers of fire emissions for each subregion? We first identified the overall trend of fire emissions at the global scale, which we decomposed into smaller subregions. We further observed areas that contribute the most to fire emission trends using $2^\circ \times 2^\circ$ pixels. Next, we selected fire emission drivers for each of the subregions from the 18 potential drivers that cover aspects of climate, fuel, and anthropogenic interventions with a causal model using multi-spatial cross convergent mapping (multispatial-CCM). Lastly, we ranked the importance of the selected drivers by their impact on fire emissions with machine learning models. We derived an understanding of the spatial-temporal dynamics of fire emissions and their underlying drivers across regions and biomes.

4.2 Data and methods

4.2.1 Overview

We used the total carbon emission data from the fourth version of Global Fire Emissions Database (GFED4s). Therefore, the term "fire emission" in this paper specifically refers to fire-derived total carbon emissions, and we used this term along this chapter for simplicity. We collected 18 candidate variables as potential drivers for diver selection. Our analysis include 3 part. 1) Identifying fire emission trends for the time period 2001-2019 at the global, subregional and pixel scales. We defined subregions as biomes within geographical regions; and set the resolution of the pixel at $2^\circ \times 2^\circ$. 2) Selecting drivers for fire emission trends from the 18 potential drivers with the causal model. The pixels that showed significant fire emission trends were used for driver selection for each subregion. The drivers we identified for fire emission trends were thereby specific to regions and biomes. 3) Using machine learning models to rank the driver importance by estimating their impacts on fire emissions at the subregional level.

4.2.2 Data

The fire emission data and the 18 candidate varaibles were the same as what we used in Chapter 3. Here, we skip the introduction of these data to avoid repetion.

4.2.3 Statistical analysis

Robust regression for trend detection

We applied robust linear regression to yield reliable estimations of the temporal trend of fire emissions [154]. Robust regression models operate by reducing the effect of points with high deviation from the mean, the regression results are less leveraged by the extremes. In our case, this means years with extreme fire emissions were given less weight in detecting a trend. This fits the purpose of this study, we focus on the long-term consistent trends rather than the variations or extreme events. We explored different robust regression techniques, but these produced very similar result for temporal trends (Appendix Figure B.2). All results in the main manuscript are from Huber regression, because it is a widely-used robust linear regression technique with applications in many fields [9, 155].

The slope of the robust linear regression was used for determining trends. As the regression was for annual fire emission against year, the direction and magnitude of the slope coefficient represent the estimated changes in fire emission per year. Based on the direction of their slope, we classified the trend of fire emission into decreasing (negative slope) and increasing (positive slope) trends. The statistical significance of the trend, i.e., the slope of the regression model, was tested by the Wald Test, and we set the significance level at 0.05, meaning a significant trend requires $p \leq 0.05$.

Identifying drivers and quantifying impacts

We follow the framework we proposed in Chapter 3 to identify drivers for fire emission trend and quantify their impacts on fire emissions. We defined subregions by biomes within geographical regions as the unit to apply this causal framework. Drivers for fire emission trends were identified for each subregion from the pixels

that showed significant trend within it by multispatial CCM. The reasons for using subregions include: 1) to satisfy the assumption of multispatialCCM that the set of different sites as spatial replicates should come from a relatively homogeneous system [131]; and 2) to make the computational time tangible for our analysis. The geopolitical division followed the basis regions defined in GFED database. We reduced the 14 basis regions to 10 for simplicity. The map of global biomes was provided by World Wildlife Fund [133], which classifies global ecosystems into 14 different biomes based on climate and vegetation. We aggregated the original 14 biomes to 8 following a previous study [111]. Details of the geographical regions can be found in Appendix Figure B.3; aggregation of biomes in Appendix Table B.1 and Figure B.4.

We obtained 44 subregions that contained at least one pixel that showed significant fire emission trend. We applied the causal model multispatialCCM to each subregion. Out of the total 44 subregions, the causal model successfully selected drivers for 31 subregions. The rest, scush as tropical dry forests in Africa, contained too few pixels with significant fire emission trends (all ≤ 3, Appendix Figure B.5) to produce a valid result. Our results on fire emission drivers represented 31 subregion, which accounted for around 93% of the global fire emissions from 2001 to 2019.

Statistical analysis was done in R [141] and Python [143]. Robust regression was implemented by `MASS` [156] package, and the significance test by `sfsmisc` [157]. Multispatial CCM was implemented by `multispatialCCM` [132]. GBDT was implemented by `LightGBM` [129], and its parameterization by `scikit-learn` [142]. SHAP explainer was implemented by `shap` using the `TreeExplainer` [135].

4.3 Results

4.3.1 Fire emission trend

At the global scale, fire emission did not show a significant trend ($p > 0.05$ for the regression slope, *Global*, Figure 4.1). This suggested the annual global fire emission did not change significantly between 2001 and 2019. The non-significant fire emission trend at the global scale was caused by the counteractive fire emission

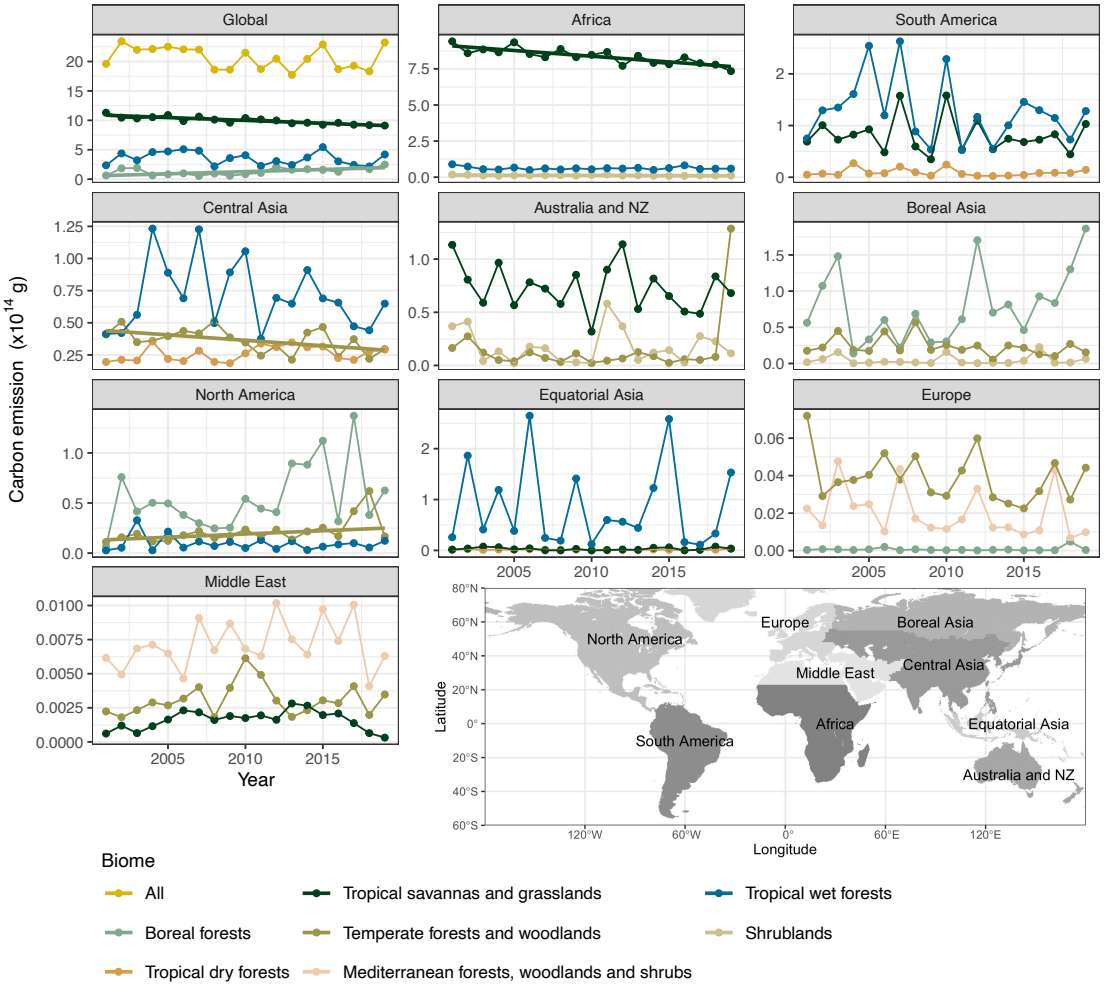

FIGURE 4.1: Global and regional carbon emissions from different biomes from 2001 to 2019 and their temporal trends. For each region, only 3 biomes with the highest emissions were included, except that subplot *Global* also included total emissions from all biomes. Regions were arranged in a decreasing order in terms of their fire emissions from left to right and up to down, and their y-axis were in different scales. Overall temporal trends determined by Huber regression were denoted by straight lines and only significant trends ($p \leq 0.05$ for slope of the regression) were displayed in the figure. A map of the regions was included in the lower right corner for reference.

trends in tropical savannas and grasslands and boreal forests. Tropical savannas and grasslands showed a significant decreasing trend of fire emissions, while boreal forests showed an increasing trend (solid green and light green lines in *Global*, Figure 4.1). Globally, tropical savannas and grasslands were the largest source of fire emissions, contributing 59% to global emissions, and boreal forests were the third largest source contributing 8% to global emissions (Appendix Figure B.6). Although emissions from tropical savannas and grasslands were a magnitude higher than from boreal forests, their increasing or decreasing rates of fire emissions were comparable. The former decreased at a rate of $-9.7 \pm 1.4 \times 10^{12} gC/year$ and the later increased at a rate of $7.4 \pm 2.2 \times 10^{12} gC/year$ (rates of fire emission trends estimated by the slope coefficients of Huber regression). In addition, tropical savannas and grasslands and boreal forests were the only 2 biomes that showed significant fire emission trends at the global scale, the other 6 biomes showed non-significant trends (Appendix Figure B.7).

More than 75% of fire emissions from tropical savannas and grasslands occurred in Africa, which also showed a significant decreasing trend, driving the global decline in fire emissions from tropical savannas and grasslands (solid green lines in *Global* and *Africa*, Figure 4.1)). Emissions from tropical savannas and grasslands in other regions, e.g., South America, Australia, Equatorial Asia, and Middle East, had marginal contributions to global emissions and all showed a non-significant trend (Figure 4.1). Tropical wet forests were the second largest source for global fire emissions, but showed no significant trend in fire emissions globally and across regions (Figure 4.1). Boreal forests showed a significant increasing trend at the global scale, while fire emissions for boreal forests in *Boreal Asia*, *North America*, and *Europe* were not significant (Figure 4.1). For the rest of the 5 biomes with lower fire emissions globally and in separate regions, their fire emission trends were mostly non-significant, except temperate forests and woodlands in Central Asia and North America, the former showed a significant decreasing trend and the latter increasing (Figure 4.1). Most regions exhibited strong interannual fluctuations in carbon emissions but non-significant trends, for example the significant spikes in annual fire emissions for tropical wet forests in South America, Central Asia and Equatorial Asia (Figure 4.1).

At the $2^\circ \times 2^\circ$ pixel scale, we detected 697 pixels that showed significant fire emission trends, which is 17% of all the pixels that experienced fire emissions. Of the

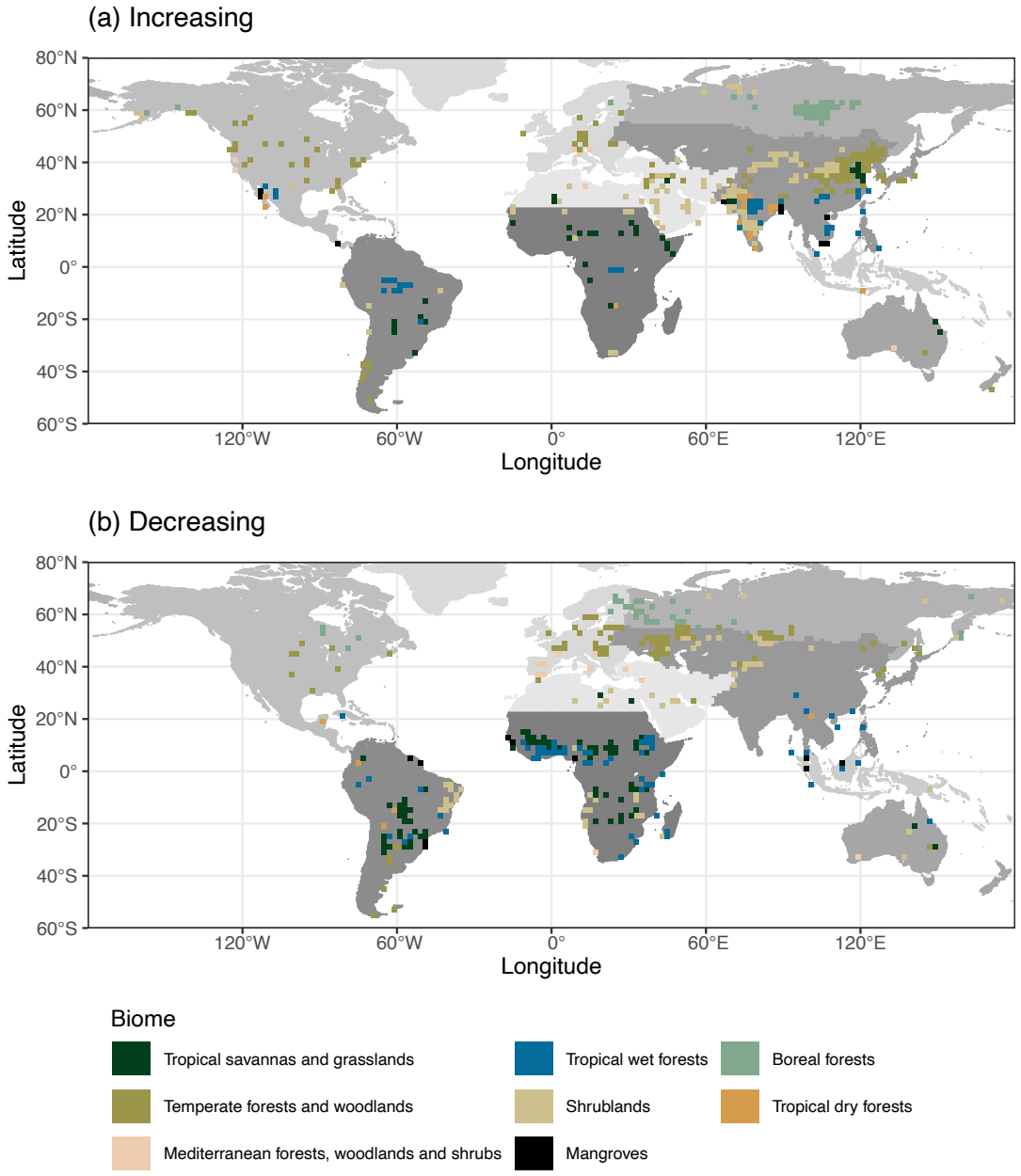

FIGURE 4.2: Pixels that showed significant (a) increasing fire emission trends and (b) decreasing fire emission trends from 2001 to 2019 ($p < 0.05$ for regression slopes). Color of the pixels indicated different biomes, and the different shades of grey in the base map indicated the regions. Fire emission trends were detected by Huber regression. Only pixels that showed significant trend were displayed on the map.

pixels that showed significant fire emission trends, 361 pixels showed an increasing trend and 336 decreasing (Figure 4.2). Pixels that showed significant trend covered a total area of around $2 \times 10^7\ km^2$, $0.9 \times 10^7\ km^2$ for increasing and $1.1 \times 10^7\ km^2$ for decreasing. A large number of pixels that showed an increasing trend were distributed in Central Asia, especially around India and north China. The dominant biomes for these pixels in Central Asia were temperate forests and woodlands, and shrublands. We also observed a large cluster of pixels with increasing fire emissions in boreal forests in the center of Boreal Asia, which is around the east of Siberia (Figure 4.2 (a)). This cluster alone contributed to increasing fire emissions at a rate of $2.8 \pm 0.7 \times 10^{12} gC/year$, slightly more than 1/3 of the overall increasing rate of fire emissions from boreal forests globally, which is $7.4 \pm 2.2 \times 10^{12} gC/year$. The large clusters of pixels that showed significant increasing trends in Boreal Asia and Central Asia accounted for 56% of that globally. Two smaller clusters of pixels that showed significant increasing fire emission trend were observed in tropical wet forests in South America and temperate forests and woodlands in Europe. The rest of pixels with increasing fire emissions in other regions did not form significant clusters.

For pixels that showed decreasing fire emission trends, about 47% were located in Africa and South America. For Africa, most of the pixels that showed decreasing trends were in the south of the equator, and were dominated by tropical savannas and grasslands, and tropical wet forests. Pixels that showed decreasing fire emission trends in South America were dominated by tropical savannas and grasslands. A considerable amount of pixels with decreasing fire emissions were observed in temperate forests and woodlands in Europe and west of Central Asia, and boreal forests closer to Europe. In total they accounted for 40% of the number of pixels that showed significant decreasing trends. The remaining pixels with decreasing fire emissions (13%) were scattered in other regions. Australia and New Zealand along with Equatorial Asia, although hotspots for fire events, only contained a few pixels that showed significant long-term fire emission trends.

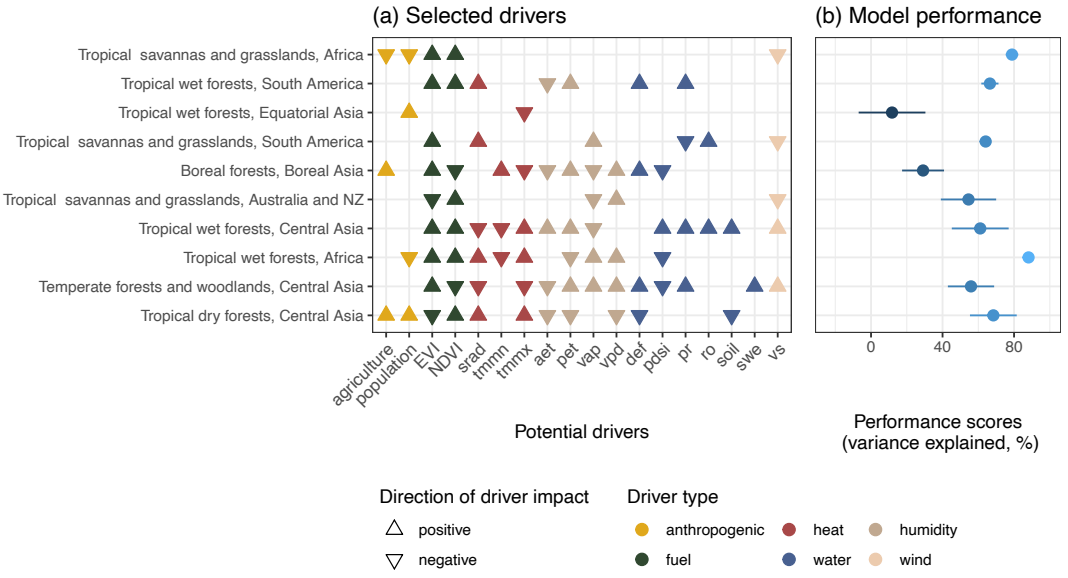

FIGURE 4.3: Drivers selected by causal model for subregions defined by region and biome (a) and their GBDT model performance with the selected drivers as model input (b). Full namaes of the drivers shown on the y axis of the left-hand plots can be found in Table 3.1. Only top 10 subregions with the highest fire emissions were displayed, and were arranged in a decreasing order by their fire emissions from top to bottom. Triangles denoted the selected drivers for each subregion. The orientation of the triangles represented the overall impact of the driver on fire emissions for the particular subregion, which were calculated by taking the average of the estimated impact on fire emissions (SHAP values). An upwards triangle means a positive impact, and downwards negative. All 18 potential drivers were divided into 6 categories, which were indicated by the color of the triangles. Model performance scores were measured by variance explained by the GBDT model with the selected drivers. The dots and horizontal lines represented the mean and standard deviation of performance scores from the 5-fold cross validation for each subregions. A high performance score means the model predicts fire emissions accurately. A negative score means the model predicts less accurately than having the mean fire emission value as a constant estimate.

4.3.2 Drivers selected by causal model and their impact on fire emissions

For all 31 subregions, the causal model reduced 18 potential drivers to between 1 and 14 drivers of fire emission trends specific to the subregion. With the selected drivers as GBDT model input, 17 subregions achieved GBDT model performance scores higher than 50% variance explained (Appendix Figure B.8). Subregions that achieved good model performance did not necessarily have large numbers of

drivers . For instance, the fire emissions from temperate forests and woodlands in South America were driven solely by wind speed (*vs*), a climatic driver, and the GBDT model scored around 50% of the variance explained; while the fire emission drivers for the same biome in Central Asia were more complex and had 13 in total, ranging from climatic to vegetation, and also achieved a performance score close to 50%. This suggested that the causal model effectively selected the drivers that have causal relations with fire emissions for most subregions.

We focused on the top 10 subregions which accounted for more than 80% of the global fire emissions from 2001 to 2019 (Figure 4.3). From these 10 subregions, 8 subregions achieved a GBDT model performance of more than 50% variance explained. Tropical wet forests in Equatorial Asia had the worst GBDT model performance score, and boreal forests in Boreal Asia also had lower scores compared to the other subregions. Fire emission drivers for the same biome across different geographical regions can be different. For example, tropical savannas and grasslands in Africa, South America, and Australia, had different drivers associated with fire emissions. Vegetation was identified as an important driver for the same biome in these three regions, but climatic drivers were different, and anthropogenic drivers were only identified for African savannas and grasslands. Likewise, fire emission drivers for different biomes within the same geographical regions can be different as well. For example, the two biomes in Africa, tropical savannas and grasslands and tropical wet forests, had very different climatic drivers. The former only had one associated with wind, while the later had multiple climatic drivers associated with heat, humidity and water.

For the top 10 subregions, fuel was the most common driver category, which was identified as a fire emission driver for 9 subregions except tropical wet forests in Equatorial Asia (Figure 4.3). The importance of the two drivers relating to fuel, *EVI* and *NDVI* , varied among subregions. *EVI* and *NDVI* were the most important drivers for tropical savannas and grasslands in Africa, the biggest contributor to global fire emissions; while they were the least important drivers for boreal forests in Boreal Asia (Figure 4.4). Typically, low fuel loads decreased fire emissions, while higher fuel loads increased fire emissions. For example, in African savannas and grasslands, lower *EVI* and *NDVI* values had a negative impact on fire emissions but an increase in *EVI* and *NDVI* resulted in a positive impact on fire emissions, and this shift from negative impact to positive occurred around the

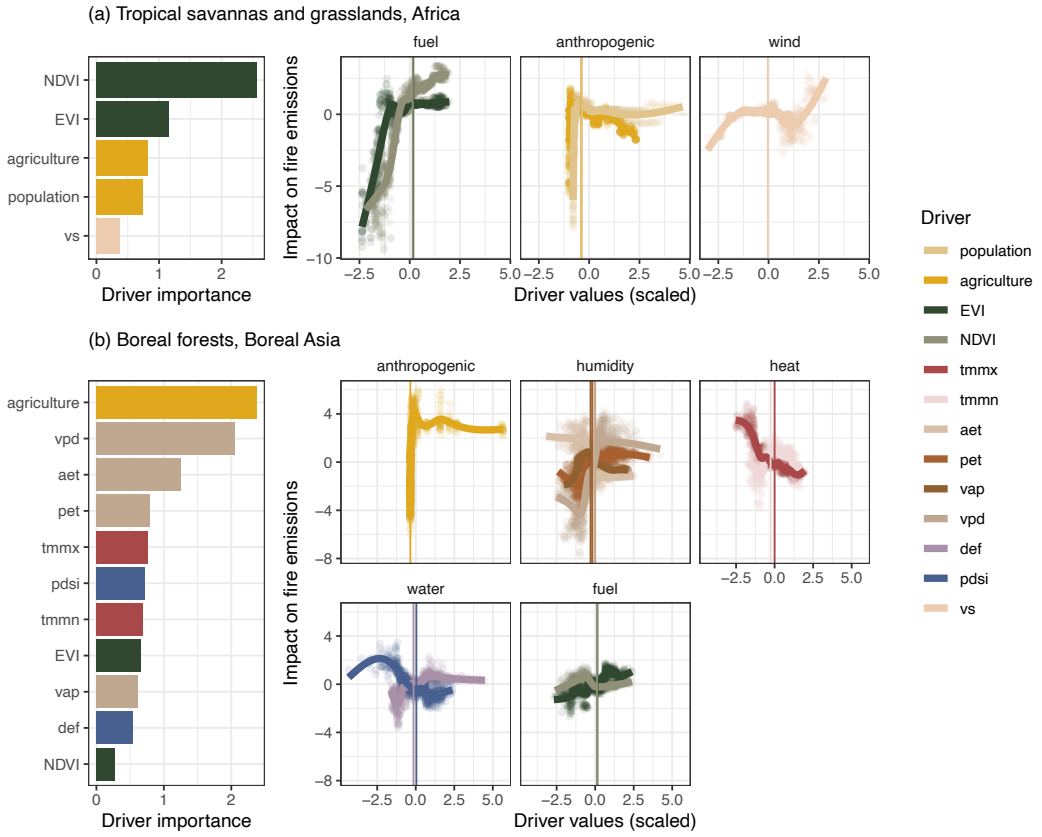

FIGURE 4.4: Driver importance and their estimated impact on fire emissions for tropical savannas and grasslands in Africa (a) and boreal forests in Boreal Asia (b). Full namaes of the drivers shown on the y axis of the left-hand plots can be found in Table 3.1. Drivers were arranged by their importance (overall impact on fire emissions) from top to bottom in a decreasing order in the bar plots. Importance of drivers were calculated by taking the mean absolute values of their estimated impact on fire emissions across the range of driver values. The estimated impact on fire emission against driver values were plotted by driver categories on the right hand side. Driver values were scaled by $(X - \bar{X})/\sigma(X)$, where X represents a driver, and $\bar{X}$ and $\sigma(X)$ its mean and standard deviation. Estimated impact on fire emissions were SHAP values calculated by SHAP explainer. Negative values of estimated impact indicated negative impact on fire emissions, and vice versa. The vertical lines in each subplot indicated the medians of the respective driver. Note that the medians of some drivers were very close and thus the vertical lines almost overlapped.

medians (Figure 4.4 (a)). Fuel had an overall positive impact on fire emissions for most subregions, highlighting the role of vegetation as having a positive relationship with fire emissions (Figure 4.3). The two drivers representing fuel, *EVI* and *NDVI*, could have opposite impacts on fire emissions for some subregions, but the overall impacts of fuel were nonetheless positive. For example, *EVI* and *NDVI* had opposite impacts on fire emissions for Asian boreal forests, *EVI* positive and

NDVI negative (Figure 4.3). However, the positive impact of *EVI* outweighed the negative impact of *NDVI* because the former ranked higher in driver importance than the latter (Figure 4.4), resulting in an overall positive impact of fuel on fire emissions. This is also true for tropical savannas and grasslands in Australia, and temperate forests and woodlands and tropical dry forests in Central Asia. Regardless of the opposite directions of the two drivers associated with fuel, the overall impacts of fuel were still positive (Figure 4.3 and Appendix Figure B.9).

At least one driver belonging to the four climatic categories - heat, water, humidity and wind - were observed for all subregions, meaning climate had a widespread effect on fire emissions for all subregions (Appendix Figure B.8). Among the four climatic categories, heat, humidity and water were more commonly observed as drivers, while wind was identified as a driver for fewer subregions (Figure 4.3 and Appendix Figure B.8). For the top 10 subregions, 8 subregions had drivers relating to heat and humidity, 7 for water; while wind was only observed in 5 of them and usually ranked low in terms of driver importance. Some subregions had more climatic drivers than others, suggesting that climate has more control over fire emissions for those regions. African tropical savannas and grasslands had only one climatic driver *vs* which was also the least important driver. On the other hand, boreal forests in Boreal Asia had 8 climatic drivers covering 3 categories, namely humidity, heat, and water; their driver importance also ranked high (Figure 4.4). Therefore, in our analysis climate played a much more important role for driving fire emissions in boreal forests in Boreal Asia than tropical savannas and grasslands in Africa.

Anthropogenic factors were identified to be fire emission drivers for 16 subregions in total, and 5 for the top 10 subregions with highest emissions. For the two anthropogenic factors, *population* was identified as a fire emission driver in more subregions than *agriculture*. This suggested anthropogenic interventions in general as reflected by *population* had a broader impact on fire emissions through different means other than agricultural activities. The impact of anthropogenic drivers on fire emissions were negative for some subregions and positive for others. For African tropical savannas and grasslands, both *population* and *agriculture* had a negative impact on fire emissions, which suggests anthropogenic interventions reduced fire emissions (Figure 4.3). When *population* and *agriculture* were low (below the medians), this negative impact was greater since their impacts were far

below 0. With the increase of the two anthropogenic factors, the impact became positive around the median values, and then decreased and became negative again (Figure 4.4). For boreal forests in Boreal Asia, the anthropogenic driver *agriculture* had an overall positive impact on fire emissions (Figure 4.3), and the pattern of its impact were quit different from that in African savannas and grasslands (Figure 4.4). After around the median of *agriculture*, its impact stayed positive and the values were far higher than that in African savannas and grasslands. This suggested that anthropogenic interventions had distinct mechanisms for the two subregions.

The impact of drivers under the same driver category for a subregion did not necessarily follow the same pattern. For example, drivers under the categories fuel and anthropogenic for tropical savannas and grasslands in Africa aligned for their impacts on fire emissions (Figure 4.4 (a)). For boreal forests in Boreal Asia, drivers under the category humidity were consistent for their overall impact on fire emissions, which was a negative impact - high humidity led to lower fire emissions. Note that *vpd* and *pet* are inversely related to humidity (Table 3.1), therefore, the positive impacts of these two drivers on fire emissions represent a negative impact of humidity (Figure 4.3). However, the patterns of impact for the 4 drivers relating to humidity were all highly nonlinear and displayed different patterns (Figure 4.4 (b)). And for this subregion Asian boreal forests, drivers under the categories heat and water had different directions of impact, and their patterns of impact differed as well.

4.4 Discussion

Our study makes an important contribution towards understanding trends and drivers of fire-derived total carbon emissions from 2001 to 2019 at a global scale and at a scale specific to biome and region. Long-term trends associated with global fire emissions have been relatively stable, a result of two counteractive fire emission trends from African savannas and grasslands and Asian boreal forests. Trends across subregions vary widely, with some subregions showing consistent increasing or decreasing trends in fire emissions, while others showing large fluctuations in annual fire emissions. Vegetation and climatic variables were major drivers for fire

emission trends across subregions, although anthropogenic variables were significant in driving the trends of fire emissions from two of the largest contributing sources, African savannas and grasslands and Asian boreal forests. These geophysical and anthropogenic drivers ranked differently in driver importance across our subregions and underlie the observed decreasing or increasing fire emission trends across time.

Our findings on fire emission trends from 2001 to 2019 aligned with many existing studies on that for burnt area. The global burnt area although shown a declining trend, the magnitude of its decline was minor according to Wu et al. [145], Andela et al. [108] and many other similar studies [107, 111]. This is mainly due to the decline of fire activities in Africa and South America, mostly of the biome tropical savannas and grassland. Decline in these regions was mainly caused by anthropogenic interventions such as urbanization and agricultural activities [108, 109, 111, 145]. While increase in burnt area were observed in many places, the increases in fire emisisons were extremely concentrated in a relatively small area, especially the Asian boreal forests.

At a global scale, vegetation was the most common important driver in fire emission trends across subregions. This corroborates with global studies that identified fuel as the most important driver for changes in global fires [111]. Vegetation generally had a positive impact on fire emissions in our results, which aligns with our understanding that fire is constrained by the availability of vegetation and other forms of fuel [33, 158]. The feedback between fire and vegetation are further complicated by climate because it affects the regeneration and flammability of vegetation [33]. In our results, climate also drove fire emission trends in most subregions, aligning with the literature that climatic conditions, especially rainfall, temperature and humidity, are important controls for global fires [24, 106]. Anthropogenic interventions were identified as drivers of fire emission trends for a smaller number of subregions compared to vegetation and climate. However, the importance of anthropogenic intervention can be dominating in some subregions, for instance African savannas and grasslands. Although previous studies in African savannas found climate conditions such as increasing moisture availability drives increases in fire using spatial data [34], this was not important for long-term trends in our analysis using time series from 2001 to 2019. This aligned with previous findings

that anthropogenic intervention through land-use conversion has been the dominant driver for decreased burnt area in African savannas over the past two decades [108]. Although anthropogenic intervention had a negative impact in Africa, it can have a positive impact on fire emissions in other subregions such as tropical wet forests in Boreal Asia and tropical dry forests in Central Asia. This corroborates with a global study that showed anthropogenic intervention could have a positive or negative effect on burnt area depending on population density and grass fraction [109]. Using fires to clear and prepare the land for crops can be the reason for the large areas that showed increasing fire emission trend in Central Asia [159]. For forested biomes, anthropogenic intervention through intensive deforestation can led to a higher risk of fires in the intact forests and consequently increasing fire emissions, which is further amplified by climate change [98, 160]. A small cluster of pixels in our study had significant increasing fire emission trends in tropical wet forests in South America, likely a result of deforestation in this region [161]. This risk of increasing fire emissions from forests associated with anthropogenic interventions and climate change has strong implications for future fire emission trends because forests have much higher fuel loads compared to savannas and grasslands, resulting in higher fire emissions per unit burnt area [101, 162].

Of the forested biomes that have higher risks of increasing fire emissions, we further identified the main contributor of increasing fire emissions, which is boreal forests in Boreal Asia. Our findings corroborates with the previous studies that identified forests and boreal forests as the reason for relatively stable fire emissions in spite of the decreased burnt area globally [101, 108, 162]. We found the increase in Asian boreal forests mainly occurred in a small cluster of pixels that showed increasing trend, belonging to the ecoregion *east Siberian taiga* [133]. This corroborates with a recent study that showed significantly increased burned area in this ecoregion from 2001 to 2020 correlate with climate conditions, namely warming and drying climates [93]. Our findings ascertained the causal relationship between these climatic conditions and the increased fire emissions in this region, especially humidity as one of the most important drivers. In addition to climate, we also found agricultural activities as the most important driver for increasing fire emissions in this region, which was unaccounted for in previous studies [93, 163].

It is worth mentioning that this study aimed to understand the past, including

the historical trend and the underlie drivers, rather than a projection of the future. However, the results can be quite similar. Wu et al. [145] predicts that 1) the decreases in burnt area in Africa and South America, where we also observed decreasing fire emissions, will continue to decrease due to anthropogenic interventions; and 2) burnt area in high altitudes will continue to increase as a result of changing climate and human ignitions, which also aligned with our findings that fire emisisons in Asian boreal forests increased due to anthropogenic intervention and drier climates.

Our study on fire emissions focused on the long-term consistent trend in fire emissions which is limited by the time period for our observation (2001-2019), and did not investigate the interannual variations or extreme fire events. While several extreme fire events have taken place in some subregions such as the wet forests in South America [164] and Equatorial Asia [99], and the savannas and woodlands in Australia [30], our study did not capture any significant long-term increasing trends in fire emissions for these subregions, and the number of pixels with significant fire emission trends were not high. However, we should be cautious to extend our results to predict future changes in fire emissions, and it is possible that fire emissions in these regions experience significant increase under future climate change and/or anthropogenic intervention. We observed subregions where fire emission trends were heavily driven by climate, such as tropical wet forests and tropical savannas in South America, and Asian boreal forests. This aligned with existing studies that highlighted the risk of climate change on fires in these regions [93, 160]. Since fire emission trends in these subregions have been heavily controlled by climate, it is likely that their future fire emissions are more vulnerable to climate change, and should receive more attention.

We are aware that our results are constrained by data availability at the temporal and spatial scale of our study. Findings from this study are based on GFED4s emissions data, which are known to underestimate burnt area because of the inability to account for small fires. This constitutes a considerable underestimation for Africa where a large proportion of fires are small fires [40, 115] amongst other regions [165]. Therefore, our findings may be underestimating a significant proportion of emissions from small sized fires [114]. In our analysis of drivers, our selection was limited by globally available datasets. For example, pasture landcover has be found to be a good indicator for anthropogenic intervention in relation to burnt

area in global studies [108, 111], but harmonized and reliable global annual time series pasture landcover data from 2001 to 2019 is lacking [166]. Missing important drivers could be a reason for poor GBDT model performance for some subregions. For example, the relatively low GBDT model performance scores for tropical wet forests in Equatorial Asia can be a result of lacking a representation of soil carbon as a driver (fuel source) and its contribution to fire emission estimates. Large areas of tropical wet forests in Equatorial Asia are peatlands, where burning of organic carbon in soil contribute greatly to the emissions [107, 167, 168].

4.5 Conclusion

Changing climate and anthropogenic interventions are major concerns for increases in fires across the world, which can have a positive feedback on climate through fire-vegetation interactions and gaseous emissions. Global databases such as GFED provide spatially explicit time series data for fire emissions, allowing us to make valuable observations on temporal trends of fire emissions at different spatial scales. Our analysis at a global scale provides a first look at fire emission trends estimated at the global, subregional and pixel ($2^\circ \times 2^\circ$) level, and the drivers for increasing or decreasing trends specific to regions and biomes. Although we observed fire emissions to be relatively stable over the years 2001-2019, special attention should be paid to boreal forests, which showed significant increasing fire emissions.

The results on fire emission trends highlighted some important regions to target for future monitoring and management, such as the ecoregion *East Siberian Taiga*. These regions deserve special attention for two reasons, 1) they showed increasing trends of fire emissions from 2001 to 2019; and 2) they are likely to be significant net carbon sources in the future.

Drivers for fire emission trends and their relative importance at the regional scale provided evidence on which geophysical and anthropogenic factors should be targeted to mitigate global fire emissions in order to optimize the outcome. For example, climatic factors, primarily humidity, and agricultural activity have been shown to drive increasing fire emissions in Asian boreal forests, predisposing this subregion to high risk of fires under climate warming. While mitigating climate change would require action at a global level, at a regional level, monitoring and

managing agricultural activities in this subregion could have an out-sized contribution towards mitigating global fire emissions.

It should be emphasized that mitigating deforestation and fires in forests and woodlands biomes is of vital importance to reducing future global carbon emissions from fires. The decreasing trends of fire emissions at the regional level were mainly found in savannas and grasslands in Africa and South America. These decreases were primarily driven by the declines in vegetation cover, indicating this decreasing trends are unlikely to continue in the future because this is a self-limiting process [33, 34]. On the contrary, the increasing trends observed in forests are more likely to continue and even accelerate in the future because of the positive feedback between fires and vegetation in these ecosystems [27, 37]. A decline in vegetation cover in forests and woodlands biomes, cause by either fires or deforestation, can result in previously intact forests being made more susceptible to fires, subjecting these ecosystems to future risks of shifting fire regimes and higher fire emissions [33, 160, 169]. This risk is further amplified by climate change due to the complex feedback between vegetation, climate and fires [33, 160]. The increases in the fire emissions from forests and woodlands from 2001 to 2019 is already comparable to the decreases in grasslands and savannas. Therefore, in order to reduce the risk of global increases in fire emissions, more efforts should be channeled to managing forests fires and deforestation.

Part II

Mechanism model

Chapter 5

Modelling degradation of forests under the pressure of anthropogenic intervention and climate change

In this chapter, I used an existing mechanism model that described the interplay between grass, savannas, and trees to describe the transition from forest to grassland under different levels of climate change and anthropogenic intervention. I simulated the transitions using scenario analysis of this model, where the levels of climate change and anthropogenic intervention were represented by two model parameters s_1 and v, respectively. With high level of climate change, the system display hysteresis, and only if the system is under low level of anthropogenic intervention, there exist a bistability between grassland and forests, whilst if the level of anthropogenic intervention is high, the system will be grass dominated. If the system were under a low level of climate change, the system displays a nonlinear response to increasing anthropogenic intervention but without hysteresis; with increasing anthropogenic intervention, the system will loss tree occupation and become more dominated by grass. In addition to the final stable states of the system, levels of anthropogenic intervention and climate change also affect the process of the transition. With higher level of climate change, a forest dominated system will degrade to a more grass dominated one in shorter time period, leaving less opportunity window for mitigation.

5.1 Introduction

The transition of ecosystem status from forests to savannas/grasslands can lead to loss of biodiversity, carbon storage, and other important ecosystem services that forest ecosystems provide to sustain human well-being. Thus, transition from forests to savannas/grasslands is often considered as an ecosystem degradation. [98, 169, 170]. This change in state is often a critical transition because of the existence of bistability between forests and savannas/grasslands. As such, this process is often characterized by abrupt changes in ecosystems that are difficult to predict and reverse, causing profound and persistent consequences [85, 146, 170].

The most widely documented drivers for forest degradation include anthropogenic interventions and climate change [98, 170]. Anthropogenic interventions include deforestation, logging, and the conversion of forests to other uses such as agricultural land [98, 160]. Anthropogenic interventions are found in almost all kinds of forest ecosystems such as tropical forests and boreal forests [160, 171, 172]. In addition to the direct removal of trees, anthropogenic interventions can make dense forests more susceptible to fire, accelerating the process of forest degradation [98, 160, 170].

Climate change is another huge concern that can lead to forest degradation. Climate can directly affect the birth, growth, and mortality of trees and other vegetation [173]. Therefore, forest ecosystems often adapt and evolve with the changing climate [27, 116]. Additionally, climate can shape forest ecosystems indirectly through the occurrence and spread of fires, which can lead to positive feedback between fires and vegetation [27, 170, 174]. Closed-canopy forests usually have cool and moist sub-canopy micro-climates that can prevent the spread of fire; while fire can transform this less fire-prone forested landscape to shrub-dominated systems that are susceptible to fires. Such positive feedback can lead to threshold behavior and regime shift of forest ecosystems to savannas and grasslands [27, 98, 174]. These regime shifts have been observed in tropical and temperate forests [174]. For other types of forest ecosystems such as boreal forests, the feedback between vegetation and fire can be negative as fires transform the landscape to be less fire-prone, thereby reducing the likelihood of future severe fires [27, 175].

Degradation of forests to savannas/grasslands as typical regime shifts can be best modeled by simple models [44, 176]. Simple mechanism model is a suitable and widely-used technique for understanding and simulating critical transitions of many

systems [44, 176, 177]. It has been used to interpret the regime shift phenomenon in a wide range of systems including ecosystems and social-ecological systems [44, 45, 85, 178]. Such models can be used for theoretical analysis and be applied to realistic systems where the data for model selection and model parameterization are sufficient [4, 44, 177–180]. The key components of the simple model include variables representing ecosystem state, external drivers, and disturbances [5, 44]. In order to be able to effectively illustrate the regime shift phenomenon, such model often reflects the interactions among different components of the system and their nonlinear response to external drivers that give rise to the critical transitions observed in the system [5, 44].

Although the phenomenon of forest degradation is well documented in existing literature, its description through simple mechanism model is relatively lacking [179, 181]. In this chapter, I used the model developed by Touboul et al. [181], which describes the interplay between grasslands, savannas and forests. With a few modifications, we can use the model to describe the process of forest degradation to savannas/grasslands under the external drivers, namely anthropogenic interventions and climate change. For this model, the underlying mechanisms that govern the degradation from forests to savannas/grasslands include 1) the competition between these species reflected by their growth rates and mortality rates, and 2) the likelihood of fires in the system, which is determined by the percentage of trees within the system [181]. The two key mechanisms involved are both affected by climate change and anthropogenic intervention, which can be controlled by parameter values in model simulations. Therefore, this model is suitable for our research purpose to investigate the role of climate change and anthropogenic interventions in the degradation of forests to savannas/grasslands. With properly designed scenarios to represent different levels of the two drivers and scenario analysis of this model, we can qualitatively investigate the impacts of the two drivers on forest degradation.

5.2 Methods

5.2.1 Model description

Our model is based on a three dimensional model developed by Touboul et al. [181], which was modified from Staver et al. [182], to describe the interplay between grass, savanna saplings, and trees. The assumption of the model is that 1) the whole system is occupied by either grass, savanna sapling, or trees; 2) grass can grow into savanna saplings, and saplings into trees; and 3) once savannas and trees die off, their space will be occupied by grass since its growth rate are far higher than the other two species. The model equation can be formalized as (5.1):

$$\begin{aligned} \frac{dG}{dt} &= \mu S + \upsilon T - \beta GT \\ \frac{dS}{dt} &= \beta GT - \omega(G)S - \mu S \\ \frac{dT}{dt} &= \omega(G)S - \upsilon T \end{aligned} \tag{5.1}$$

where G, S, and T represents fractions of the space occupied by grass, savanna saplings and tress, respectively; μ and υ are the mortality rates of savanna saplings and trees; β is the birth rate of savanna saplings; and $\omega(G, S, T)$ is the recruitment rate from savanna saplings to trees.

The influence of fires is embedded in $\omega(G)$, which is the recruitment rate of savannas to tree. It is a sigmoid function describing the nonlinear response between fires and the vegetation of the system. If the system is dominated by grass (high G values), the system is prone to fire, thus the recruitment rate from savanna saplings to trees is low; whilst if the system is dominated by trees (high T values), the system is less prone to fire and tree recruitment rate can be high [179, 181]. This nonlinear responses can be formalized as (5.2):

$$\omega(G) = \omega_0 + \frac{\omega_1 - \omega_0}{1 + exp\{[-G - \gamma(1 - G) + \theta_1]/s_1\}} \tag{5.2}$$

Following the assumption that the whole system is occupied by either grass, savanna sapling, or trees, the three dimensional model (5.1) is constrained by $G+S+T = 1$. Therefore, the three dimensional system equation can be in fact reduced to

TABLE 5.1: Model parameters and their default values used in the analysis

Parameters	**Meaning**	**Default values**
μ	savanna mortality rate	0.2
υ	tree mortality rate	0.1
β	savanna birth rate	0.45
ω	savanna to tree recruitment rate (response to fire), a function of G	$\omega_0 = 0.9$, $\omega_1 = 0.2$, $\gamma = 0.5$, $\theta_1 = 0.4$, $s_1 = 0.01$

two dimensions. In this model, savanna saplings is more or less a transient state between grass and trees, because this model assumes that grass grows into savannas and then to trees given the right conditions [179, 181]. In order to simplify our analysis, the following analysis only focus on grass and trees, namely G and T, whilst savanna saplings S will be skipped, but still implied by G and T due to this constraint $G + S + T = 1$.

The meaning of all model parameters and their default values used in our analysis are summarized in Table 5.1. All default values were set according to the default values in Touboul et al. [181]'s analysis. The values of the parameters s_1 and υ that were used in the design of scenario analysis were also within the range used inTouboul et al. [181]'s analysis, and some other relevant studies [179, 183].

5.2.2 Scenarios for climate change and anthropogenic intervention

This model (5.1) has been rigorously analyzed from the mathematical point of view in previous studies [179, 181]. Therefore, I skipped the sensitivity analysis and only focused on specific parameters for designing scenarios. This made the analysis exclusively focusing on climate change and anthropogenic intervention as drivers for changing fire regimes, which is the main contribution of this chapter.

For the scenario analysis, I used parameter υ to control the level of anthropogenic intervention. Typically, υ refers to the natural mortality rate of the trees. For simplicity, I assumed that υ represents the total tree mortality rate from natural causes and through deforestation, and that for a particular system, the natural tree mortality rate will be relatively fixed. Hence, by varying υ values, we are in fact setting different levels of anthropogenic interventions for deforestation. I set $\upsilon = 0.1$ to represent low human intervention, because according to Schertzer et al. [179] the

TABLE 5.2: Parameter values and the represented scenario.

Parameters	Scenario
$\upsilon = 0.1$, $s_1 = 0.05$	low anthropogenic intervention, low climate change
$\upsilon = 0.1$, $s_1 = 0.01$	low anthropogenic intervention, high climate change
$\upsilon = 0.2$, $s_1 = 0.05$	high anthropogenic intervention, low climate change
$\upsilon = 0.2$, $s_1 = 0.01$	high anthropogenic intervention, high climate change

value is close to the natural tree mortality rate. As explained above, the increment of υ from 0.1 to 0.2 represents the loss of trees from deforestation, and therefore $\upsilon = 0.2$ was used for high anthropogenic intervention scenarios (Table 5.2).

The effect of climate change on vegetation through fire activities was represented by parameter s_1. The ω function (5.2) is a sigmoid function of G, represents the transitioning from a fire-resistant system where forests dominate to a grass dominant fire-prone one [179, 181]. The parameter s_1 controls the sharpness of this function, which is the response pattern of fire regime change driven by climate change. Lower values of s_1 represent steeper response, meaning the shifts of fire regimes can be significantly more abrupt (Appendix Figure C.1). This aligned with existing understanding that climate change accelerates changing fire regimes in many regions [24, 99]. Therefore, I set $s1 = 0.05$ for low climate change scenarios, and $s1 = 0.01$ for high climate change scenarios, because the response is comparably steep.

Combining the two parameters, υ and s_1, I obtained 4 scenarios in total (Table 5.2). The 4 scenarios covered different levels of anthropogenic interventions and climate change. The 4 scenarios were used to investigate the stable states of the system and the possible critical transitions from forests to grasslands.

5.2.3 Numerical analysis for stable states

Stable states in the context of ecological modelling is defined by where derivatives of all system states equal 0. In our system of equations, according to the definition the stable states can be obtained by solving the following equations:

$$\begin{aligned} \frac{dG}{dt} &= \mu S + \upsilon T - \beta G T \quad &= 0 \\ \frac{dT}{dt} &= \omega(G) S - \upsilon T \quad &= 0 \end{aligned} \tag{5.3}$$

which yields the analytical solution for the stable states as follows:

$$\begin{aligned} f(G) &= \frac{\mu(1-G)}{\mu - \upsilon + \beta G} - \frac{\omega(G)(1-G)}{\upsilon + \omega(G)} \\ &= 0 \end{aligned} \tag{5.4}$$

By finding the root of (5.4), we can obtain the percentage of space occupied by grass at stable states, and then the percentage of trees by plugging the value back to (5.3). Depending on the parameter values, the system can have one or multiple roots, indicating that the system can have one stable state or multiple stable states. The stable states can be either grass dominated or forest dominated depending which vegetation occupies more space. Our purpose is to investigate under different scenarios of climate change and human intervention, whether the stable state of the system is dominated by grass or forests, or whether the system is bistable.

I used Newton's method for our numerical analysis of stable states because it is an efficient and robust algorithm for root finding [81]. I used the widely applied implementation of this method in `SciPy` [184], a widely used Python package.

5.2.4 Simulating trajectories for shifting system status

This step is to simulate the process of a system undergoing a degradation process from tree dominated to grass dominated under the pressure of climate change and anthropogenic intervention. I set the starting point of the trajectories for simulation as the stable state of the system with low level of anthropogenic intervention and low level of climate change. The stable state of the system under this scenario is supposed to have the highest percentage of space occupied by trees among the four scenarios. With this starting point, setting the model parameters according to the rest of the other three scenarios means the system can experience certain degrees of degradation with decreasing percentage of space occupied by trees. Therefore, I set the initial state of the model according to the stable state of the scenario with low anthropogenic intervention and low climate change, and then set the model parameter to other scenarios. Subsequently, I ran the model according to (5.1) to obtain the trajectories of system degradation.

I used the Runge–Kutta method for model integration to simulate the trajectories of system degradation from tree dominated to grass dominated. The Runge-Kutta method is the most commonly used numerical method for integrating differential equations [81], which in our case is the forest-savanna-grass model. I implemented the Runge–Kutta method through Python package `SciPy` [184].

5.3 Results

5.3.1 Stable states under different scenarios

For the 4 scenarios described above, the system displays bistability where the system can be either dominated by grass or trees for certain values of υ if the level of climate change was high ($s_1 = 0.01$). If the level of climate change is high and the level of anthropogenic intervention is low ($\upsilon = 0.1$), the system is bistable; while if the level of anthropogenic intervention is high ($\upsilon = 0.2$), the system becomes grass dominated (Figure 5.1). For scenarios where the level of climate change is low ($s_1 = 0.05$), the system is nonlinear but does not display bistability. We can see that with a higher level of climate change, the system experiences an abrupt increase in percentage of space occupied by grass moving from low anthropogenic intervention to high anthropogenic intervention. Though not a discontinuous regime shift, the system still gradually moves from being grass dominated to tree dominated (Figure 5.1).

5.3.2 Trajectories for system degradation

Under high anthropogenic intervention ($\upsilon = 0.2$), the system undergoes a degradation process where the percentage of space occupied by trees decreased significantly while that of grass increased with either a higher level of climate change or low (Figure 5.2). However, with high level of climate change, the system converged to a status with lower percentage of space occupied by trees and higher percentage by grass; while with lower level of climate change, the degree of degradation, namely loss of tress, was less severe. Additionally, with higher level of climate change, the speed of system degradation was much faster, with the time needed for the

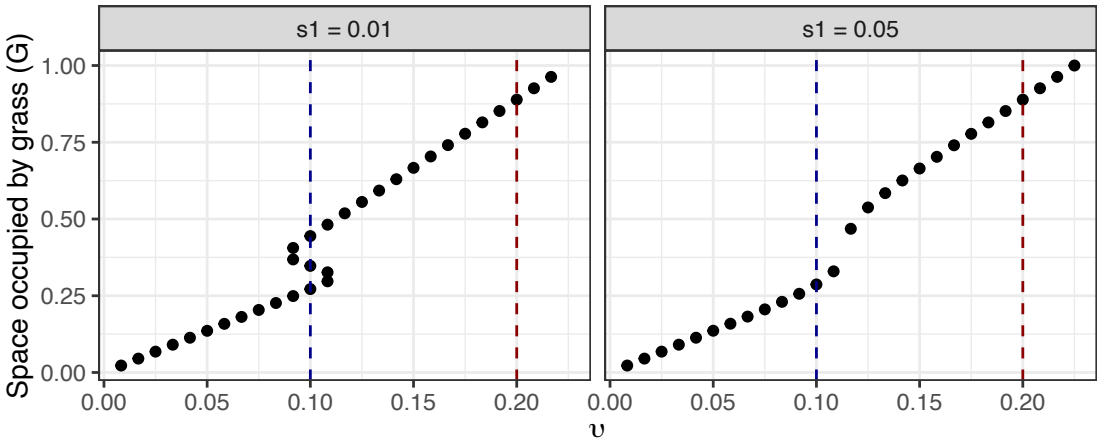

FIGURE 5.1: Stable states of the grass-forest system for the four scenarios. Dots indicate grass occupancy G for given υ values. Dashed lines indicate where $\upsilon = 0.1$ (blue) and $\upsilon = 0.2$ (red), representing low and high levels of anthropogenic interventions, respectively. The values of s_1 in the two subplots are 0.01 and 0.05, representing high and low levels of climate change.

system to converge to the degraded statues significantly shorter, as compared to the scenario with a lower level of climate change(Figure 5.2).

5.4 Discussion

In this chapter, I investigated the effect of anthropogenic intervention and climate change on forest ecosystems with a numerical analysis of a simple model describing the competition among grass, savannas, and trees. Anthropogenic intervention was represented by the parameter υ, which is the tree mortality rate, and was restricted to deforestation in our analysis. Climate change was represented by the parameter s_1, which reflects the response of the system to fires, because this response is also heavily controlled by climate. Our results showed that the status of the forest system, indicated by the percentage of space occupied by grass (G) or trees (T) is more controlled by anthropogenic intervention, while the level of climate change can affect whether the system display bistability and hysteresis. Therefore, for a tree dominated forest system, if the level of anthropogenic intervention is high, the system will degrade into a grass dominated one. Climate change played an important role in the process of degradation. With higher levels of climate change, the system will degrade to a status with less trees and more grass in a higher degradation rate.

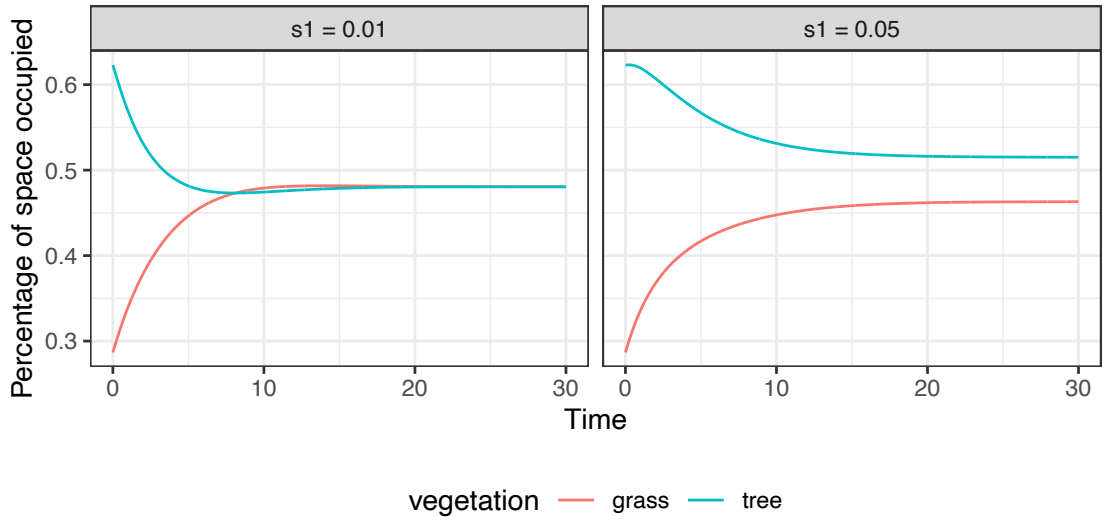

FIGURE 5.2: Trajectories of degradation from tree dominated to grass dominated. The blue and red lines represent percentage of space occupied by trees and grass. The starting point of the trajectories are tree dominated where the percentage of space occupied by trees are much higher than than grass in the system. Both plots are under high levels of anthropogenic intervention ($\upsilon = 0.2$), the plot on the left hand side is under higher level of climate change ($s_1 = 0.01$), and the right hand side lower ($s_1 = 0.05$).

Our analysis is quite simplified in a way that the effect of human intervention and climate change is entirely decoupled into two terms in the model, namely υ and s_1. This simplification has its validity as it aligns with our understanding of the mechanism of the two factors as drivers of forests degradation, 1) anthropogenic intervention through deforestation can accelerate the loss of trees [109, 171]; and 2) climate change in the form of drier and warmer climates can increase the likelihood of fires [99, 106]. Nevertheless, decoupling the two aspects neglects the fact that oftentimes the two terms have complex interactions, and cannot be treated as entirely independent. For instance, climate change can also affect the tree mortality rate which is the term υ [173], but I only used this term to represent the level of anthropogenic intervention in our design of scenarios. Similarly, I assume that the response of the system to fires is only affected by climate change, while anthropogenic intervention through deforestation and logging can also increase the sensitivity of the system to fires [98]. In addition, I only focused on the two parameters while all other parameters were set at fixed values at different levels of anthropogenic intervention and climate change. This may not be realistic as different levels of anthropogenic intervention and climate change could lead to changes

in other parameter values. For instance, higher levels of climate change could affect the growth rates of the vegetation [80, 93], which is the parameter β.

However, as the model used in this chapter is already quite a simplified one, taking into account of the complex interactions and effects of anthropogenic intervention and climate change in theory makes sense, but can not make the analysis more realistic due to the limitation of the simplicity of the model itself. The beauty of such minimal model is to capture the main mechanism and provide a plausible explanation to the phenomenon observed [44, 78, 82]. As such, I believe the analysis is sufficient to make the point that the both anthropogenic intervention and climate change can have significant impact on forest degradation and that the two have an synergetic effect, although it may only be applied to certain systems.

There are many factors that can drive the transitioning from forests to savannas besides climate change and anthropogenic intervention discussed in this chapter. One important factor that has been investigated widely is the role of large herbivores, which can drive the forests-savannas transitions through selective feeding [183, 185–187]. The mechanism in which herbivores shape this transition is very similar to fires, both followed type III response which can be described by a sigmoid function such as the ω function in (5.2) in many ecosystems [130, 146, 183, 188, 189]. We did not include this driver because the model used in this chapter is not designed to describe the changes in herbivore. If we wish to understand the role of fires and large herbivores in driving forests-savannas transition, a more complicated model capable of integrating spatial dynamics is required [130, 190].

This chapter is supposed to serve as a preliminary exploration to test the possibility of using this model to investigate the role of fire and anthropogenic intervention through deforestation in driving the forests degradation. The plan for this chapter is to find forest-savanna mosaic ecosystems, which there are actually quite many distributed around the globe [133], where the sequential observational data is available and can be used to parameterize this model. In this way, we can better understand the process of forests degradation under these pressures.

Chapter 6

Quantifying the risk of irreversible degradation for ecosystems: a probabilistic method based on Bayesian inference

Ecosystem degradation are usually abrupt and unexpected shifts in ecosystem states that are difficult to reverse. Some ecosystems may even subject to high risks of irreversible degradation (RID) as a result of undesirable resilience. In this paper, we proposed a probabilistic method to quantify RID by measuring the probability of recovering threshold being unattainable under real world scenarios. Bayesian inference was used for parameter estimation. Then the posteriors were used to calculate the thresholds and thereby the probability of it being unattainable, a.k.a RID. We applied this method to lake eutrophication as an example. Our case study supported our hypothesis that ecosystem could suffer from high RID, as shown by the lake with a RID of 72% at the whole lake level. Spatial heterogeneity of RID was significant, certain regions were more vulnerable while others had higher chances of recovery. This spatial heterogeneity could be an important factor to take into account for mitigation. We also found that both pulse disturbances and ecosystem-based solutions could provide positive opportunities for recoveries of such ecosystems. Pulse disturbances had most significant influence on regions with higher RID. While ecosystem-based solutions performed best for regions with moderate RID, reducing RID to almost 0.Our method provide a

practical way to identify sensitive regions for conservation as well opportunities for mitigation, applicable to a wide range of ecosystems.

Findings in this chapter highlighted the worst scenario of irreversible degradation, raising further requirements and challenges for sustainability. All nonlinear systems with alternative stable state are subject to this risk, and ecosystem management for such systems can benefit from closing examining this risk. Although the model used in this chapter is not designed to describe the fire-vegetation dynamics, the workflow described in this chapter can be easily converted and applied to relevant models such as the model explored in Chapter 5. If putting under that context, the RID measured from the model (5.1) represents the risk of irreversible degradation from dense forests to grasslands and savannas, which is also an important type of ecosystem degradation driven by many factors such as climate change and deforestation. This of course requires data from suitable ecosystems that can be used for parameter estimation. And this was left as one of my future work.

6.1 Introduction

Degradation of ecosystems are usually unexpected and abrupt shifts in ecosystem state [47, 146, 191]. The degraded state will be stabilized by its internal reinforcing feedback and therefore resistant to mitigation [5, 192]. In worse scenarios, degradation becomes irreversible if the internal reinforcing feedback are too strong to break [193]. While most existing studies focused on the amount of disturbance that will cause the shift of an ecosystem to an undesirable regime and the threshold associated with degradation [45, 194–196], the uncertainty and risk of recovery threshold being unattainable have been less characterized in detail. Nevertheless, this risk should be an extremely important concern as it decides whether the degradation will be reversible or not[47, 193]. Under the context of global ecosystem degradation [197, 198], this risk will have a profound influence.

In theory, when ecosystems lose key species or functional groups, they lose the ability for reorganization and transition into a desirable regime, and are subjected to the risk of irreversible degradation [146, 199]. Our efforts in restoration of particular ecosystems can be extremely difficult [41, 85, 197]. Previous studies argued that the internal reinforcing feedback and complex cross-scale interactions

are responsible for difficult reversals [41, 197, 198, 200]. We hypothesized that the intrinsic risk of irreversible degradation could be another important reason that makes reversal of ecosystem degradation even more difficult.

To verify our hypothesis, we proposed a probabilistic indicator, risk of irreversible degradation (RID), to quantify the risk of an ecosystem degradation being irreversible. It is defined by the probability of threshold for recovery (T_2) being unattainable under real world scenarios. The risk of irreversible degradation could be considered as an extreme case of undesirable resilience where the ecosystems are highly stable under the degraded regime and resistant to external changes [5, 201, 202]. Traditional resilience indicators, following the original definition of resilience, are usually representations of how much changes the system could withstand before flipping into another regime [5, 180, 194, 203, 204]. These indicators are less applicable to systems subject to high risks of irreversible shift, as it makes little sense to quantify resilience based on an unrealistic threshold that could never be achieved.

While we also found some probabilistic representations for resilience and regime shift, these did not emphasize the extreme case of irreversible degradation. Moreover, their viability and dynamics are mostly associated with external environments rather than the ecosystem itself [178, 188, 205, 206]. In other words, the risk mostly arise from the external environmental changes rather than the internal dynamics of ecosystem itself. We adopted Bayesian inference that allowed dynamic perspectives regarding parameterization [90]. Different from the frequentist approach where parameter values are treated as a fixed value, Bayesian inference treat parameters as random variables that vary with certain probabilities [90, 123]. Therefore, the uncertainty arise from the parameters that are representations of internal processes and properties of the ecosystem [123, 207, 208]. Following this, the risk measured in Bayesian approaches also arise from parameters, suggesting the risks are associated with the intrinsic properties of the ecosystem as well. Distribution of threshold could be derived from parameter posteriors since the threshold can be calculated by certain function of parameters. Thereafter, the risk of irreversible degradation could be easily obtained according to its definition. Another advantage of Bayesian method is that we could make full use of the knowledge we build about the system [90]. When given new data, the previous posterior could then be used as a prior that will be updated according to the new information. This progressive process

suits the purpose of adaptive management and could therefore be a promising tool in management practice [209, 210].

We applied our method to the eutrophication of freshwater ecosystems driven by increasing phosphorous (P) inputs. Accumulating empirical evidence supported that internal sediment release alone contribute much more than external inputs [207, 211]. This suggest the possibility of irreversible eutrophication, and therefore suits our study purpose here. We first tried to quantify the undesirable resilience as the risk of irreversible degradation; and then investigated the influence of several aspects that might provide opportunity for mitigation. We included the following aspects: i) spatial heterogeneity; ii) interactive effects of pulse disturbances and l_P reduction as long-term press; and iii) changes in internal ecosystem attributes resulted from ecosystem recovery, as reflected by the overall changes in parameter values.

By investigating on these aspects, we could be able to identify possible way of reducing RID and opportunities for more efficient mitigation. Spatial heterogeneity and connectivity between different parts of the ecosystems are considered to be an important source of ecosystem resilience [201, 212]. As a result of spatial heterogeneity, RID could vary between different parts as well. This suggests that certain parts could be more susceptible to irreversible degradation, while other parts could be more amenable [213]. Identification of the more vulnerable part could serve for conservation priority before degradation and leveraging mitigation effects after degradation [85, 146, 214]. Minimal models, although widely applied in regime shift studies, are often flawed by their homogeneity assumption. This is because the main motivation for minimal models is to capture the nonlinear dynamics and dominating mechanisms that give rise to regime shifts [44, 177]. This can be overcame by adding interaction terms to the original model functions, so that it could be used to reflect spatial dynamics [188, 215, 216]. Therefore, we first modified the original model by adding exchange terms and then explored spatial heterogeneity in undesirable resilience for each part of the system.

The irreversible degradation we defined here was with respect to long-term external drivers, also known as press [188, 217]. However, regime shift could also be realized by pulse disturbances, strong and short-term disturbance that could lead to huge fluctuations in system state [5, 188]. Given strong enough disturbance that the brings the system state across the boundary of alternative stable state (the unstable

equilibrium), the system can then gradually converge to the desirable state [5, 188]. Therefore, it is important to take into consideration this trigger in order to better characterize the risk of irreversible degradation [191, 218]. To reflect this interactive effect of pulse and press, we applied both long term l_P reduction as press and random noises as pulse in our simulation. Backward shift from degraded regime to the desirable regime was then compared with the stationary RID calculated by thresholds.

Increasing research argued that ecosystem-based management and nature-based solutions could be better ways for conservation and protection [219–221]. We testified the usefulness of ecosystem recovery on ecosystems with high RID. By investigating the effects of changing parameter values on RID, we could get insights on the performance of ecosystem recovery. Moreover, by doing this, we could identify the ecosystem attributes that are most efficient in lowering RID.

6.2 Methodology

The indicator was defined by probability of T_2 being unrealistic. Since we often do not know the real distribution of T_2, we can therefore calculate its frequency based on large random sampling as an approximation. The calculation of RID can then be expressed as (6.1)

$$RID = \mathbf{P}(T_2 < T_2^c) = \frac{n(T_2 < T_2^c)}{n(T_2)} \tag{6.1}$$

where T_2^c represented the critical threshold for environmental pressure, under which will be unattainable in real world scenarios; $\mathbf{P}(T_2 < T_2^c)$ represented the probability for T_2 below T_2^c; $n(T_2 < T_2^c)$ and $n(T_2)$ represented number of samples $T_2 < T_2^c$ and the total sample size, respectively. We directly used the probability of $T_2 < T_2^c$ as an indicator of risk so that the expression looks more compact. This itself implied the unstated loss function should be $L = \mathbb{1}_{\{T_2 < T_2^c\}}(T_2)$, mapping all $T_2 < T_2^c$ to 1 and the rest to 0. It is one of the typical loss functions. Our rationale for using this binary loss function was that we only care about whether the degradation will be irreversible or not. The risk function, as the expectation of the loss function defined above, become the probability written as (6.1). For our case of lake eutrophication

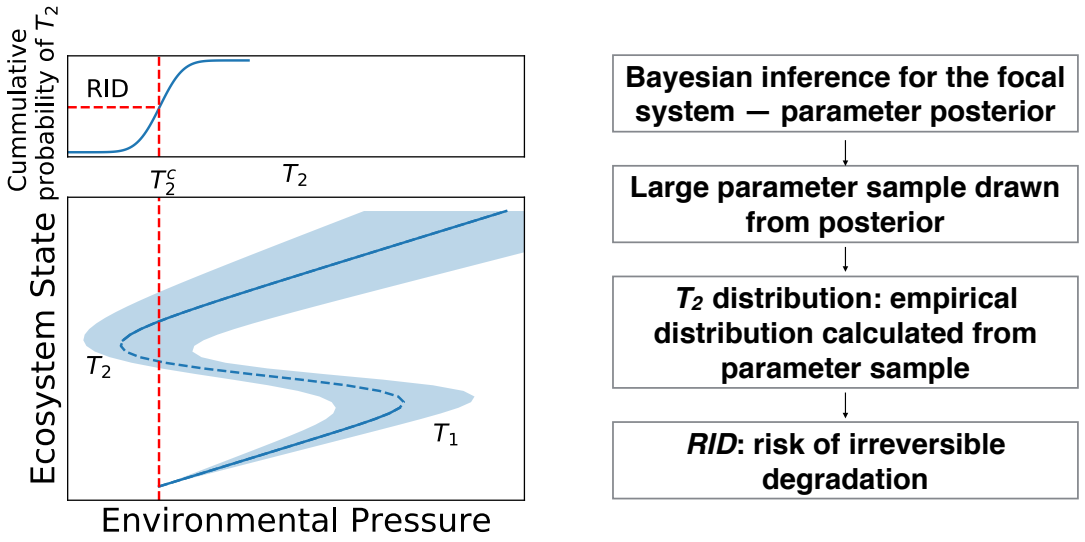

FIGURE 6.1: Procedures for calculating risk of irreversible degradation. We used higher values of ecosystem state to represent the degraded state. This is to be consistent with the model where high values of P represents more eutrophic state. Therefore, T_1 is the threshold for degradation, and threshold T_2 is the threshold for recovery.

driven by increasing P load (l_P), $T_2^c = 0$ because it is unrealistic to reduce l_P to below 0.

To calculate RID, there are mainly two steps: i) Bayesian inference for parameter distributions; and ii) calculation of threshold based on parameter sample drawn from posteriors of Bayesian inference. We also did some dynamic simulations to investigate how factors, including spatial heterogeneity, pulse disturbances and ecosystem recovery, influenced RID (Figure 6.1). In the following part, we elaborated on each step of our method.

6.2.1 Model Description

We selected the classic P driven eutrophication model for our case since it was a good representation of the ecosystem and illustrated our method well. The model for the whole lake followed (6.2) [193].

$$\frac{dP}{dt} = l_P - sP + r\frac{P^q}{P^q + m^q} \tag{6.2}$$

where P represented the state variable, water P concentration; l_P represented the external P load, r represented the potential sediment release; m was the half-saturation coefficient where the actual P release reached half of its potential and q was the shape parameter that controls the steepness of response between actual sediment P release and P.

For estimation of each subunit within the lake, we added an exchanging term between each unit, and obtained (6.3):

$$\frac{dP_i}{dt} = l_{Pi} - s_i P_i - \sum_{j=1}^{n} e_{ij} P_i + \sum_{j=1}^{n} \frac{w_j}{w_i} e_{ji} P_j + r_i \frac{P_i^{q_i}}{P_i^{q_i} + m_i^{q_i}} \tag{6.3}$$

$$\frac{dP}{dt} = \sum_{i=1}^{n} w_i \frac{dP_i}{dt} = l_P - \sum_{i=1}^{n} w_i s_i P_i - \sum_{i=1}^{n} w_i r_i \frac{P_i^{q_i}}{P_i^{q_i} + m_i^{q_i}} \tag{6.4}$$

where all the subscripts i denoted the respective parameters for the ith subunit; e_{ij} represented the outflow rate from subunit i to its neighbouring subunit j; and e_{ji} the outflow rate from subunit j to i; w_i represented the weight assign to each subunit according to their water volume (water volume of subunit i over the total water volume of the lake). The second equation acted as a regularization term to ensure mass balance such that the sum of all subunits will not deviate too much from the whole lake level.

6.2.2 Solving differential equations for threshold

Following our rationale on irreversible degradation, in order to quantify RID, we need to calculate the threshold for recovery (T_2). T_2 is the minimal l_P value for degraded regime. As regimes are defined by a fixed point, they could be obtained by setting (6.2) to 0:

$$\begin{aligned} l_P^* - sP^* + \frac{rP^{*q}}{P^{*q} + m^q} &= 0 \\ l_P^* = sP^* - \frac{rP^{*q}}{P^{*q} + m^q} & \end{aligned} \tag{6.5}$$

where l_P^* and P^* denote l_P and P at equilibrium. Thresholds, as local maximum or minimum, could be found by taking derivative with respect to P^*:

$$\frac{dl_P^*}{dP^*} = s - \frac{d}{dP^*}(\frac{rP^{*q}}{P^{*q} + m^q}) = 0 \tag{6.6}$$

By solving (6.6), we obtained P^* at the threshold, and then l_P^* threshold could be obtained by plugging in P^* to (6.5). Note that for illustration purpose, we usually plot P^* against l_P^*, indicating l_P is the control variable and P the response variable. But to be written as a function, we can only write l_P^* as a function of P^* since each l_P^* could map to more than one P^* when an alternative stable state comes into existence.

Similarly, the threshold for each subunit could be found by solving (6.7):

$$\frac{dl_{Pi}^*}{dP_i^*} = (-s_i - \sum_{j=1}^{n} e_{ij} + \frac{w_j}{w_i}\sum_{j=1}^{n} e_{ji}) + \frac{d}{dP_i^*}(\frac{r_i P_i^{*q_i}}{P_i^{*q_i} + m_i^{q_i}}) = 0 \tag{6.7}$$

6.2.3 Parameter inference and risk of irreversible degradation

The parameter posterior is calculated according to Bayes' theorem (6.8).

$$p(\theta|X) = \frac{p(X|\theta)p(\theta)}{p(X)} \tag{6.8}$$

where X and θ represented data and parameters, respectively. $p(\theta|X)$ denoted the posterior, the probability distribution of θ given X; $p(X|\theta)$ denoted likelihood function, the probability of X given parameter θ; $p(\theta)$ denoted the prior assigned to θ before the inference. $p(X)$ denoted the marginalized probability of X which will be a constant.

For our process-based model that involves multiple parameters and noisy observation data, the inference was conducted according to (6.9) [43, 222]:

$$p(\theta|\mathbf{y},\mathbf{x},\sigma,\alpha) \propto p(\mathbf{y}|\mathbf{x},\theta,\sigma)p(\theta|\alpha) \tag{6.9}$$
$$p(\mathbf{y}|\mathbf{x},\theta,\sigma) = \prod_{n=1}^{N} \mathcal{N}(\mathbf{y}|f(\mathbf{x},\theta),\sigma)$$

where $\mathbf{y}$ represented the observation and $\mathbf{x}$ the input; then $p(\mathbf{y}|\mathbf{x},\theta,\sigma)$ was the likelihood function measuring the likelihood of observations under the given input, model parameters and another parameter σ. It followed a normal distribution with mean $f(\mathbf{x},\theta)$ and variance σ^2. The rationale for doing this was that the observations always involve with noise that can not be explained by the variables included in the model, which in our case means P can not be perfectly modelled by the parameters l_P, s, r, m, and q. Typically, this kind of noise follows a normal distribution [218]. The function $f(\mathbf{x},\theta)$ here should be consistent with (6.2) or (6.3) according to the object of the inference. And the $p(\theta|\alpha)$ is the prior set with parameters α, which in our case would be the upper and lower bounds of the uniform distributions.

Since we can not obtain a closed form solution for parameter distributions, we used Markov Chain Monte-Carlo simulation to get an approximation instead [223]. Therefore, we need to set up the prior and the Markov Chain for the inference. For the priors, considering that great variation exist among different lakes, and no specific information on the mean and variance of parameters for our lake was available, we adopted uniform distributions as priors. The upper and lower bounds for our uniform priors were given such that they covered the range of that found in the literature [193, 218]. The posterior was simulated with the Differential Evolution Markov Chain Monte-Carlo algorithm (DEMCzs), a differential evolution MCMC method [222]. Convergence was checked through Gelman-Rubin diagnostic [224]. We computed two chains with the DEMCzs, each with 500000 iterations, and our model converged on all parameters (Gelman-Rubin's test of convergence below 1.05 for all parameters).

Parameter sample was drawn from the posterior. The first half of the chains were discarded to make sure we only sampled after convergence. The size of our parameter sample was 5000. After we obtained the parameter sample, we calculated the values of T_2 under each parameter combination. This gave us a set of T_2 with size 5000, equal to the the size of parameter sample. For a particular combination of parameter values in the sample, in which each parameter has a specific value, we

can calculate whether the system is irreversible or not depending on the value of T_2 calculated from (6.1), $T_2 < 0$ means irreversible. Bases on all results calculated for the whole parameter sample (5000 combinations in total), we can calculate RID, which is the probability of the system being irreversible among all sample. High RID values indicate the system is difficult to reverse.

The data we used for model parameter estimation included 1) monthly observation of phosphorous concentration (P) from 4 monitoring site relatively evenly distributed on Erhai (please refer to Figure D.1 for the location of the lake and the monitoring sites) over the time period of 2009 - 2011 (36 data points in total); 2) total external load of phosphorous input to the lake (l_p) based on previous monitoring data, this is also aggregated to the monthly level to match the P data. At the whole lake level, P were averaged over the whole lake. All parameters, namely s, r, q, and m, were estimated through Bayesian estimation. The fitness of the parameterized model to the observations can be found in Figure D.2. For model of all subunits, another parameter $e_{i,j}$ were estimated for each subunit respectively based on the data observed for each subunit. Their respective fitness of the parameterized model can be found in Figure D.3.

6.2.4 Simulation under dynamic scenarios

Calculation of RID was a reflection of the intrinsic characteristic of the lake, indicating the possibility of transition back to the desirable regime after degradation. While this theoretical result could be influenced by processes and changes at different scales. To make our results a better reflection of the real world as well as identifying possible mitigation opportunities, we conducted simulations under several dynamic scenarios in addition to the calculation of threshold.

Interactive effect of pulse and press on *RID*

To simulate the interactive effect of pulse and press on regime shift, in addition to load reduction as a typical long-term press, we added a white-noise term to represent pulses. The model function could be written as (6.10):

$$\frac{dP}{dt} = l_P - sP + r\frac{P^q}{P^q + m^q} + \sigma dW \sigma dW \tag{6.10}$$

where $\sigma dW \sigma dW$ denoted the white-noise. σ reflected strength of random disturbances. The noise was assumed to obey a normal distribution because distributions of noise are well-described by normal distributions in a wide array of contexts [188, 218].

Since a random noise was added into the equation, we can not get the equilibrium by directly solving the equations. Instead, the stable states were obtained by running the model for long iterations until the final state became steady. The initial P was set to higher than that at T_2 ($1.2 \times P_{T_2}$) to ensure the system started from a degraded regime. Reduction rate was set proportional to T_1 (from 100% to 0), the threshold for degradation. This can not guarantee a recovery but lower than T_1 could make the system become bistable and therefore shift from a eutrophic regime to a clear regime. After long iterations, if P at stable states were lower than that of T_2, we consider the system to be recovered. Calculation under the same parameter sample could give the probability of recovery under the dynamic scenarios accordingly. By comparing this result with previous RID, we can have further insights on the recovery process for systems with high undesirable resilience.

RID under ecosystem recovery

In addition to reducing external environmental pressure, the ecosystem status can be possibly reversed by ecosystem recovery measures that target at the internal components of the ecosystem itself. These internal components can be represented by the model parameters and are often referred to as "slow variables", changes in which can also lead to regime shifts [4, 5, 85]. For example, the parameter r in the model ((6.2)) indicates the maximal sediment release rate, an internal component of the system, and lowering this rate (smaller values of r) can also trigger the regime shift from eutrophic state to clear state [218, 225]. We tried to reveal the effect of ecosystem recovery on RID. Ecosystem-based recoveries will lead to changes in ecosystem attributes. We represented this by overall changes in parameter values. We retained the shape of parameter distributions but increase or decrease their sample values by proportion. RID was calculated for changes in different parameter values. Each time one of the parameters was set proportional to its original values in the sample while other parameters remained unchanged. By comparing RID under all these variations, we could conclude the usefulness of ecosystem recovery for systems subject to high undesirable resilience, as well as

the performance of revising different attributes of the systems in different spatial units.

In this paper, all simulations were carried out in R software [226]. Bayesian inference was implemented by package BayesianTools [222]. Data for parameter inference and related simulations (including lake morphology, water quality and P load) was based on Lake Erhai, one of the largest lakes in southeast China. Details of this lake could be found in Appendix (Figure D.1).

6.3 Results

6.3.1 *RID* at different spatial scales

The probability distribution of T_2 for the whole lake resembled a normal distribution with some skewness (upper plot in Figure 6.2). The value of T_2 ranged from -0.10 to 0.05 $mgP \cdot m^{-3} \cdot month^{-1}$, and the probability of $T_2 < 0$ should be high. This could be better illustrated by the cumulative probability for T_2 (lower plot in Figure 6.2). RID, according to our definition, was the cumulative probability at $T_2 = 0$. At the whole lake level, RID was 71.6%. This result supported that Lake Erhai suffered from high risk of irreversible degradation. Therefore, it is a proper example for our study object in this paper.

Calculation for each subunit showed differentiated RID among the 4 subunits. RID for subunits 1 and 4 were substantially lower than the other two subunits (Figure 6.2). Subunit 1 had the lowest RID of 16.9%. Subunit 4 had relatively low risk as well, with a RID of 40.9%. While RID for subunits 2 and 3 were significantly higher, 86.8% and 95.3% respectively (Table 6.1). This result supported our hypothesis on spatial heterogeneity of RID. Subunits 1 and 4 had RID lower than that of the whole lake, while subunits 2 and 3 had RID higher than that of the whole lake (Figure 6.2). This indicated higher chances of recovery for subunits 1 and 4; while subunits 2 and 3 will be more resistant to mitigation.

The reason for differentiated spatial RID, for our case here, could be attributed to the hydrology conditions. It could be seen from the parameter posteriors for inflow/outflow (s) and exchange rate (e). The inflow and outflow rate for subunits 1 and 4 were much higher than that of subunits 2 and 3. Better hydrodynamic

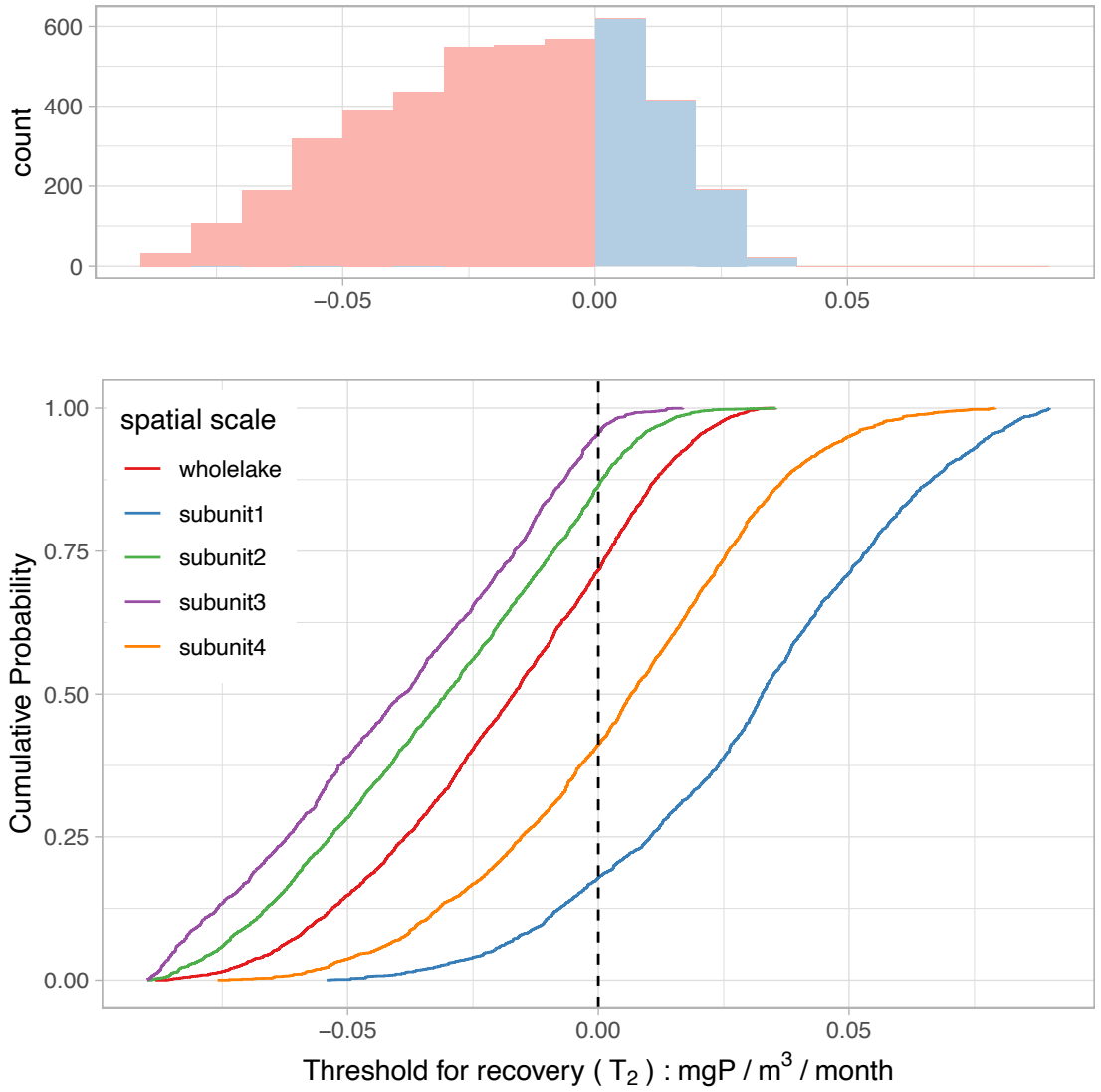

FIGURE 6.2: Risk of irreversible degradation measured at different spatial scales. The x axis represented T_2, the threshold for recovery. The upper panel showed the histogram of T_2 at the whole lake level; the lower panel showed the cumulative probability of T_2 for both whole lake level and different subunits. Cumulative probabilities at $T_2 = 0$ equal the RID as T_2^c for our case here equals 0.

conditions for subunits 1 and 4 lead to lower RID and less undesirable resilience. Another possible reason, although not directly reflected in our data, could be the relatively larger shore area (Appendix Figure D.4). Since shore area could play an important role in the reduction of nutrients and recovery of eutrophication, it is possible that subunits 1 and 4 could have better chance of recovery due to higher portion of shore area.

TABLE 6.1: Risk of irreversible degradation at the whole lake level and for each subunit.

Whole lake	Subunit 1	Subunit 2	Subunit 3	Subunit 4
0.716	0.173	0.864	0.957	0.411

6.3.2 *RID* under interactive effect of pulse and press disturbances

For all subunits, as reduction rate increase, the recovery rate increased as well (Figure 6.3). Subunit 1, with RID much lower than other subunits, displayed a distinct response pattern. It responded relatively proportional to load reduction in an approximately linear way. Other subunits were much less responsive at low reduction rates, and only became more responsive at high reduction rates.

Adding of pulse disturbances (σ values higher than 0) imposed a positive influence on recovery rate. For all subunits under all reduction rates, pulse disturbances led to higher recovery rates. This positive influence tend to be more significant for subunits with higher RID, as recovery rate of subunits 2, 3 and 4 differentiated more significantly under different σ values. This could be that subunits with low RID were already mostly reversible even without external disturbances. While for subunits with high RID, they were more reliant on external disturbances to provide the opportunities to trigger the backward regime shift. Without external disturbances to drive their state beyond the boundary for alternative state, these subunits will have a much lower chance for recovery.

This also explained why this positive influence became more significant with more intense disturbances (increasing σ). The disturbance intensity required to trigger the shift were decided by the difference between current system state and the boundary for alternative stable state. The higher σ values, the higher probability of disturbance intensity live up to this requirement, and therefore higher chances for recovery.

We might have noticed that certain discrepancy existed between the recovery rate and that indicated by RID. By definition, the recovery rates of reduction rate equals to 1 and σ equals to 0 were supposed to be $1 - RID$, but they were somewhat different (Appendix Figure D.4). This was caused by different final P for all subunits. To calculate RID, we assumed that all subunits will have the same P

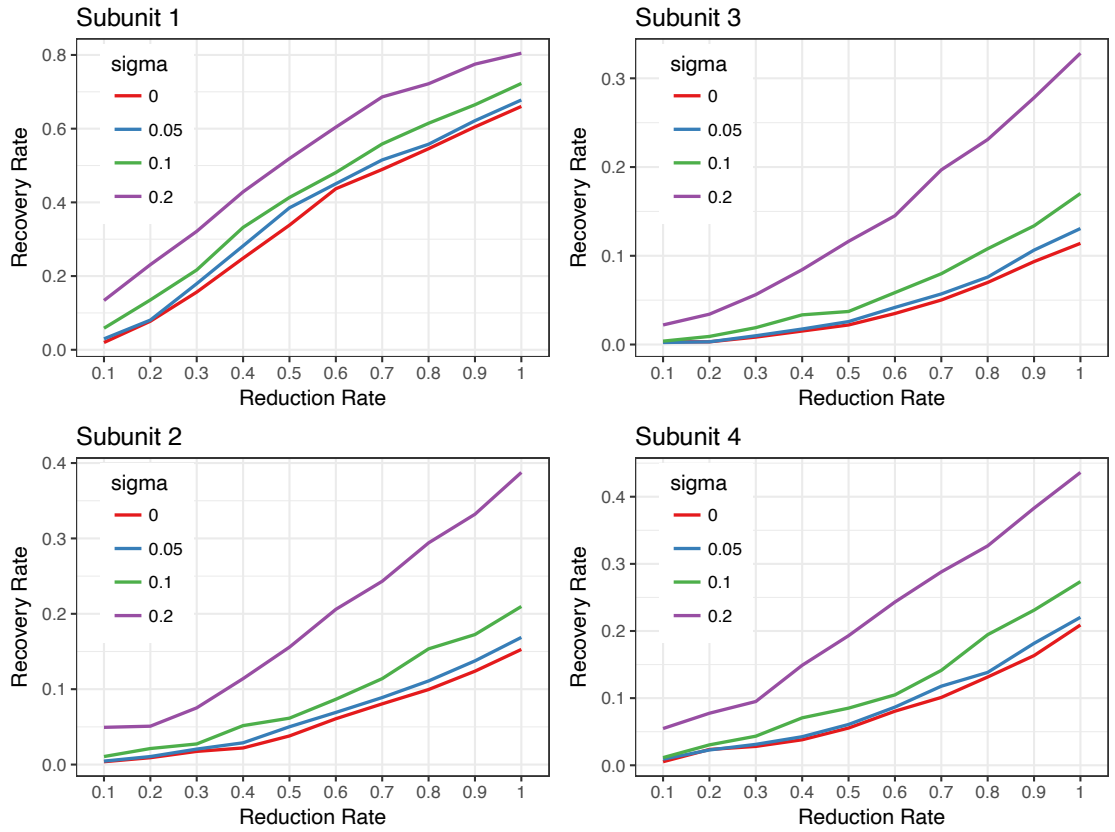

FIGURE 6.3: Recovery rate for each subunits under different load reduction rate and intensity of external disturbance. Recovery rate is defined by the probability of the lake recovered to the clear state (stable state of P lower than that at T_2) from the eutrophic state with the parameter samples drawn from their posteriors. Reduction rate indicates the percentage of l_p reduced compared to the previous l_p that sustained the eutrophic state, which was set at T_1 for the starting point of the simulated trajectories. Higher reduction rate means lower l_p for the trajectory simulation, and recovery rate of 1 means $l_p = 0$. The parameter σ values represented intensities of internal disturbance, higher σ values represent more intense internal disturbances.

under equilibrium. But this is not entirely true considering all the process happening at different rates in subunits. Still, subunits with higher RID will have lower recovery rate; while subunits with lower RID will be more likely to recover. This consistency suggested that RID was nevertheless a good representation of recovery probability even under dynamic simulation.

6.3.3 Influence of ecosystem restoration

Varying parameter values could influence RID, but the effect of different parameters differed in different subunits (Figure 6.4). For all subunits, m and r were the most influential parameters for RID. Decrease in r and increase in m could lower RID. This influence was consistent and most obvious in all subunits. Both r and m were relevant to sediment release, r being the potential for sediment release and m being the half saturation coefficient. Decrease in r and increase in m indicates less sediment release rate under the same P. This means high sediment release could be the main reason for irreversible degradation, and decrease in sediment release could make the degraded regime less resilient.

Parameter s, loss rate through outflow and sedimentation, could lower RID with increasing parameter values (Figure 6.4). This result suggested higher loss rate through outflow and sedimentation could make the system less resilient in degraded regime. It had much more influence on subunits 2, 3 and 4, while less influential in subunit 1. This was caused by the relatively high loss rate in subunit 1. Therefore, s cast stronger limits on reversal of subunits 2, 3 and 4.

Effects of parameter e, the exchange rate, on the 4 subunits were contradictory. Increase of e could lead to lower RID in subunit 1, but higher RID in subunits 2 and 3. For subunit 4, e did not seem to make an obvious difference (Figure 6.4). This was due to the difference in net contribution of exchange. For subunit 1, exchange between neighboring subunits acted as a net sink; while for subunits 2 and 3 it was a net source. Therefore, increase of e could decrease RID in subunit 1 while increase RID in subunits 2 and 3.

For all subunits, q displayed little influence on RID (Figure 6.4). Parameter q was the shape parameter that represented the nonlinear response of sediment release to P. This result suggested that all subunits are highly nonlinear and changes of q in this range (-50% to +50%) were not enough to induce a significant influence on the reversibility of system degradation.

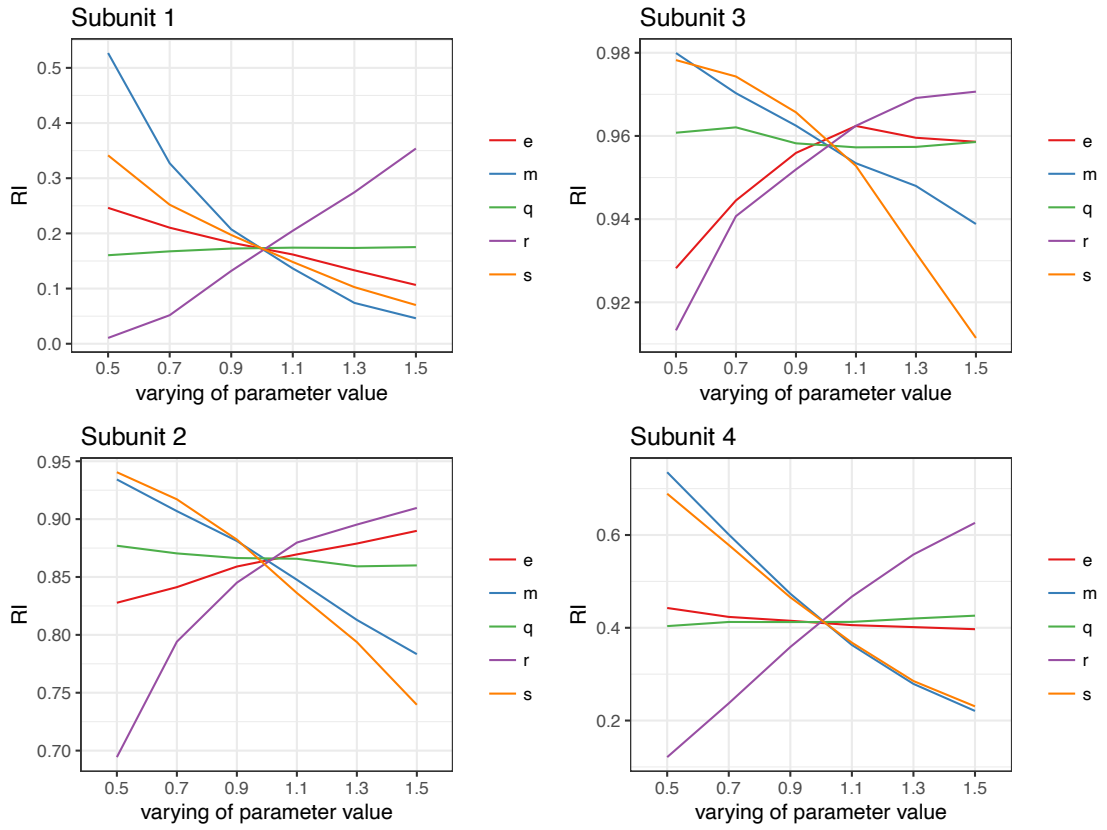

FIGURE 6.4: Variation in risk of irreversible degradation (RID) when parameter values varied under ecosystem recovery. Varying in parameter values were set proportional to the original parameter sample drawn from their posterior. All parameter values ranged from 50% to 150% of its original values. RID were calculated under the varying of each parameters when other parameters remained unchanged.

6.4 Discussion

Our results showed that ecosystem recovery could be a more efficient way for mitigation of systems with high RID. As reflected in our model results, varying in model parameter values changed the undesirable resilience significantly (Figure 6.4). Ecosystem recovery led to improvements in ecosystem attributes, and therefore T_2 gradually tends towards the positive side. Some of the conclusions we reach at can be inferred from the model itself by pure math, the contribution of this chapter is to give a quantitative representation the risk and other relevant measures derived from it. For example, mathematically speaking, we can infer the existence of irreversible degradation, our results confirmed this with a real world case study by combining the model and observational data with Bayesian inference and simulations. In additions, the effect of changing parameter values on RID

can also be inferred from the model qualitatively, while we demonstrated it with specific numbers with the simulations.

We can have better intuitions on irreversible degradation when relating to the fundamental theory of catastrophe bifurcation, which is the theoretical basis for regime shift [47, 180]. Catastrophe bifurcation was originally widely observed in the field of physics and engineering. It describes the situation where the system first changes smoothly with external drivers until the threshold where it jumps discontinuously to another state; while the recovery does not follow the same trajectories but the driver needs to be reverted far back from the previous threshold [81]. This phenomenon is known as hysteresis, and later is widely observed in ecological and social systems [47, 191, 227]. In physics and engineering, it is quite common that the critical transition in a catastrophe bifurcation will be irreversible. For example, the collapse of a bridge after the pressure exceeds the threshold. [81]. There is no other way to bring back the bridge other than building a new bridge. For ecosystems, the rebuilding process might be obscured by their complexity and on-going dynamics of the system itself. But still we should realize the essence of a regime shift lies in the change of ecosystem structure and function [146, 212]. Therefore, after the collapse of the ecosystem, rebuilding the system seem to be the most straightforward way. Especially when confronted with high risks of irreversible degradation. Because reducing environmental pressures might never achieve this goal.

In addition, ecosystem recovery is a good way to build resilience into the system so that it will be less vulnerable to changes. Although our result only revealed the positive effect of disturbances, because our system are subject to high RID. We should be aware that the effect of disturbances could act both ways. It could bring the system from a desirable regime to a degraded regime, as well the other way around. For systems with high RID, the degraded state could be a much stronger attractor [202, 218]. This makes the system liable to secondary degradation. Ecosystem recovery could be a way to prevent secondary degradation, since it could skew the dominant attractor from the undesirable regime to the desirable regime, making the desirable regime more resilient [178, 191].

Nevertheless, reducing external environmental pressure is still important in a way that it is the preliminary requirement for the existence of a desirable regime [85, 191]. Also without reduction of external environmental pressure, the system will

be held in a vulnerable position [5]. Just like after rebuilding of the bridge, we still need to carefully maintain the pressure within the threshold.

Moreover, quantifying the risk of irreversible degradation could have a profound influence on perceptions of ecosystem degradation and ecosystem management. Much emphasis has been put on avoiding and reversal of ecosystem degradation for sustainable development [228]. To achieve this, threshold for degradation and the associated uncertainty has been widely studied as it determined the boundary for sustainable development [1, 47]. Safe operating space was proposed as a practical guide to this problem. It requires anthropogenic intervention to be maintained under the threshold for degradation, avoiding the existence of alternative stable states [1, 198]. In this way, the risk of degradation was controlled at the highest level. For systems with high RID, the safe operating space might not be allowed since it is rare for the system to have only one desirable regime without an alternative stable state (Figure 6.1). This raised further challenges for safe operating space and imposed higher requirement for sustainable development.

At the same time, the spatial aspect of our method could be especially meaningful. Spatial heterogeneity associated with responses and risks is an important factor for conservation. Identification of this spatial pattern could provide information on conservation priority and mitigation opportunities for leveraging effects [229, 230]. We testified the spatial heterogeneity of RID in a freshwater ecosystem. This spatial heterogeneity could be even more evident in other ecosystems. Aquatic ecosystems are more free-flowing compared to other ecosystems where all inorganic material move and exchange at a lower rate such as terrestrial ecosystems. As a result, spatial heterogeneity due to different morphology and geophysical conditions such as temperature and nutrient content intrinsic to each subunit are more significant due to the slow internal exchange process. This gives a good reason for wider application of our method on other type of ecosystems.

Now that we have seen an successful application of our proposed method, we would like to further argue its generalization to other models and even other ecosystems. For instance, the model we used to display the workflow of estimating the risk of irreversible degradation is a rather simplified one. In practice, some more complicated process-based model are often desired, such as PCLake. In order to apply these models, parameter estimation is also required [202, 205, 213]. If we can use this framework to estimate some of the key parameters, then it will also be possible

to estimate RID with PCLake and other models alike. In addition, the framework we proposed to estimate RID is not limited to freshwater ecosystems. While we demonstrated our method with a freshwater ecosystem, the method was not tailored to this specific ecosystem but more of a general framework applicable to a wide range of ecosystems. Increasing model studies on all kinds of ecosystems and application of Bayesian inference for model parameterization ensured the basis for wider application of our method [207, 231].

Promising as our method is, the main challenge remains with the uncertainty. In a sense, RID quantified a certain fraction of the uncertainty associated with T_2, the probability of it falling below 0. Since RID itself is derived from uncertainty, it will be complicated if we wish to further analyze its uncertainty. Nevertheless, with such significant results, both for RID at the whole lake level and spatial differentiated RID (Figure 6.2), it should be convincing enough to draw our attention to this risk of irreversible degradation.

6.5 Conclusions

We proposed a novel indicator RID that measured the risk of an ecosystem degradation being irreversible, in terms of the uncertainty associated with T_2. By adopting Bayesian inference, the whole framework for implementing this indicator was straightforward and flexible, convenient for management practice.

By applying RID to the example of lake eutrophication of Lake Erhai, we testified that the ecosystem could suffer from high RID, as shown by the RID of 72% at the whole lake level in our case. This finding suggested that we should be more aware of ecosystem degradation, because the consequences could be more severe, and therefore raise further challenges for sustainability.

On the other hand, by applying RID, we also identified the following opportunities for mitigation.

- We found spatial heterogeneity could provide opportunity windows as certain regions could have higher chances of recovery. We also need to pay more attention to regions that are more susceptible to irreversible degradation.

- External pulse disturbances could have an overall positive influence on ecosystem recovery for ecosystems with high RID. Because it could drive the ecosystem beyond the boundary for alternative stable states and therefore trigger the shift towards a desirable regime without further reducing environmental pressures.

- We showed that ecosystem recovery from ecosystem-based management could be more efficient for such systems. Changes in certain ecosystem attributes could lower RID significantly.

From the findings of our study, we concluded that RID could be a meaningful and useful indicator. In addition to the model used as an example in this chapter, it has high potential for future application to a wide range of ecosystems. The most relevant one for the topic of this thesis is the forest-savanna model (5.1) explored in Chapter 5. Incorporating RID with the model (5.1) gives a measure of the risk of irreversible degradation from forests to savannas, a typical type of ecosystem degradation obsered in many regions across the world. Many ecosystems are undergoing transitions from forests to savannas, such as Amazon forests [98, 169]. It has already been pointed out by many researchers that this degradations can be difficult or even impossible to reverse [27, 169]. Having a quantitative measure of the risk of irreversible degradation for these forest ecosystems provides more evidence to support this argument, and can lead to better forests management. On the other hand, with the accumulating satellite observations that can be used to estimate vegetation covers and fires at a large spatial scale and a fine spatial-temporal resolution [107, 152, 232], fitting the model to real-world data has been made possible. Therefore, it is feasible to combine data with the theoretical model (5.1) discussed in Chapter 5, and then integrate the paramterized model with the indicator proposed in this chapter.

Chapter 7

Conclusion and future work

7.1 Main conclusions

In this thesis, I try to understand the changing fire activities through the lens of causality, and the chapters included were all centerred around this topic. I answered this question from at least two perspectives with two different techniques, statistical model (Chapters 3 and 4) and process-based model (Chapters 5 and 6) (please refer to Figure 1.1). In this way, I gave a more comprehensive picture of how fire activities are modified by different environmental stressors and how different systems might respond. The main findings of each chapter are summarized below.

In the first part, I mainly employed machine learning techniques to explore the drivers and their contributions to fire emissions. I first proposed a novel causal framework for understanding drivers of environmental changes, which was built on state-of-the-art causal inference and interpretable machine learning model. I tested the validity of this framework by applying it to some of the well studied regions covering different continents and biomes across the world. I found that the drivers identified by this framework mostly aligned with our findings of these regions from existing literature. Thus, I argued that the causal framework proposed is valid and has the potential to be applied to generate new insights for understanding drivers of fire activities in other parts of the world especially the relatively understudied parts of the world.

I subsequently applied the causal framework to investigate drivers of fire emissions at a scale specific to region and biome. I found that at the global scale, fire-derived carbon emissions was relatively stable, because I observed a non-significant trend in global fire emissions. This was mainly caused by two counteractive trend in fire-derived carbon emissions, a decreasing fire emissions in African savannas and grassland, and an increasing fire emissions in Asian boreal forests. The drivers for the two counteractive trends were different according our results using the proposed causal framework. The decrease in African savannas and grassland was mainly caused by decreased vegetation cause by anthropogenic interventions through agricultural expansion. Whilst the increase in Asian boreal forests was mainly caused by agricultural activities and climate change, especially by drier climates. Our results in the two particular regions as well as in other regions highlighted the importance of vegetation as a primary driver for changes in fire emissions over the past decades. In addition, although a number of studies pointed out that anthropogenic interventions may have outweighed other environmental changes for causing shifting fire activities, our findings showed that for most part of the world, environmental changes, including vegetation and climates, are still dominant drivers for changing fire emissions.

The second part of the thesis used simple mechanism models to understand the drivers for regime shifts in ecosystems. In Chapter 5, I used a grass-savanna-forest model to understand the stable states of the ecosystem under different scenarios of anthropogenic intervention and climate change. I found that under high levels of climate change, the system displays bistability and hysteresis, indicating that the system can undergo abrupt shifts from being forest dominated to grass dominated with increasing anthropogenic intervention. Moreover, due to the hysteresis, once the system is degraded into a grass dominant one, reverting the ecosystem status is much more difficult. Under a low level of climate change, the system is nonlinear but does not exhibit bistability. Thus, with increasing anthropogenic intervention, the system can still experience abrupt degradation from being forest dominated to grass dominated, but the reversal process requires less time and reduction in anthropogenic intervention.

The last chapter was also built on simple mechanism model, and went a step further on ecosystem bistability and the phenomenon of hyeteresis. I proposed a probabilistic approach to quantify the risk of irreversible ecosystem degradation in the

presence of hysteresis for a particular system. The probabilistic approach depends on Bayesian inference for model parameter estimation, by using a probabilistic distribution for all model parameters. Based on their probabilistic distributions, I can estimate the probability of the threshold for ecosystem recovery being unattainable, which is defined as the risk of irreversible degradation. I applied the approach to a real world case study, which is to quantify the irreversible degradation of a freshwater ecosystem. This application suggest that this approach I proposed is valid and has the potential to be applied to other ecosystems given a reliable simple mechanism model is available.

7.2 Future work

I think that the first part is more completed, as the two chapters of this part, namely Chapter 3 and Chapter 4, are closely linked and form a consistent system, I first proposed a causal framework, tested it, and then applied it to a global analysis. All these steps were also centered on the same topic, which is understanding the drivers of fire-derived carbon emissions. As I also discussed in Chapter 3, the causal framework I proposed is highly generalized and can be applied to other systems in order to investigate the drivers of the observed changes. The application is not limited to fire emission or other aspects related to fire activities. Moreover, as I argues in Chapter 3, techniques of causal analysis should be more extensively applied if the researchers wish to make claims such as drivers and causes for an observation. Thus, I do think the causal framework driver wider application in the field of ecology.

Although I believe the causal framework can be applied to many other systems, a more relevant application to further my own research can be a small-scale study to understand drivers of fire activities. The advantages of small-scale application is that we can have a good understanding of the system, so that we can make better judgement for part of the results given by the analysis. In addition, for a small-scale study, the available data can be more abundant, and therefore the analysis can be more inclusive. In Chapter 3 and Chapter 4 of this thesis, the variables I included was limited by the availability of global long-term data. Thus, I only included two variables to represent the social aspects of the system, namely population density and percentage of agricultural land. If I narrow down to a small system that has

been widely studied, I can have better representations of the social aspects because of the data accumulated from past studies focusing on the region.

For the second part, the two chapters may seem somewhat unrelated at first, because the two models used in the two chapters are different models, although both are simple mechanism models used to describe ecosystem regime shift. As mentioned before, Chapter 5 is a rather naive analysis, which is designed to provide a theoretical starting point for applying such models to real world systems. If I can find a real world system where I can apply the model described in Chapter 5, I can then combine it with the approach described in Chapter 6 in order to investigate the regime shifts and irreversible degradation of forests ecosystems to grasslands and savannas.

To further the work I did in the second part of this thesis, I can start by applying the model analyzed in Chapter 5 to a real world forest ecosystem through model parameterization with observational data. This should be practical because degradation of forests to savannas and grasslands driven by climate change and human intervention have been widely observed in forest ecosystems. One of the most well-known example is the Amazon forest [169]. Significant degradation in Amazon forests to savannas can lead to loss of biodiversity and carbon storage, thus has drawn wide attention [160, 169]. And the most recognized drivers for Amazon forests degradation has been drier climates caused by climate change and anthropogenic intervention through deforestation [160, 161]. Therefore, the model in Chapter 5 precisely captured the underlying mechanism of the degradation process in Amazon forests and similar tropical forest ecosystems. With the advancement in satellite observation, long-term vegetation data and other relevant data, for instance climate conditions and agricultural activities, are becoming more and more accessible, making this following analysis through model parameterization more feasible. Given that I successfully applied the model in Chapter 5 to a real world case study, application of the approach in Chapter 6 to measure the risk of irreversible degradation of the forest ecosystem is relatively straightforward. The only preliminary requirement for measuring this risk is to have a reliable model and the required data to fit the model.

The application of Chapter 5 and Chapter 6 are not limited to the forest ecosystems described in Chapter 5. There are observations in other types of forested ecosystems where bistability and hysteresis are observed, thus degradation can have vital

consequences. For instance, the bistability between peatlands and forests observed in boreal Europe have drawn great attention recently [233]. Similarly, the shift in ecosystem status from peatlands to degraded forests are characterized by abrupt changes in ecosystem status that are difficult to reverse or even irreversible [233]. Although the model described in Chapter 5 is not designed for regime shifts in such ecosystems because the mechanism governing the shift are different, it is promising to develop suitable models from the same line of thinking.

In conclusion, I do see further application of the model and probabilistic approach I described in Chapter 5 and Chapter 6 of this thesis. In the future, given the time for collecting data and test out the model, I am confident that I can have a more solid case study to test the model, and also have a better understanding of the regime shifts in forests ecosystems and their risk of irreversible degradation.

Appendix A

Supporting material for Chapter 3

Data and Methods

Potential Drivers for fire emissions

All meteorological variables and vegetation indices were accessed through Google Earth Engine [234] with the help of the Python package `geedataextract` [235]. Source data for climatic variables including *aet*, *def*, *pdsi*, *pet*, *pr*, *ro*, *soil*, *srad*, *swe*, *tmmn*, *tmmx*, *vap*, *vpd*, and *vs* were obtained from TERRACLIMATE [236]. Vegetation indices *EVI* and *NDVI* were obtained from NASA's MOD13Q1.006 Terra Vegetation Indices 16-Day Global 250m product [232].

Population data was downloaded from WorldPop. The data estimated population density at the spatial resolution of 1 km on annual basis. It is available from 2000 to 2020.

The land cover data is provided by Copernicus Global Land Service. The data classified the land surface into 22 classes at a spatial resolution of 300m, and is available from 1992 to present with one year delay. The original 22 land cover classes was defined by the United Nations Food and Agriculture Organization's Land Cover Classification System. We reduced the 22 land use classes to 2 categories, agricultural and non-agricultural, and calculated the percentage of agricultural land. Because agricultural expansion is a typical and driver for fires [104, 111]. We performed this reduction of land use classes according to the User Guide provided by

TABLE A.1: Transformation from land cover types to percentage of agricultural land.

Original LCCS land cover classes	**IPCC classes**	**Percentage of agricultural land**
10, 11, 12 for Rainfed cropland	Agriculture	1
20 for Irrigated cropland	Agriculture	1
30 for Mosaic cropland (>50%) / natural vegetation (tree, shrub, herbaceous cover) (<50%)	Agriculture	0.75
40 for Mosaic natural vegetation (tree, shrub, herbaceous cover) (>50%) / cropland (<50%)	Agriculture	0.25
Rest	Non-agriculture	0

this database, where the 22 categories were mapped to 6 IPCC land use categories that explicitly contains agricultural land. Six of the original 22 classes belong to agricultural land, and the rest to the other non-agricultural categories. Among the 6 classes belonging to agricultural land, rainfed cropland and irrigated cropland were fully used for agriculture, and their percentages of agricultural land were counted as 1; for the mosaic croplands, the one with $> 50\%$ cropland was counted as 0.75 and the one with $< 50\%$ 0.25. The rest classes unrelated to agriculture were counted as 0 (Supplementary Table S.1).

Causal model

Fire activities are recognized as nonlinear and complex [27, 52, 130]. Therefore, multispatialCCM suits the purpose of identifying causality for complex systems. Before applying multispatialCCM, we first make sure the nonlinear signal of the response variable, in our case fire emission, is not dominated by noise by testing its auto-predictability because applying CCM to systems dominated by noise is inappropriate [7]. We first verified that the system was not dominated by noise with the function that has been incorporated into the R package implementing multispatialCCM.

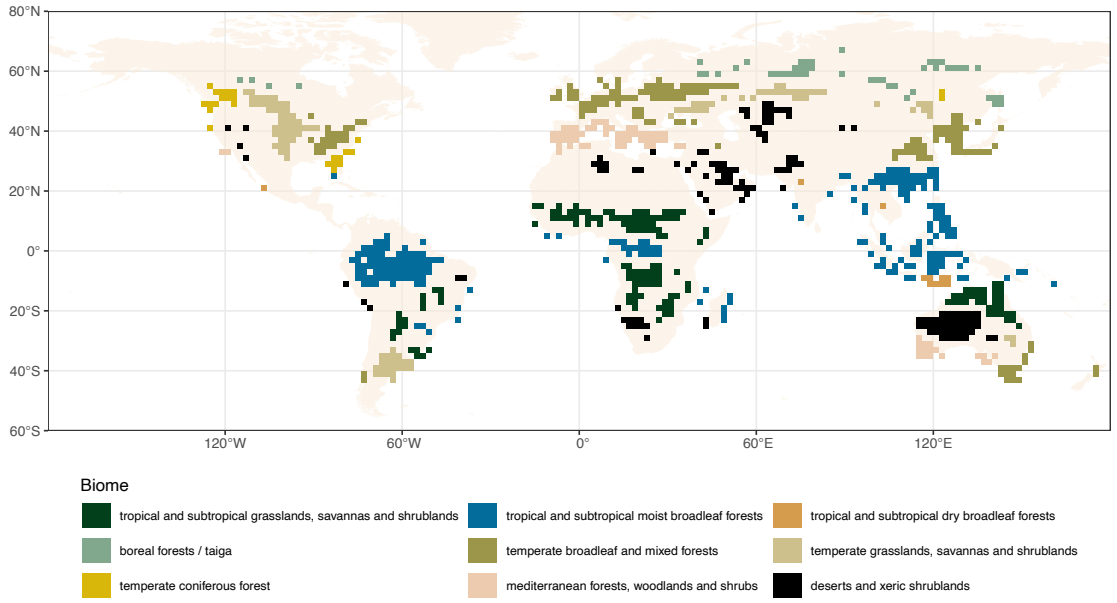

FIGURE A.1: Pixels that experienced fire emissions every year from 2001 to 2019. The color of pixels denote the biome.

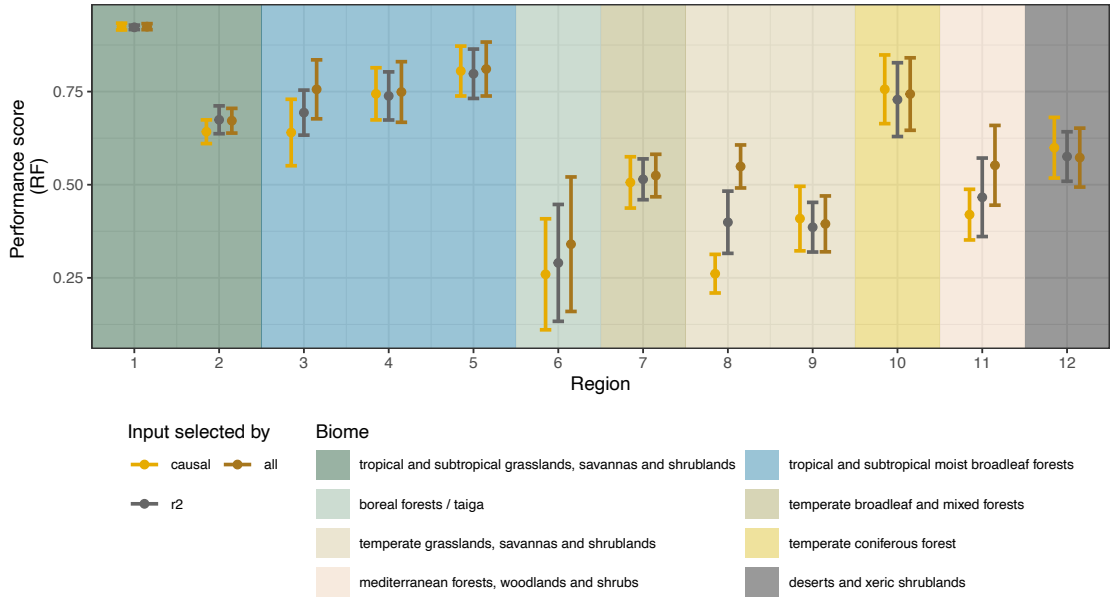

FIGURE A.2: Random forest model performance scores for all regions with the the same number of input selected by the causal model and by correlations (highest r^2). Each boxplot displays performance scores of the model calculated by a 5-fold cross validation.

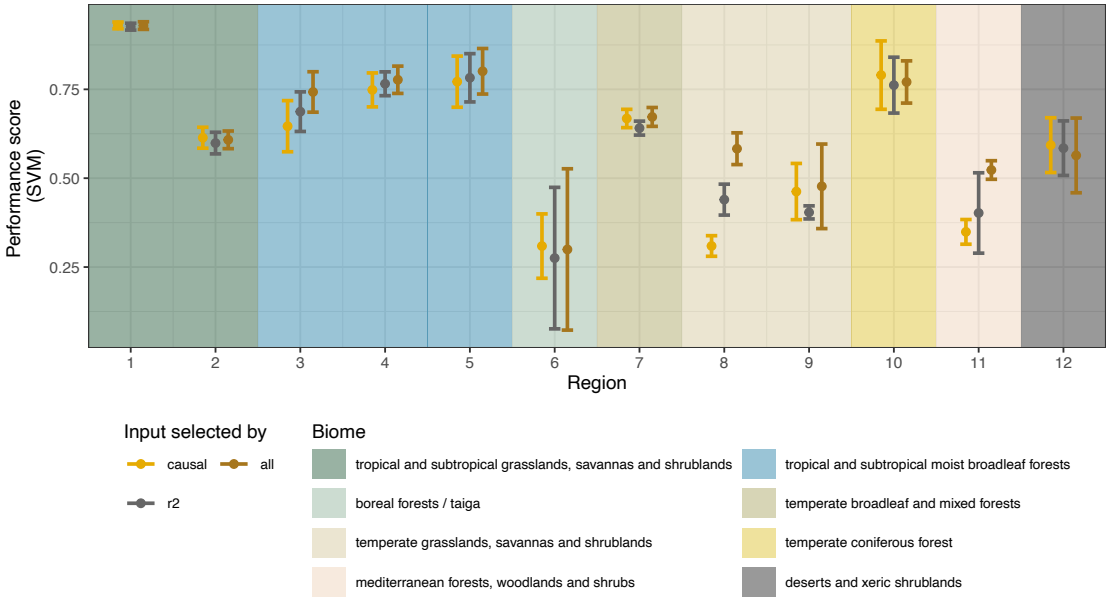

FIGURE A.3: Support vector machine model performance scores for all regions with the the same number of input selected by the causal model and by correlations (highest r^2). Each boxplot displays performance scores of the model calculated by a 5-fold cross validation.

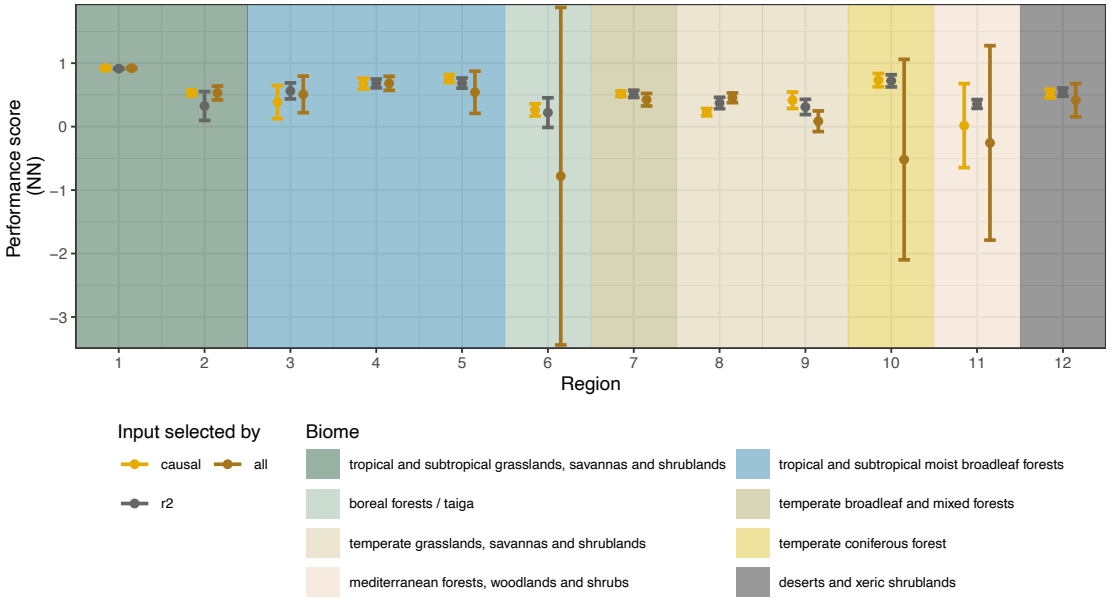

FIGURE A.4: Neural network model performance scores for all regions with the the same number of input selected by the causal model and by correlations (highest r^2). Each boxplot displays performance scores of the model calculated by a 5-fold cross validation.

Appendix B

Supporting material for Chapter 4

Data and Methods

Defining subregions for applying causal model

Subregions were defined by combinations of geographical regions and biomes. For geographical regions, we used the basis regions defined in GFED [152, 162] and merged some of the original basis regions to reduce the number from 14 to 9 (see Supplementary Figure S3). We followed [111] for definitions of 8 biomes based on the original definitions by [133] (see Supplementary Figure S4). We merged some of the regions for simplicity although we still had 43 subregions after the merges. Additionally, keeping all 14 basis regions will lead to many small subregions that only contain a few pixels that showed significant fire emission trends. Such subregions are not able to produce a valid result of the causal model because of the small sample size thus undermine the spatial coverage of our results. For example, originally South America were divided into two parts by the equator, this will also divide the subregion tropical wet forest in South America into two parts, above and below the equator. The part above the equator will be too small to be analyzed by the causal model. It will be reasonable and more efficient to merge the two parts and only retain South America as a whole in our analysis. The merges that produced North America, Africa, and Central Asia followed the same reasoning (Supplementary Figures S3 and S4).

TABLE B.1: Aggregation of biomes from the original 14 biomes to the 8 biomes.

Original biomes	**Aggregated biomes**
Boreal forests / Taiga	Boreal forests
Mangroves	Mangroves
Mediterranean Forests, woodlands and shrubs	Mediterranean forests, woodlands and shrubs
Montane grasslands and shrublands	Shrublands
Tundra	Shrublands
Deserts and xeric shrublands	Shrublands
Temperate broadleaf and mixed forests	Temperate forests and woodlands
Temperate Coniferous Forest	Temperate forests and woodlands
Temperate grasslands, savannas and shrublands	Temperate forests and woodlands
Tropical and subtropical dry broadleaf forests	Tropical dry forests
Tropical and subtropical grasslands, savannas and shrublands	Tropical savannas and grasslands
Flooded grasslands and savannas	Tropical savannas and grasslands
Tropical and subtropical moist broadleaf forests	Tropical wet forests
Tropical and suptropical coniferous forests	Tropical wet forests

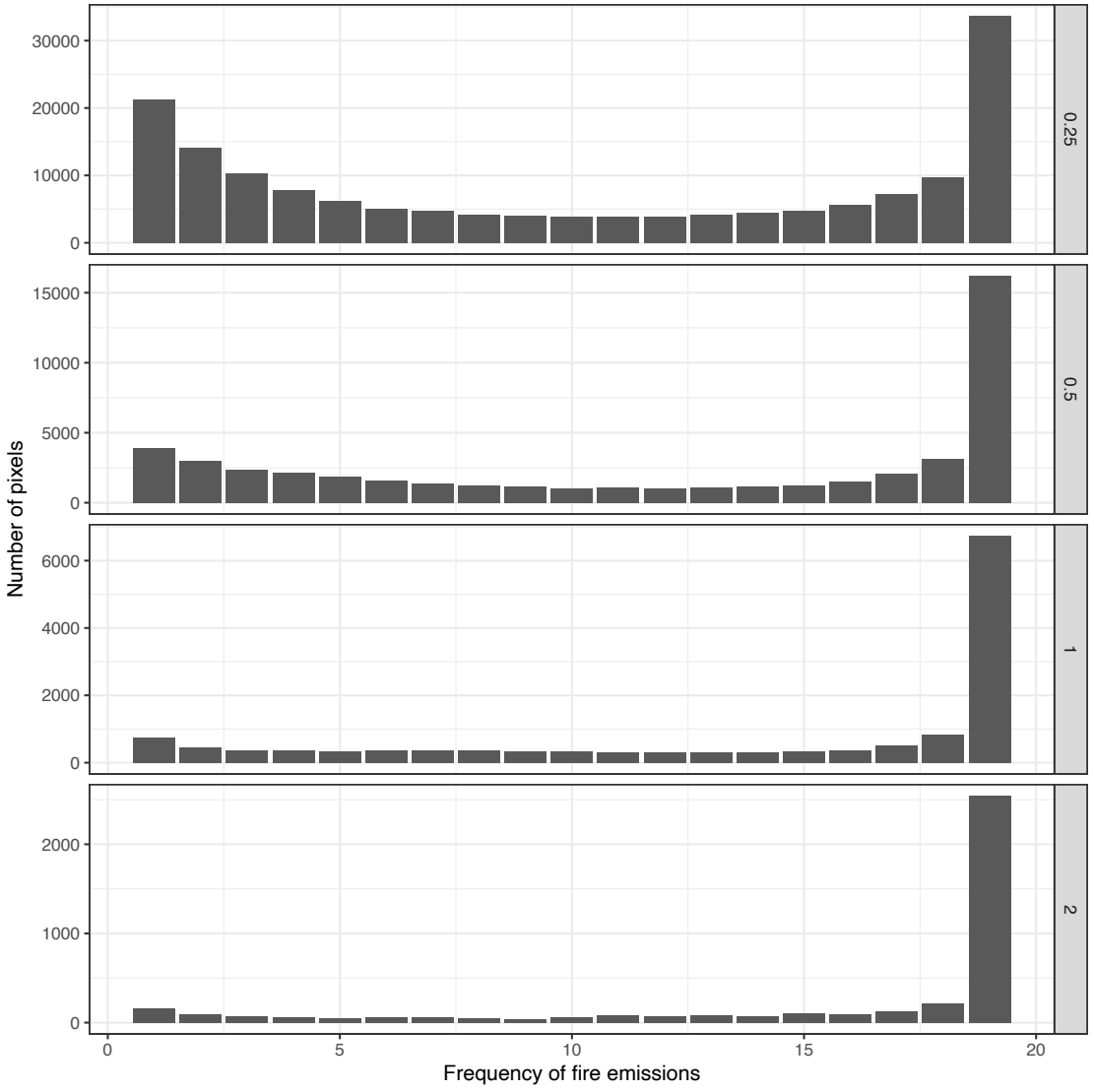

FIGURE B.1: Histograms for fire frequencies under different spatial resolutions ($0.25° \times 0.25°$, $0.5° \times 0.5°$, $1° \times 1°$ and $2° \times 2°$, in a top-down order). Original resolution of the dataset is $0.25° \times 0.25°$. We aggregated it to the rest three coarser resolutions. Frequency was calculated by the number of years with non-zero annual emissions. Counts of pixels with 0 frequency were not displayed as they were not included in the subsequent modelling analysis either.

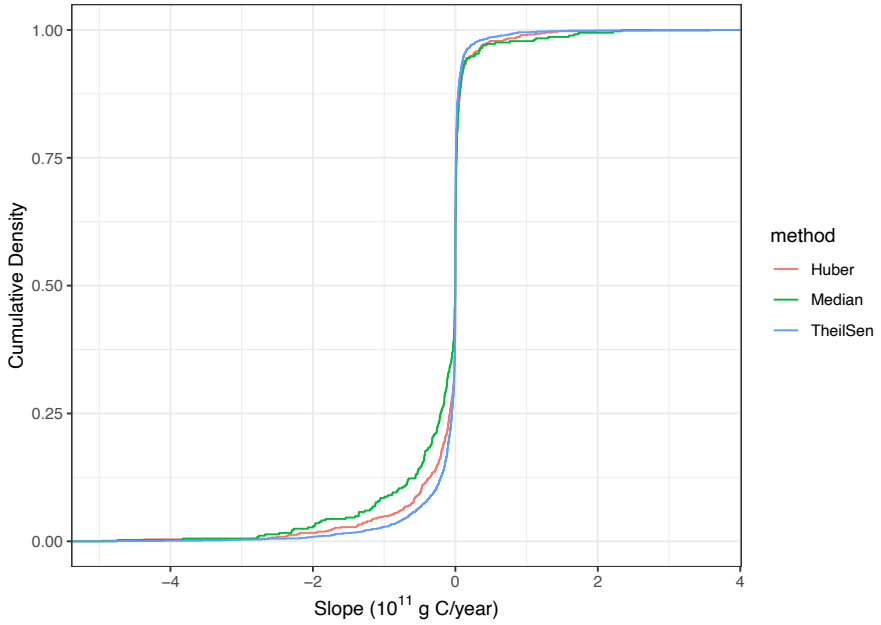

FIGURE B.2: Distributions of fire emission trends (estimated regression slope) quantified by different robust regression techniques. Huber regression is the one we presented in the manuscript. Here we compared it with the other two commonly-used robust regression techniques: median regression and Theil-Sen regression. Only significant pixels were included in the figure, and their distributions mostly overlapped.

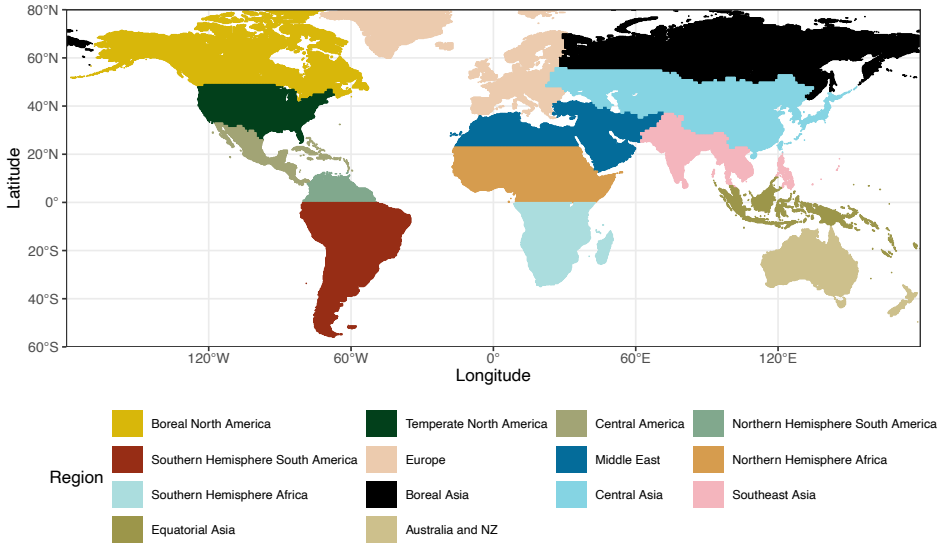

(A)

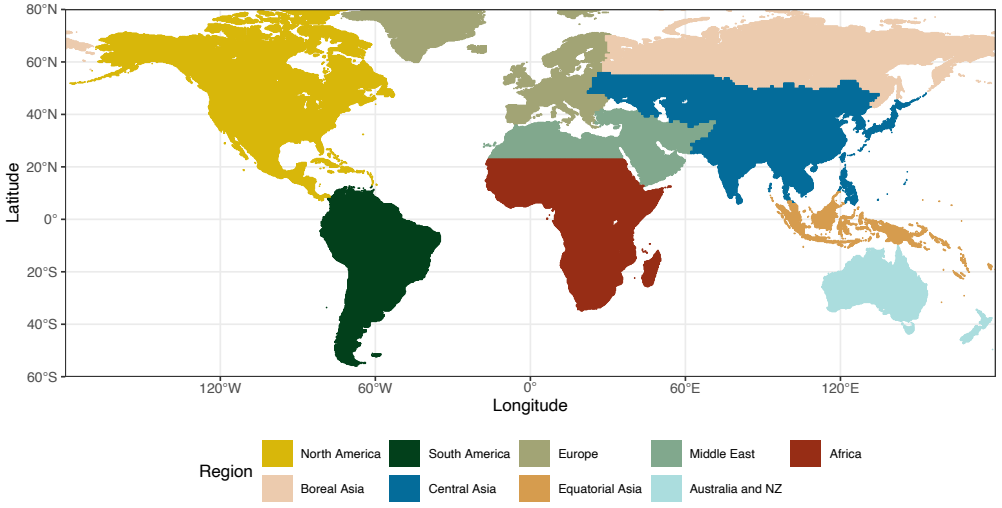

(B)

FIGURE B.3: Maps for global geographical regions (a) originally defined in GFED dataset and (b) after merging.

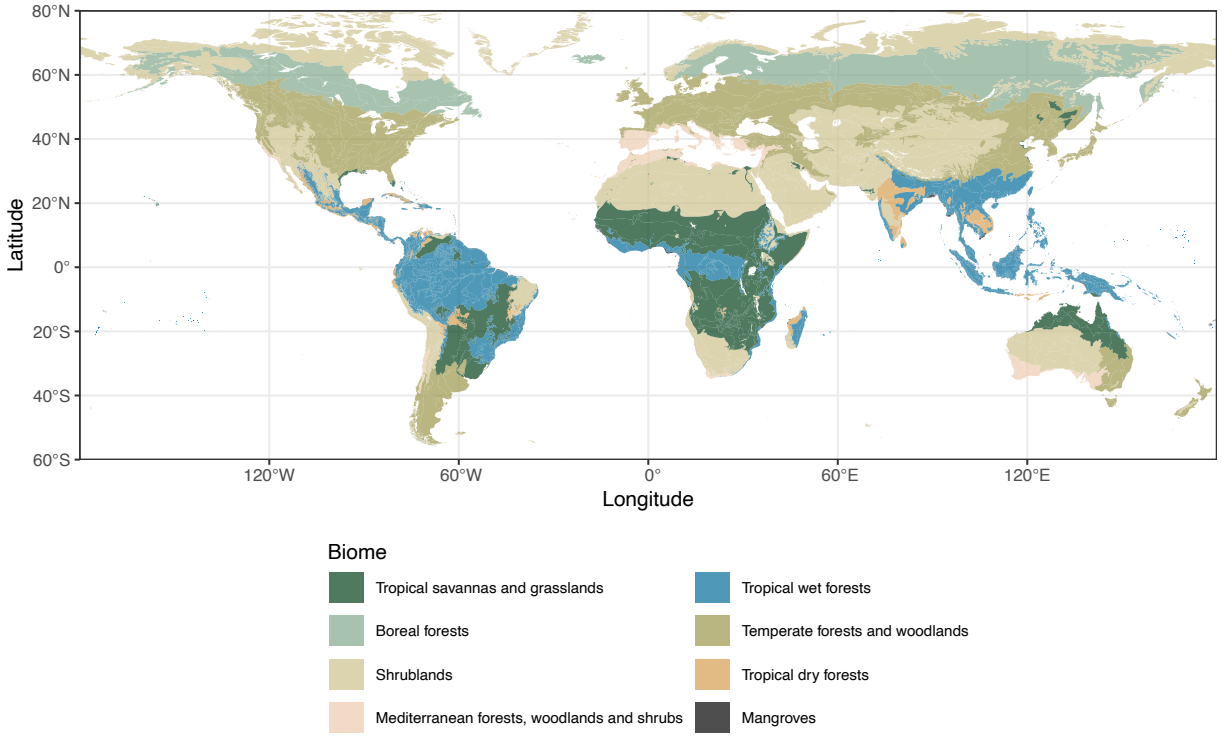

FIGURE B.4: Map of global distribution of the 8 biomes.

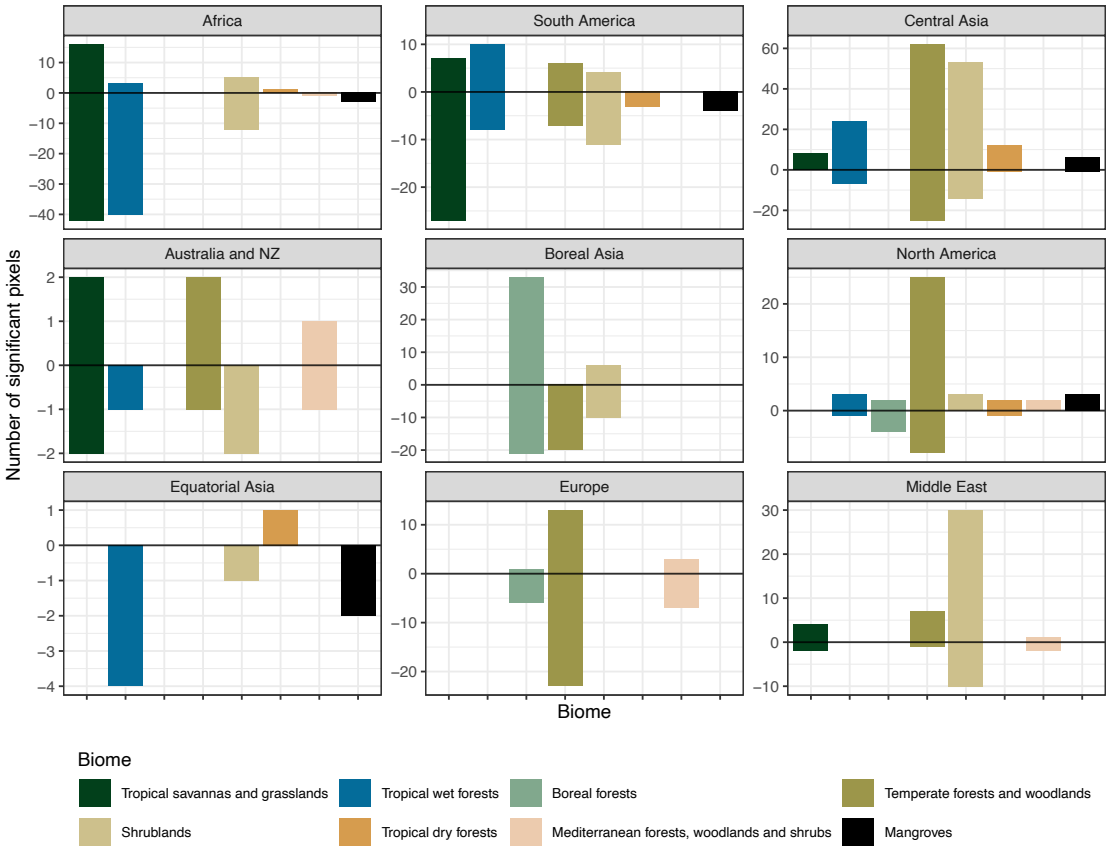

FIGURE B.5: Number of pixels that showed significant fire emission trends for subregions defined by region and biome. Bars above 0 represented number of pixels with increasing trend, and bars below 0 that with decreasing trend. Regions were arranged in a decreasing order in terms of their total fire emissions from 2001 to 2019.

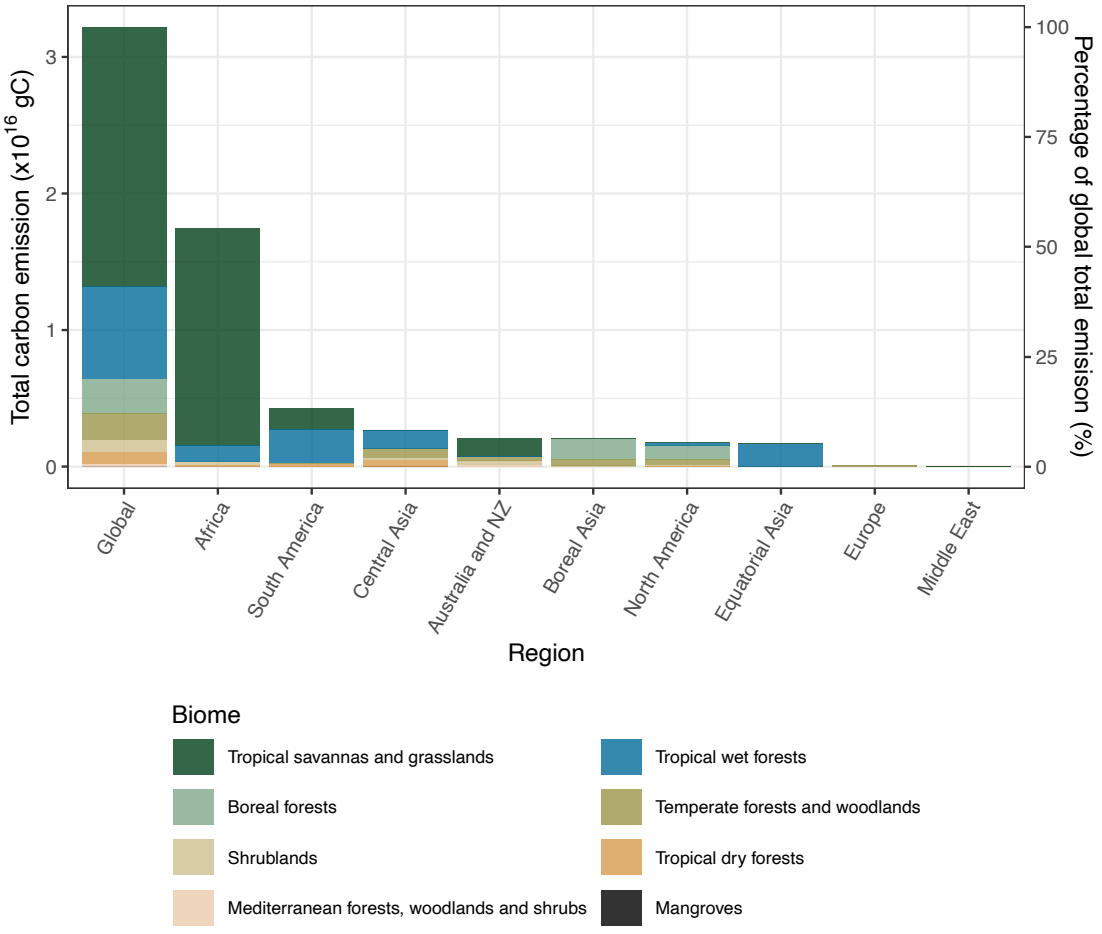

FIGURE B.6: Total fire emissions and contributions to global fire emission calculated for regions and biomes from 2001 to 2019.

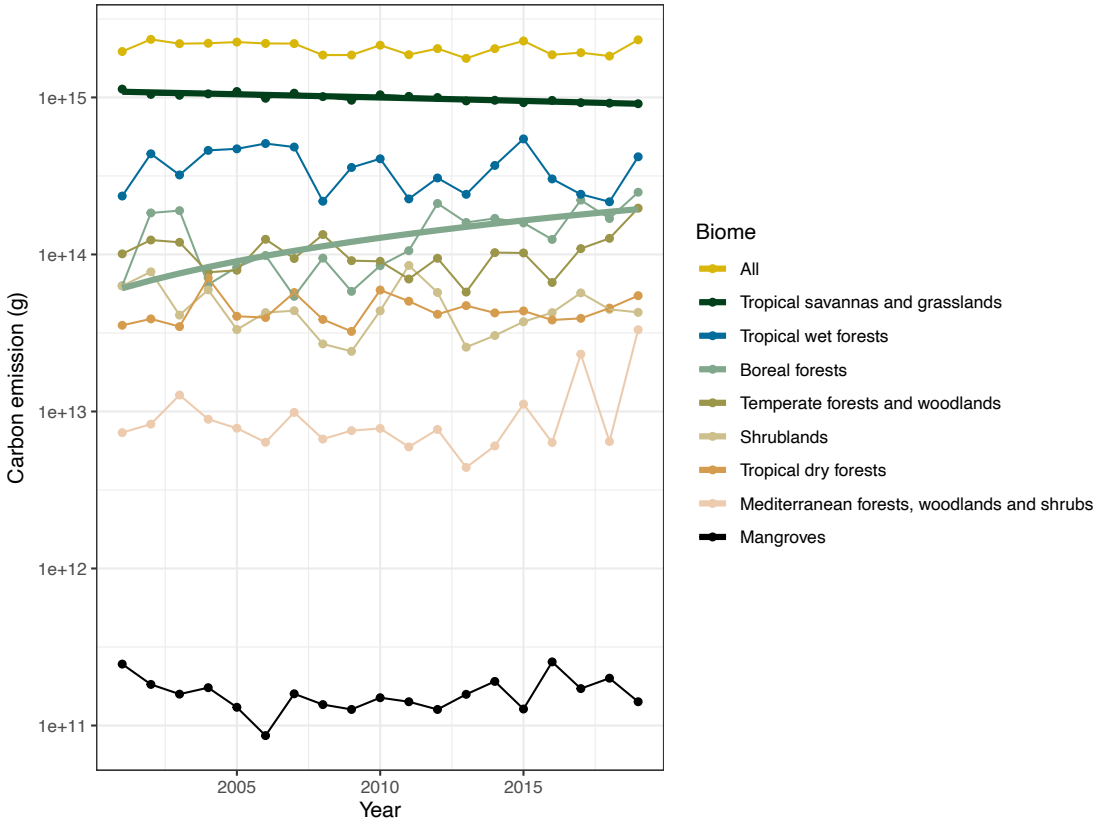

FIGURE B.7: Fire emission trends estimated for 8 biomes at the global scale and for total fire emissions. Solid straight lines represented significant fire emission trends ($p \leq 0.05$ for regression slope) and non-significant trends were not displayed. The solid straight lines were slightly curved due to the log scale for y-axis fire emissions.

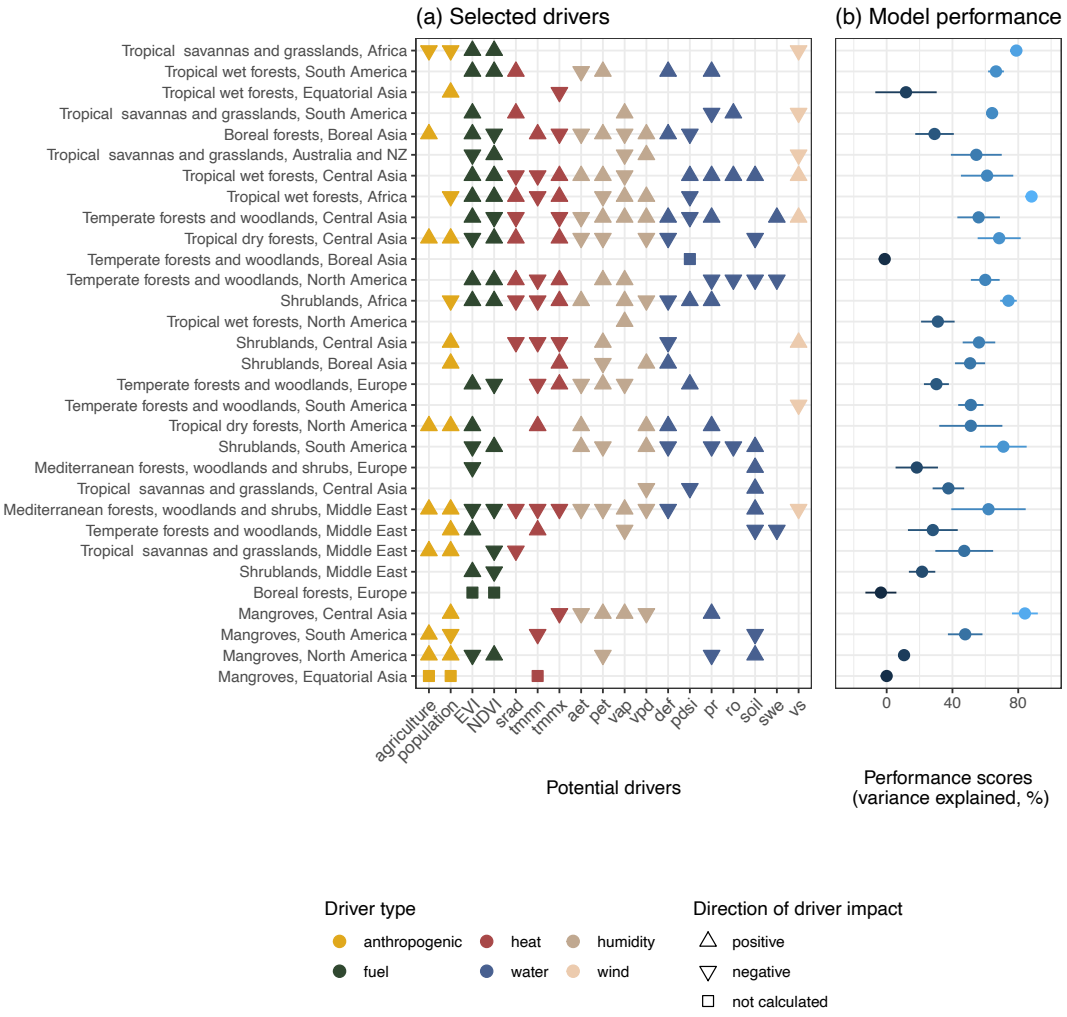

FIGURE B.8: Drivers selected by causal model and GBDT model performances for subregions defined by region and biome. For each subregion, the selected drivers were denoted by triangles or squares. Drivers were divided into 6 categories and denoted by colors. Subregions were arranged in a decreasing order in terms of their fire emissions from top to bottom. Orientation of the triangles showed the overall direction of the driver impact on fire emissions, upward triangles meaning increasing in drivers has positive impact on fire emissions and downward negative. For subregions with negative GBDT model performance, impact of their drivers were not measured and drivers were denoted by squares. Model performances were measured by variance explained by the model. Points and error bars showed the mean and standard deviation of the performance scores evaluated by the 5-fold nested cross-validation.

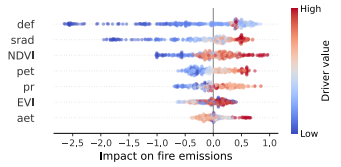

(A) Tropical wet forests, South America

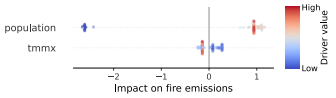

(B) Tropical wet forests, Equatorial Asia

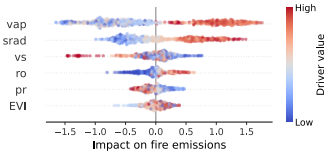

(C) Tropical savannas and grasslands, South America

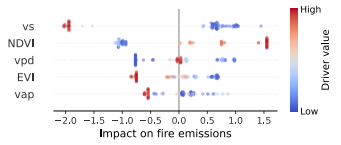

(D) Tropical savannas and grasslands, Australia and NZ

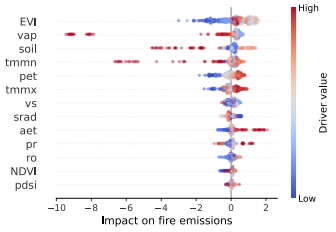

(E) Tropical wet forests, Central Asia

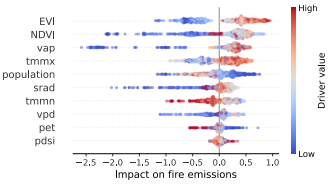

(F) Tropical wet forests, Africa

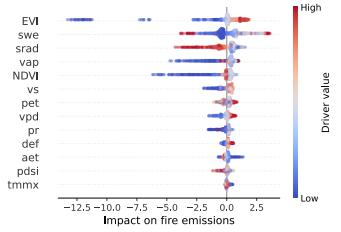

(G) Temperate forests and woodlands, Central Asia

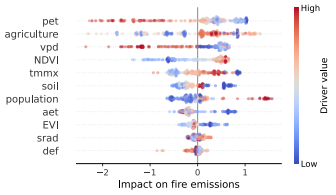

(H) Tropical dry forests, Central Asia

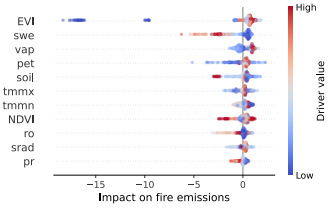

(I) Temperate forests and woodlands, North America

FIGURE B.9: Driver importance for subregions. Drivers are sorted by their importance (impact on fire emissions) from top to bottom in a decreasing order. For each driver, the horizontal beeswarm plot displayed the estimated contribution to fire emission under different driver values, which is equivalent to the figures for each driver in Figure 4 in the main text but squeezed to save space. Colors indicated the lower or higher values of the driver. Negative values of estimated impact indicated negative impact on fire emissions, and vice versa.

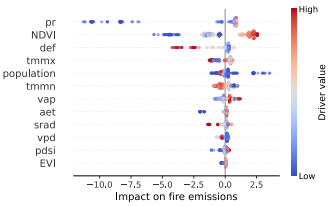

(J) Shrublands, Africa

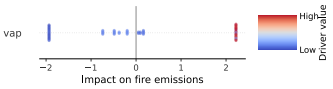

(K) Tropical wet forest, North America

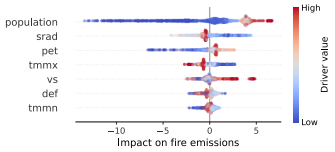

(L) Shrublands, Central Asia

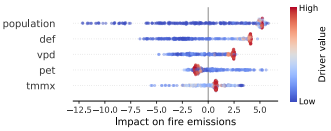

(M) Shrublands, Boreal Asia

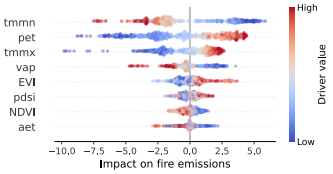

(N) Temperate forests and woodlands, Europe

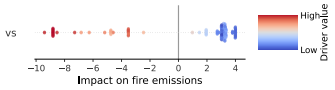

(O) Temperate forests and woodlands, South America

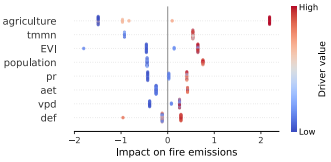

(P) Tropical dry forests, North America

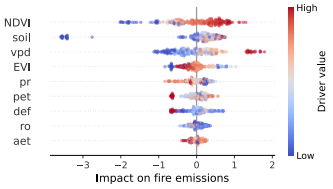

(Q) Shrublands, South America

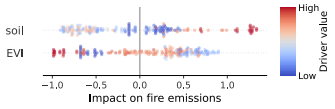

(R) Mediterranean forests, woodlands and shrubs, Europe

FIGURE B.9: Driver importance for subregions. Drivers are sorted by their importance (impact on fire emissions) from top to bottom in a decreasing order. For each driver, the horizontal beeswarm plot displayed the estimated contribution to fire emission under different driver values, which is equivalent to the figures for each driver in Figure 4 in the main text but squeezed to save space. Colors indicated the lower or higher values of the driver. Negative values of estimated impact indicated negative impact on fire emissions, and vice versa.

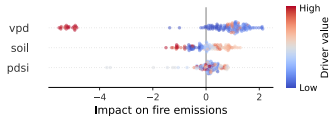

(S) Tropical savannas and grasslands, Central Asia

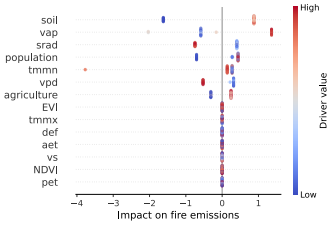

(T) Mediterranean forests, woodlands and shrubs, Middle East

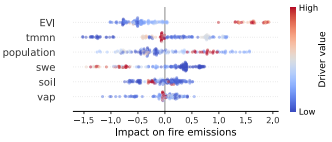

(U) Temperate forests and woodlands, Middle East

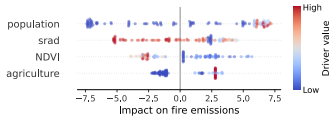

(V) Tropical savannas and grasslands, Middle East

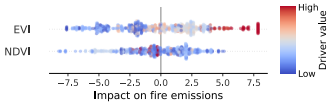

(W) Shrublands, Middle East

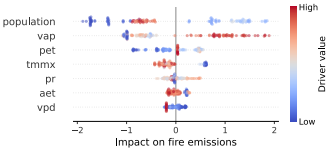

(X) Mangroves, Central Asia

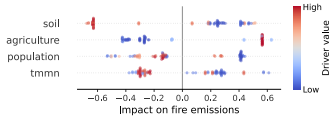

(Y) Mangroves, South America

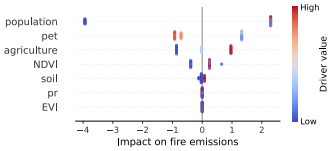

(Z) Mangroves, North America

FIGURE B.9: Driver importance for subregions. Drivers are sorted by their importance (impact on fire emissions) from top to bottom in a decreasing order. For each driver, the horizontal beeswarm plot displayed the estimated contribution to fire emission under different driver values, which is equivalent to the figures for each driver in Figure 4 in the main text but squeezed to save space. Colors indicated the lower or higher values of the driver. Negative values of estimated impact indicated negative impact on fire emissions, and vice versa.

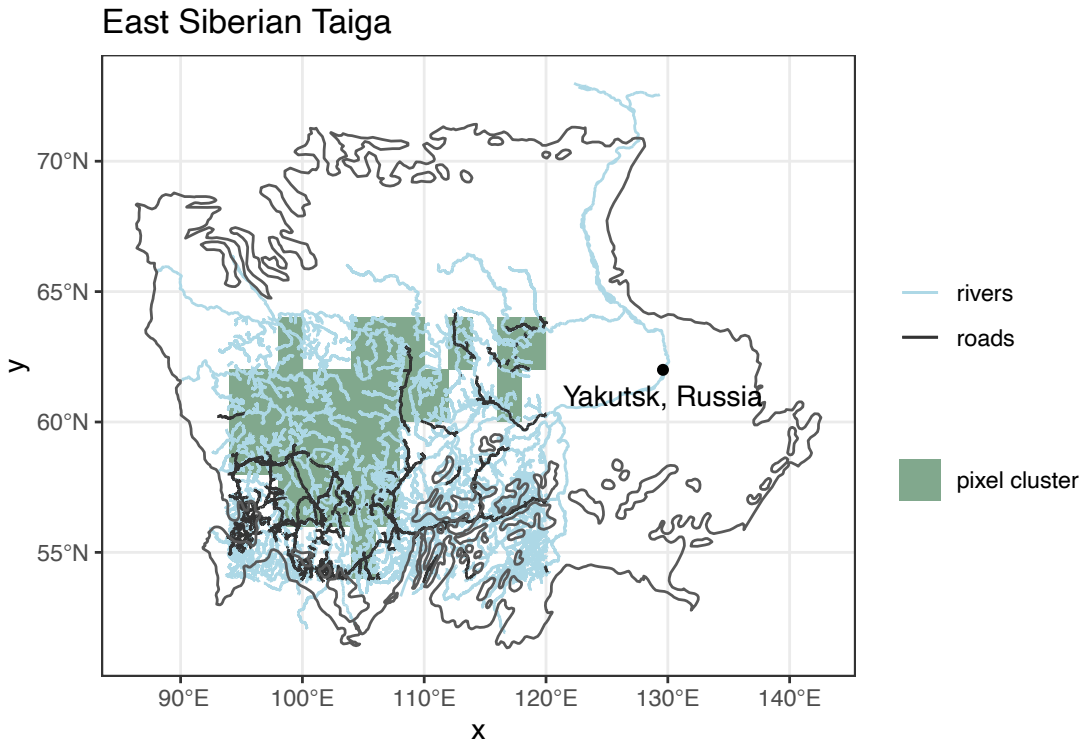

FIGURE B.10: The cluster of pixels that showed significant increasing fire emissions in Asian boreal forests fall within the ecoregion East Siberian Taiga. The nearest city from this cluster is Yakutsk, Russia. A number of rivers and roads pass the pixel clusters, which could be the reason that agricultural activities was identified as a fire emission driver for this cluster.

Appendix C

Supporting material for Chapter 5

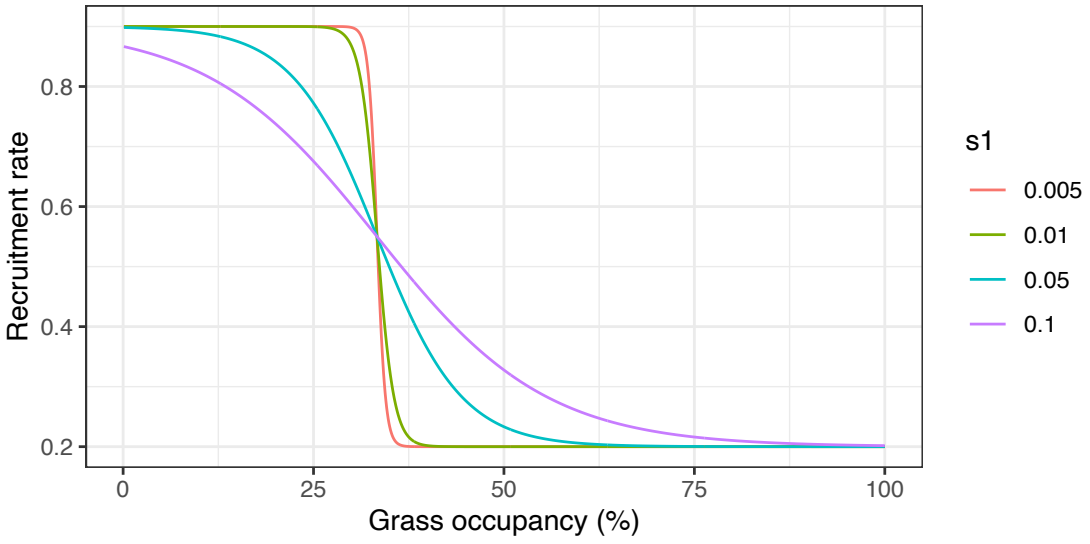

FIGURE C.1: Recruitment rate (ω) from savannas to trees controlled by grass occupation rate. Levels of climate change are represented by s_1 values. Other parameter values of the response function ω were set at the default. Lower values of s_1 represent higher levels of climate change as the response is sharper; and higher values of s_1 represent lower levels of climate change as the response become more smooth.

Appendix D

Supporting material for Chapter 6

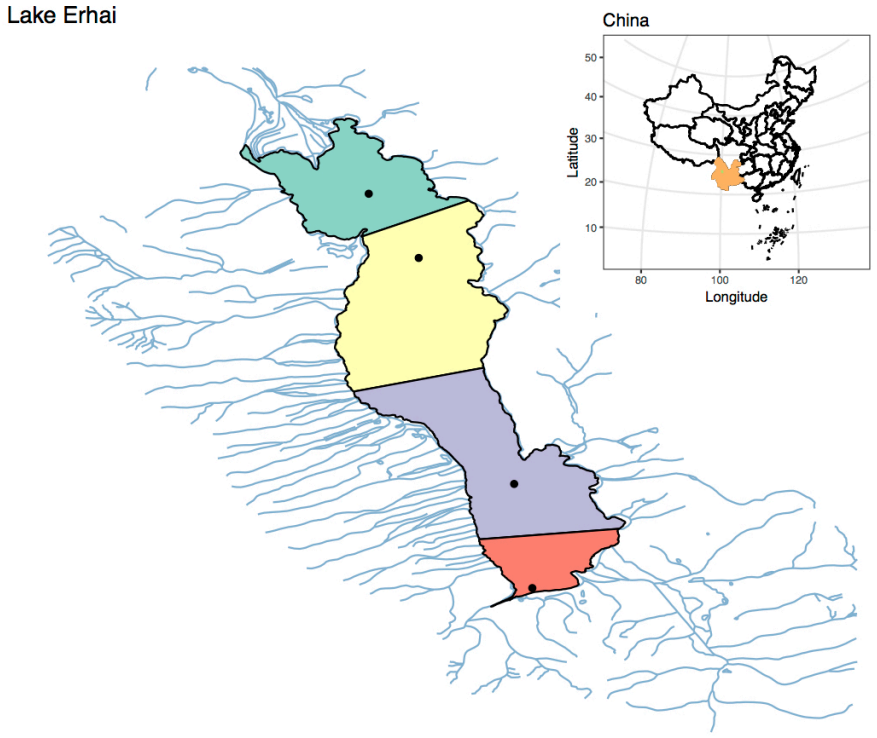

FIGURE D.1: Division of the lake based on the monitoring site. The lake was divided into 4 subunits based on proximity polygons. Number of subunits was decided by the availability of water quality data and the corresponding monitoring site. The nearest point will be categorized into the same subunit as the monitoring site. External load was based on different inflows, and then assigned to each subunit based on their location.

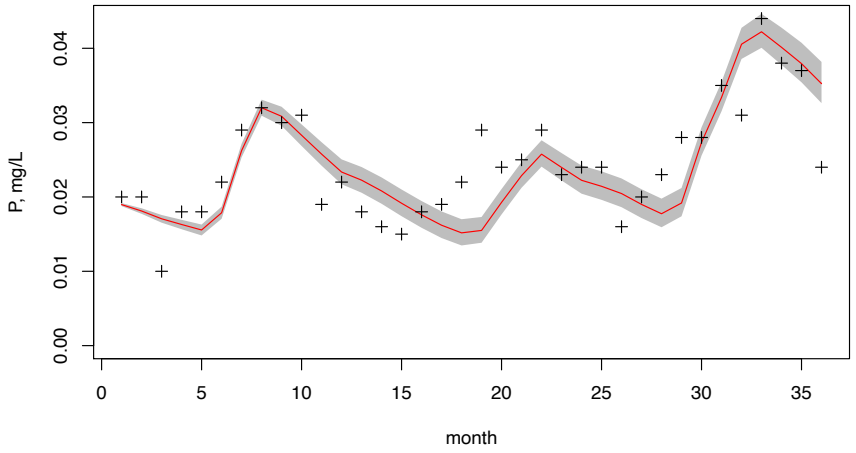

FIGURE D.2: Comparison between simulation and observation of TP at the whole lake level. Points represented the observations, red line represented the mean of estimation, and the gray area represented the 95% confidence interval.

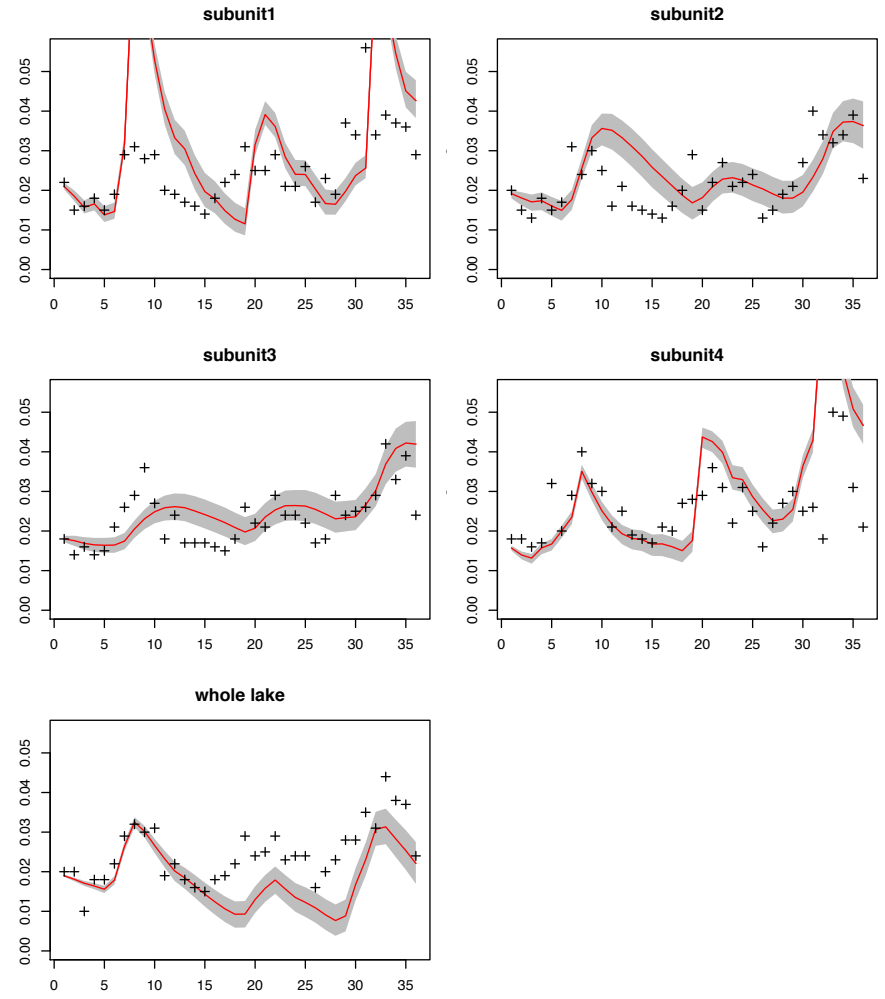

FIGURE D.3: Comparison between simulation and observation of TP for different subunits and the whole lake calculated from subunits.

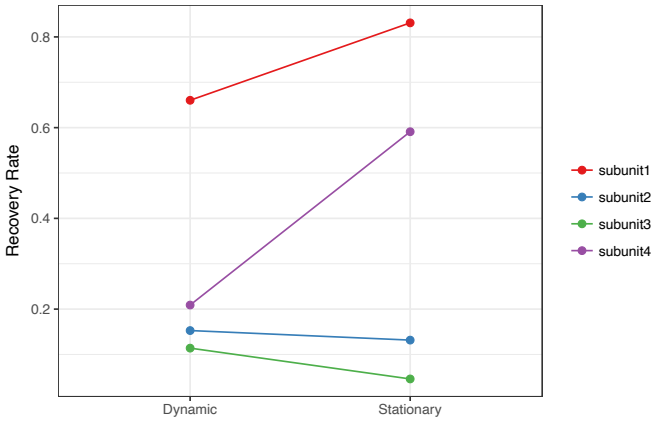

FIGURE D.4: Comparison of recover rate given by RID (stationary, 1-RID) and under dynamic simulation under 100% external load reduction. Recovery rate under dynamic simulation are slightly higher than indicated by RID for subunits with high RID, namely subunits 2 and 3. While that for subunits with low RID are lower.

List of Author's Publications

Journal articles

- Sifeng Wu, Stuart William Smith, and Janice Ser Huay Lee. "Geophysical and anthropogenic drivers for global and regional fire emission trends from 2001 to 2019." *under review*. preprint: https://doi.org/10.21203/rs.3.rs-1537229/v1
- Sifeng Wu, Zhongyao Liang, and Yong Liu. "Quantifying the risk of irreversible degradation for ecosystems: A probabilistic method based on Bayesian inference." Ecological Indicators 107 (2019): 105621

Conference

- Sifeng Wu and Janice Ser Huay Lee. Geophysical and anthropogenic drivers for global and regional fire emission trends from 2001 to 2019, EGU General Assembly 2022, Vienna, Austria, 23–27 May 2022, EGU22-6879, https://doi.org/10.5194/egu22-6879, 2022.

Bibliography

[1] Johan Rockström, Will Steffen, Kevin Noone, Åsa Persson, F Stuart Chapin III, Eric F Lambin, Timothy M Lenton, Marten Scheffer, Carl Folke, Hans Joachim Schellnhuber, et al. A safe operating space for humanity. *Nature*, 461(7263):472, 2009. 1, 28, 99

[2] Rachel E Mason, Joseph M Craine, Nina K Lany, Mathieu Jonard, Scott V Ollinger, Peter M Groffman, Robinson W Fulweiler, Jay Angerer, Quentin D Read, and Peter B Reich. Evidence, causes, and consequences of declining nitrogen availability in terrestrial ecosystems. *Science*, 376(6590):eabh3767, 2022. ISSN 0036-8075.

[3] Luke T Kelly, Katherine M Giljohann, Andrea Duane, Núria Aquilué, Sally Archibald, Enric Batllori, Andrew F Bennett, Stephen T Buckland, Quim Canelles, and Michael F Clarke. Fire and biodiversity in the Anthropocene. *Science*, 370(6519):eabb0355, 2020. ISSN 0036-8075. 1, 4, 28

[4] Marten Scheffer, Stephen R Carpenter, Timothy M Lenton, Jordi Bascompte, William Brock, Vasilis Dakos, Johan Van de Koppel, Ingrid A Van de Leemput, Simon A Levin, and Egbert H Van Nes. Anticipating critical transitions. *science*, 338(6105):344–348, 2012. ISSN 0036-8075. 1, 11, 28, 71, 91

[5] Brian H Walker, Stephen R Carpenter, Johan Rockstrom, Anne-Sophie Crépin, and Garry D Peterson. Drivers, "slow" variables, "fast" variables, shocks, and resilience. *Ecology and Society*, 17(3), 2012. 5, 18, 71, 82, 83, 84, 85, 91, 99

[6] John M Anderies, Jean-Denis Mathias, and Marco A Janssen. Knowledge infrastructure and safe operating spaces in social–ecological systems. *Proceedings of the National Academy of Sciences*, 116(12):5277–5284, 2019. ISSN 0027-8424. 1, 28

[7] George Sugihara, Robert May, Hao Ye, Chih-hao Hsieh, Ethan Deyle, Michael Fogarty, and Stephan Munch. Detecting causality in complex ecosystems. *Science*, 338(6106):496–500, 2012. ISSN 0036-8075, 1095-9203. doi: 10.1126/science.1227079. 1, 10, 11, 15, 30, 35, 110

[8] Paul J Ferraro, James N Sanchirico, and Martin D Smith. Causal inference in coupled human and natural systems. *Proceedings of the National Academy*

of Sciences, 116(12):5311–5318, 2019. ISSN 0027-8424. 1, 5, 10, 22, 28, 29, 30, 44, 45, 46

[9] Trevor Hastie, Robert Tibshirani, and Jerome Friedman. *The Elements of Statistical Learning*. Springer, New York, 2009. 1, 6, 17, 29, 31, 36, 37, 38, 51

[10] Judea Pearl. Causal inference in statistics: An overview. *Statistics surveys*, 3:96–146, 2009. 2, 16, 29, 45, 46

[11] Judea Pearl and Dana Mackenzie. *The Book of Why: The New Science of Cause and Effect*. Basic books, 2018. ISBN 0-465-09761-8. 1, 2, 10, 12, 13, 16, 19, 22, 29, 38, 44, 46

[12] Jeremy Ginsberg, Matthew H. Mohebbi, Rajan S. Patel, Lynnette Brammer, Mark S. Smolinski, and Larry Brilliant. Detecting influenza epidemics using search engine query data. *Nature*, 457(7232):1012–1014, 2009. ISSN 1476-4687. doi: 10.1038/nature07634. 2

[13] David Lazer, Ryan Kennedy, Gary King, and Alessandro Vespignani. The Parable of Google Flu: Traps in Big Data Analysis. *Science*, 343(6176): 1203–1205, 2014. doi: 10.1126/science.1248506. 2

[14] Clive WJ Granger and Paul Newbold. Spurious regressions in econometrics. *Journal of econometrics*, 2(2):111–120, 1974. 2

[15] Daniel Kahneman. *Thinking, Fast and Slow*. Macmillan, 2011. 2

[16] Jonathan G Richens, Ciarán M Lee, and Saurabh Johri. Improving the accuracy of medical diagnosis with causal machine learning. *Nature communications*, 11(1):1–9, 2020. ISSN 2041-1723. 2, 29

[17] Fabian Dablander. An introduction to causal inference. 2020. 2, 4

[18] Nassim Taleb. *Fooled by Randomness: The Hidden Role of Chance in Life and in the Markets*, volume 1. Random House Incorporated, 2005. 2

[19] Daniel Kahneman, Olivier Sibony, and Cass R Sunstein. *Noise: A Flaw in Human Judgment*. Little, Brown, 2021. 3

[20] Marta R Costa-jussà. An analysis of gender bias studies in natural language processing. *Nature Machine Intelligence*, 1(11):495–496, 2019. ISSN 2522-5839.

[21] Eirini Ntoutsi, Pavlos Fafalios, Ujwal Gadiraju, Vasileios Iosifidis, Wolfgang Nejdl, Maria-Esther Vidal, Salvatore Ruggieri, Franco Turini, Symeon Papadopoulos, and Emmanouil Krasanakis. Bias in data-driven artificial intelligence systems—An introductory survey. *Wiley Interdisciplinary Reviews: Data Mining and Knowledge Discovery*, 10(3):e1356, 2020. ISSN 1942-4787.

[22] George Adigbli. Race, science and (im)precision medicine. *Nature Medicine*, 26(11):1675–1676, 2020. ISSN 1546-170X. 3

[23] Richard Dawkins, Roderick Strange, and Charles Simonyi Professor of the Public Understanding of Science Richard Dawkins. *The Extended Phenotype: The Long Reach of the Gene*. Oxford University Press, 1999. ISBN 978-0-19-288051-2. 3, 4

[24] Sally Archibald, Caroline ER Lehmann, Jose L Gómez-Dans, and Ross A Bradstock. Defining pyromes and global syndromes of fire regimes. *Proceedings of the National Academy of Sciences*, 110(16):6442–6447, 2013. ISSN 0027-8424. 4, 20, 48, 49, 62, 74

[25] Alan H. Taylor, Valerie Trouet, Carl N. Skinner, and Scott Stephens. Socioecological transitions trigger fire regime shifts and modulate fire–climate interactions in the Sierra Nevada, USA, 1600–2015 CE. *Proceedings of the National Academy of Sciences*, 113(48):13684–13689, 2016. ISSN 0027-8424, 1091-6490. doi: 10.1073/pnas.1609775113.

[26] David B. Lindenmayer and Chris Taylor. New spatial analyses of Australian wildfires highlight the need for new fire, resource, and conservation policies. *Proceedings of the National Academy of Sciences*, 117(22):12481–12485, 2020. ISSN 0027-8424, 1091-6490. doi: 10.1073/pnas.2002269117.

[27] Kendra K. McLauchlan, Philip E. Higuera, Jessica Miesel, Brendan M. Rogers, Jennifer Schweitzer, Jacquelyn K. Shuman, Alan J. Tepley, J. Morgan Varner, Thomas T. Veblen, Solny A. Adalsteinsson, Jennifer K. Balch, Patrick Baker, Enric Batllori, Erica Bigio, Paulo Brando, Megan Cattau, Melissa L. Chipman, Janice Coen, Raelene Crandall, Lori Daniels, Neal Enright, Wendy S. Gross, Brian J. Harvey, Jeff A. Hatten, Sharon Hermann, Rebecca E. Hewitt, Leda N. Kobziar, Jennifer B. Landesmann, Michael M. Loranty, S. Yoshi Maezumi, Linda Mearns, Max Moritz, Jonathan A. Myers, Juli G. Pausas, Adam F. A. Pellegrini, William J. Platt, Jennifer Roozeboom, Hugh Safford, Fernanda Santos, Robert M. Scheller, Rosemary L. Sherriff, Kevin G. Smith, Melinda D. Smith, and Adam C. Watts. Fire as a fundamental ecological process: Research advances and frontiers. *Journal of Ecology*, 108(5):2047–2069, 2020. ISSN 1365-2745. doi: 10.1111/1365-2745.13403. 4, 20, 30, 33, 46, 48, 49, 66, 70, 101, 110

[28] John T Abatzoglou, A Park Williams, Luigi Boschetti, Maria Zubkova, and Crystal A Kolden. Global patterns of interannual climate–fire relationships. *Global Change Biology*, 24(11):5164–5175, 2018. ISSN 1354-1013. 4, 20

[29] Florent Mouillot and Christopher B. Field. Fire history and the global carbon budget: A fire history reconstruction for the 20th century. *Global Change Biology*, 11(3):398–420, 2005. ISSN 1354-1013, 1365-2486. doi: 10.1111/j.1365-2486.2005.00920.x. 4

[30] Ivar R van der Velde, Guido R van der Werf, Sander Houweling, Joannes D Maasakkers, Tobias Borsdorff, Jochen Landgraf, Paul Tol, Tim A van Kempen, Richard van Hees, and Ruud Hoogeveen. Vast CO2 release from Australian fires in 2019–2020 constrained by satellite. *Nature*, 597(7876):366–369, 2021. ISSN 1476-4687. 4, 19, 20, 22, 49, 64

[31] Jin-Soo Kim. Extensive fires in southeastern Siberian permafrost linked to preceding Arctic Oscillation. *SCIENCE ADVANCES*, page 8, 2020.

[32] Luca Tacconi. Preventing fires and haze in Southeast Asia. *Nature Climate Change*, 6(7):640–643, 2016. ISSN 1758-678X, 1758-6798. doi: 10.1038/nclimate3008. 4, 19, 20

[33] Matthew D Hurteau, Shuang Liang, A LeRoy Westerling, and Christine Wiedinmyer. Vegetation-fire feedback reduces projected area burned under climate change. *Scientific Reports*, 9(1):1–6, 2019. ISSN 2045-2322. 4, 20, 62, 66

[34] Caroline ER Lehmann, T Michael Anderson, Mahesh Sankaran, Steven I Higgins, Sally Archibald, William A Hoffmann, Niall P Hanan, Richard J Williams, Roderick J Fensham, and Jeanine Felfili. Savanna vegetation-fire-climate relationships differ among continents. *Science*, 343(6170):548–552, 2014. ISSN 0036-8075. 4, 20, 62, 66

[35] M Hamilton, J Salerno, and A P Fischer. Cognition of complexity and trade-offs in a wildfire-prone social-ecological system. *Environmental Research Letters*, 14(12):125017, 2019. ISSN 1748-9326. doi: 10.1088/1748-9326/ab59c1. 4, 20, 30, 49

[36] Julia Martinez-Fernandez, Isabel Banos-Gonzalez, and Miguel Angel Esteve-Selma. An integral approach to address socio-ecological systems sustainability and their uncertainties. *Science of The Total Environment*, 762:144457, 2021. ISSN 0048-9697. 4, 20

[37] Mark A. Adams. Mega-fires, tipping points and ecosystem services: Managing forests and woodlands in an uncertain future. *Forest Ecology and Management*, 294:250–261, 2013. ISSN 03781127. doi: 10.1016/j.foreco.2012.11.039. 5, 66

[38] Erin J. Hanan, Jianning Ren, Christina L. Tague, Crystal A. Kolden, John T. Abatzoglou, Ryan R. Bart, Maureen C. Kennedy, Mingliang Liu, and Jennifer C. Adam. How climate change and fire exclusion drive wildfire regimes at actionable scales. *Environmental Research Letters*, 16(2):024051, 2021. ISSN 1748-9326. doi: 10.1088/1748-9326/abd78e. 5

[39] Sally Archibald. Managing the human component of fire regimes: Lessons from Africa. *Philosophical Transactions of the Royal Society B: Biological Sciences*, 371(1696):20150346, 2016. doi: 10.1098/rstb.2015.0346. 5

[40] Paul Laris. On the problems and promises of savanna fire regime change. *Nature Communications*, 12(1):4891, 2021. ISSN 2041-1723. doi: 10.1038/s41467-021-25141-1. 5, 64

[41] Magnus Nyström, Albert V Norström, Thorsten Blenckner, Maricela de la Torre-Castro, Johan S Eklöf, Carl Folke, Henrik Österblom, Robert S Steneck, Matilda Thyresson, and Max Troell. Confronting feedbacks of degraded marine ecosystems. *Ecosystems (New York, N.Y.)*, 15(5):695–710, 2012. 5, 82, 83

[42] Egbert H. van Nes, Marten Scheffer, Victor Brovkin, Timothy M. Lenton, Hao Ye, Ethan Deyle, and George Sugihara. Causal feedbacks in climate change. *Nature Climate Change*, 5(5):445–448, 2015. ISSN 1758-678X, 1758-6798. doi: 10.1038/nclimate2568. 5, 30, 35, 45

[43] Christopher M Bishop. *Pattern Recognition and Machine Learning*. Springer, 2006. 6, 88

[44] Tatiana Filatova, J Gary Polhill, and Stijn Van Ewijk. Regime shifts in coupled socio-environmental systems: Review of modelling challenges and approaches. *Environmental modelling & software*, 75:333–347, 2016. ISSN 1364-8152. 6, 11, 18, 70, 71, 79, 84

[45] Graeme S Cumming and Garry D Peterson. Unifying research on social–ecological resilience and collapse. *Trends in Ecology & Evolution*, 32 (9):695–713, 2017. 6, 71, 82

[46] DW Schindler, FAJ Armstrong, SK Holmgren, and GJ Brunskill. Eutrophication of Lake 227, Experimental Lakes Area, northwestern Ontario, by addition of phosphate and nitrate. *Journal of the Fisheries Board of Canada*, 28(11):1763–1782, 1971. ISSN 0706-652X. 9, 10

[47] Marten Scheffer, Steve Carpenter, Jonathan A Foley, Carl Folke, and Brian Walker. Catastrophic shifts in ecosystems. *Nature*, 413(6856):591–596, 2001. ISSN 1476-4687. 9, 11, 82, 98, 99

[48] Mark Parascandola. Two approaches to etiology: The debate over smoking and lung cancer in the 1950s. *Endeavour*, 28(2):81–86, 2004. ISSN 0160-9327. 10

[49] Kaitlin Kimmel, Laura E Dee, Meghan L Avolio, and Paul J Ferraro. Causal assumptions and causal inference in ecological experiments. *Trends in Ecology & Evolution*, 36(12):1141–1152, 2021. ISSN 0169-5347. 10, 28, 29

[50] Suchinta Arif, Nicholas AJ Graham, Shaun Wilson, and M Aaron MacNeil. Causal drivers of climate-mediated coral reef regime shifts. *Ecosphere*, 13(3): e3956, 2022. ISSN 2150-8925. 10, 11, 29

[51] Jianguo Liu, Thomas Dietz, Stephen R Carpenter, Marina Alberti, Carl Folke, Emilio Moran, Alice N Pell, Peter Deadman, Timothy Kratz, and Jane Lubchenco. Complexity of coupled human and natural systems. *science*, 317 (5844):1513–1516, 2007. ISSN 0036-8075. 10

[52] Erica A. Newman, Maureen C. Kennedy, Donald A. Falk, and Donald McKenzie. Scaling and complexity in landscape ecology. *Frontiers in Ecology and Evolution*, 7:293, 2019. ISSN 2296-701X. doi: 10.3389/fevo.2019.00293. 10, 33, 110

[53] Anil Seth. Granger causality. *Scholarpedia*, 2(7):1667, 2007. 10, 13, 14, 16

[54] Francis Galton. Regression towards mediocrity in hereditary stature. *The Journal of the Anthropological Institute of Great Britain and Ireland*, 15: 246–263, 1886. 12

[55] Karl Pearson and Alice Lee. On the laws of inheritance in man: I. Inheritance of physical characters. *Biometrika*, 2(4):357–462, 1903. 12

[56] Karl Pearson. The grammar of science. *Nature*, 46(1185):247–247, 1892. 12

[57] Sewall Wright. Correlation and causation. *Journal of Agricultural Research*, 7(7):557–585, 1921. 12, 16

[58] Clive WJ Granger. Investigating causal relations by econometric models and cross-spectral methods. *Econometrica: journal of the Econometric Society*, pages 424–438, 1969. 13, 14, 15, 30

[59] Yonghong Chen, Steven L Bressler, and Mingzhou Ding. Frequency decomposition of conditional Granger causality and application to multivariate neural field potential data. *Journal of neuroscience methods*, 150(2):228–237, 2006. 14, 15

[60] Winrich A Freiwald, Pedro Valdes, Jorge Bosch, Rolando Biscay, Juan Carlos Jimenez, Luis Manuel Rodriguez, Valia Rodriguez, Andreas K Kreiter, and Wolf Singer. Testing non-linearity and directedness of interactions between neural groups in the macaque inferotemporal cortex. *Journal of neuroscience methods*, 94(1):105–119, 1999. 14

[61] Yonghong Chen, Govindan Rangarajan, Jianfeng Feng, and Mingzhou Ding. Analyzing multiple nonlinear time series with extended Granger causality. *Physics letters A*, 324(1):26–35, 2004. 14

[62] Nicola Ancona, Daniele Marinazzo, and Sebastiano Stramaglia. Radial basis function approach to nonlinear Granger causality of time series. *Physical Review E*, 70(5):056221, 2004. 14

[63] Frédéric Barraquand, Coralie Picoche, Matteo Detto, and Florian Hartig. Inferring species interactions using Granger causality and convergent cross mapping. *Theoretical Ecology*, 14(1):87–105, 2021. 14, 15

[64] Clive William John Granger and Paul Newbold. *Forecasting Economic Time Series*. Academic Press, 2014. 15, 38

[65] Karl J Friston, André M Bastos, Ashwini Oswal, Bernadette van Wijk, Craig Richter, and Vladimir Litvak. Granger causality revisited. *Neuroimage*, 101: 796–808, 2014. 15

[66] Sewall Wright. The relative importance of heredity and environment in determining the piebald pattern of guinea-pigs. *Proceedings of the National Academy of Sciences of the United States of America*, 6(6):320, 1920. 15, 16

[67] Arthur S Goldberger. Structural equation methods in the social sciences. *Econometrica: Journal of the Econometric Society*, pages 979–1001, 1972. 16

[68] Judea Pearl. Graphs, causality, and structural equation models. *Sociological Methods & Research*, 27(2):226–284, 1998. 16, 30, 45

[69] Kenneth A Bollen and Judea Pearl. Eight myths about causality and structural equation models. In *Handbook of Causal Analysis for Social Research*, pages 301–328. Springer, 2013. 16, 44

[70] Sylvain Christin, Éric Hervet, and Nicolas Lecomte. Applications for deep learning in ecology. *Methods in Ecology and Evolution*, 10(10):1632–1644, 2019. ISSN 2041-210X. doi: 10.1111/2041-210X.13256. 17, 22, 29

[71] Mark D Verhagen. Identifying Model Complexity: A Machine Learning Framework. 2021. 17, 29, 45

[72] Holger Schielzeth. Simple means to improve the interpretability of regression coefficients. *Methods in Ecology and Evolution*, 1(2):103–113, 2010. ISSN 2041-210X. doi: 10.1111/j.2041-210X.2010.00012.x. 17, 29

[73] Christoph Molnar. *Interpretable Machine Learning*. lulu.com, 2020. 17, 30, 31, 37

[74] Sally S.-C. Wang, Yun Qian, L. Ruby Leung, and Yang Zhang. Interpretable machine learning prediction of fire emissions and comparison with FireMIP process-based models. Preprint, Biosphere Interactions/Atmospheric Modelling/Troposphere/Physics (physical properties and processes), 2021. 20, 21, 22, 37, 44

[75] Cynthia Rudin. Stop explaining black box machine learning models for high stakes decisions and use interpretable models instead. *Nature Machine Intelligence*, 1(5):206–215, 2019. 17

[76] Scott M Lundberg and Su-In Lee. A unified approach to interpreting model predictions. In *Advances in Neural Information Processing Systems*, volume 30. Curran Associates, Inc., 2017. 17, 31, 37

[77] Erik Štrumbelj and Igor Kononenko. Explaining prediction models and individual predictions with feature contributions. *Knowledge and Information Systems*, 41(3):647–665, 2014. ISSN 0219-1377, 0219-3116. doi: 10.1007/s10115-013-0679-x. 17, 37

[78] Volker Grimm. Mathematical models and understanding in ecology. *Ecological modelling*, 75:641–651, 1994. 18, 79

[79] David J Currie. Where Newton might have taken ecology. *Global ecology and biogeography*, 28(1):18–27, 2019. 18

[80] Gerhard Krinner, Nicolas Viovy, Nathalie de Noblet-Ducoudré, Jérôme Ogée, Jan Polcher, Pierre Friedlingstein, Philippe Ciais, Stephen Sitch, and I Colin Prentice. A dynamic global vegetation model for studies of the coupled atmosphere-biosphere system. *Global Biogeochemical Cycles*, 19(1), 2005. 18, 79

[81] Steven H Strogatz. Nonlinear dynamics and chaos: With applications to physics, biology, chemistry, and engineering. pages 72–86. CRC Press, 2018. 18, 75, 76, 98

[82] Robert M May and George F Oster. Bifurcations and dynamic complexity in simple ecological models. *The American Naturalist*, 110(974):573–599, 1976. ISSN 0003-0147. 18, 79

[83] Stephen R Carpenter. Ecological futures: Building an ecology of the long now. *Ecology*, 83(8):2069–2083, 2002. 18

[84] Matthew R Evans, Volker Grimm, Karin Johst, Tarja Knuuttila, Rogier De Langhe, Catherine M Lessells, Martina Merz, Maureen A O'Malley, Steve H Orzack, Michael Weisberg, et al. Do simple models lead to generality in ecology? *Trends in ecology & evolution*, 28(10):578–583, 2013. 18

[85] Marten Scheffer and Stephen R Carpenter. Catastrophic regime shifts in ecosystems: Linking theory to observation. *Trends in Ecology & Evolution*, 18(12):648–656, 2003. 18, 46, 70, 71, 82, 84, 91, 98

[86] Xi Zhang, Xingrong Zhao, Zhujun Jiang, and Shuai Shao. How to achieve the 2030 CO2 emission-reduction targets for China's industrial sector: Retrospective decomposition and prospective trajectories. *Global environmental change*, 44:83–97, 2017. ISSN 0959-3780. 19

[87] Junnian Wu, Guangying Pu, Yan Guo, Jingwen Lv, and Jiangwei Shang. Retrospective and prospective assessment of exergy, life cycle carbon emissions, and water footprint for coking network evolution in China. *Applied Energy*, 218:479–493, 2018. 19

[88] Rob J Swart, Paul Raskin, and John Robinson. The problem of the future: Sustainability science and scenario analysis. *Global environmental change*, 14(2):137–146, 2004. 19

[89] SP Seitzinger, E Mayorga, AF Bouwman, C Kroeze, AHW Beusen, G Billen, G Van Drecht, E Dumont, BM Fekete, J Garnier, et al. Global river nutrient export: A scenario analysis of past and future trends. *Global Biogeochemical Cycles*, 24(4), 2010. 19

[90] Aaron M Ellison. Bayesian inference in ecology. *Ecology letters*, 7(6):509–520, 2004. 19, 83

[91] Sean R Connolly, Sally A Keith, Robert K Colwell, and Carsten Rahbek. Process, mechanism, and modeling in macroecology. *Trends in Ecology & Evolution*, 32(11):835–844, 2017. 19

[92] Trevor J Hefley, Mevin B Hooten, Robin E Russell, Daniel P Walsh, and James A Powell. When mechanism matters: Bayesian forecasting using models of ecological diffusion. *Ecology Letters*, 20(5):640–650, 2017. 19

[93] Anna C Talucci, Michael M Loranty, and Heather D Alexander. Siberian taiga and tundra fire regimes from 2001–2020. *Environmental Research Letters*, 17(2):025001, 2022. ISSN 1748-9326. doi: 10.1088/1748-9326/ac3f07. 19, 20, 22, 63, 64, 79

[94] Jocelyne Shimin Sze, Jefferson, and Janice Ser Huay Lee. Evaluating the social and environmental factors behind the 2015 extreme fire event in Sumatra, Indonesia. *Environmental Research Letters*, 14(1):015001, 2019. ISSN 1748-9326. doi: 10.1088/1748-9326/aaee1d. 19, 20, 22, 45, 49

[95] Stijn Hantson, Salvador Pueyo, and Emilio Chuvieco. Global fire size distribution is driven by human impact and climate. *Global Ecology and Biogeography*, 24(1):77–86, 2015. ISSN 1466-822X. 20

[96] Matthias Forkel, Wouter Dorigo, Gitta Lasslop, Emilio Chuvieco, Stijn Hantson, Angelika Heil, Irene Teubner, Kirsten Thonicke, and Sandy P Harrison. Recent global and regional trends in burned area and their compensating environmental controls. *Environmental Research Communications*, 1 (5):051005, 2019. ISSN 2515-7620. doi: 10.1088/2515-7620/ab25d2. 20, 48

[97] Vivek K Arora and Joe R Melton. Reduction in global area burned and wildfire emissions since 1930s enhances carbon uptake by land. *Nature Communications*, 9(1):1–10, 2018. ISSN 2041-1723. 20

[98] Paulo Eduardo Barni, Anelícia Cleide Martins Rego, Francisco das Chagas Ferreira Silva, Richard Anderson Silva Lopes, Haron Abrahim Magalhaes Xaud, Maristela Ramalho Xaud, Reinaldo Imbrozio Barbosa, and Philip Martin Fearnside. Logging Amazon forest increased the severity and spread of fires during the 2015–2016 El Nino. *Forest Ecology and Management*, 500: 119652, 2021. ISSN 0378-1127. 20, 46, 63, 70, 78, 101

[99] Robert D. Field, Guido R. van der Werf, Thierry Fanin, Eric J. Fetzer, Ryan Fuller, Hiren Jethva, Robert Levy, Nathaniel J. Livesey, Ming Luo, Omar Torres, and Helen M. Worden. Indonesian fire activity and smoke pollution in 2015 show persistent nonlinear sensitivity to El Niño-induced drought. *Proceedings of the National Academy of Sciences*, 113(33):9204–9209, 2016. ISSN 0027-8424, 1091-6490. doi: 10.1073/pnas.1524888113. 20, 22, 49, 64, 74, 78

[100] Cathy Whitlock, Philip E Higuera, David B McWethy, and Christy E Briles. Paleoecological perspectives on fire ecology: Revisiting the fire-regime concept. *The Open Ecology Journal*, 3(1), 2010. 20

[101] Bo Zheng, Philippe Ciais, Frederic Chevallier, Emilio Chuvieco, Yang Chen, and Hui Yang. Increasing forest fire emissions despite the decline in global burned area. *Science Advances*, 7(39):eabh2646, 2021. ISSN 2375-2548. doi: 10.1126/sciadv.abh2646. 20, 21, 22, 48, 49, 63

[102] Xu Yue and Nadine Unger. Fire air pollution reduces global terrestrial productivity. *Nature communications*, 9(1):1–9, 2018. ISSN 2041-1723. 20

[103] Pierre Friedlingstein, Michael O'Sullivan, Matthew W. Jones, Robbie M. Andrew, Judith Hauck, Are Olsen, Glen P. Peters, Wouter Peters, Julia Pongratz, Stephen Sitch, Corinne Le Quéré, Josep G. Canadell, Philippe Ciais, Robert B. Jackson, Simone Alin, Luiz E. O. C. Aragão, Almut Arneth, Vivek Arora, Nicholas R. Bates, Meike Becker, Alice Benoit-Cattin, Henry C. Bittig, Laurent Bopp, Selma Bultan, Naveen Chandra, Frédéric Chevallier, Louise P. Chini, Wiley Evans, Liesbeth Florentie, Piers M. Forster, Thomas Gasser, Marion Gehlen, Dennis Gilfillan, Thanos Gkritzalis, Luke Gregor, Nicolas Gruber, Ian Harris, Kerstin Hartung, Vanessa Haverd, Richard A. Houghton, Tatiana Ilyina, Atul K. Jain, Emilie Joetzjer, Koji Kadono, Etsushi Kato, Vassilis Kitidis, Jan Ivar Korsbakken, Peter Landschützer, Nathalie Lefèvre, Andrew Lenton, Sebastian Lienert, Zhu Liu, Danica Lombardozzi, Gregg Marland, Nicolas Metzl, David R. Munro, Julia E. M. S. Nabel, Shin-Ichiro Nakaoka, Yosuke Niwa, Kevin O'Brien, Tsuneo Ono, Paul I. Palmer, Denis Pierrot, Benjamin Poulter, Laure Resplandy, Eddy Robertson, Christian Rödenbeck, Jörg Schwinger, Roland Séférian, Ingunn Skjelvan, Adam J. P. Smith, Adrienne J. Sutton, Toste Tanhua, Pieter P. Tans, Hanqin Tian, Bronte Tilbrook, Guido van der Werf, Nicolas Vuichard, Anthony P. Walker, Rik Wanninkhof, Andrew J. Watson, David Willis, Andrew J. Wiltshire, Wenping Yuan, Xu Yue, and Sönke Zaehle. Global carbon budget 2020. *Earth System Science Data*, 12(4):3269–3340, 2020. ISSN 1866-3508. doi: 10.5194/essd-12-3269-2020. 20, 22, 48

[104] Matthew W Jones, Cristina Santín, Guido R van der Werf, and Stefan H Doerr. Global fire emissions buffered by the production of pyrogenic carbon. *Nature Geoscience*, 12(9):742–747, 2019. ISSN 1752-0908. 20, 109

[105] Bailu Zhao, Qianlai Zhuang, Narasinha Shurpali, Kajar Köster, Frank Berninger, and Jukka Pumpanen. North American boreal forests are a large carbon source due to wildfires from 1986 to 2016. *Scientific Reports*, 11(1): 1–14, 2021. ISSN 2045-2322. 20

[106] Jennifer K Balch, John T Abatzoglou, Maxwell B Joseph, Michael J Koontz, Adam L Mahood, Joseph McGlinchy, Megan E Cattau, and A Park Williams. Warming weakens the night-time barrier to global fire. *Nature*, 602(7897): 442–448, 2022. ISSN 1476-4687. 20, 62, 78

[107] Guido R van der Werf, James T Randerson, Louis Giglio, Thijs T Van Leeuwen, Yang Chen, Brendan M Rogers, Mingquan Mu, Margreet JE Van Marle, Douglas C Morton, and G James Collatz. Global fire emissions estimates during 1997–2016. *Earth System Science Data*, 9(2):697–720, 2017. ISSN 1866-3508. 20, 21, 33, 34, 48, 49, 62, 65, 101

[108] N. Andela, D.C. Morton, L. Giglio, Y. Chen, G.R. van der Werf, P.S. Kasibhatla, R. S. DeFries, G. J. Collatz, S. Hantson, S. Kloster, D. Bachelet, M. Forrest, G. Lasslop, F. Li, S. Mangeon, J. R. Melton, C. Yue, and J.T. Randerson. A human-driven decline in global burned area. *Science*, 356 (6345):1356–1362, 2017. ISSN 0036-8075. doi: 10.1126/science.aal4108. 20, 45, 48, 49, 62, 63, 65

[109] W Knorr, A Arneth, and L Jiang. Demographic controls of future global fire risk. *Nature Climate Change*, 6(8):781–785, 2016. ISSN 1758-6798. 20, 45, 62, 63, 78

[110] Ben Collen and Emily Nicholson. Taking the measure of change. *Science*, 346(6206):166–167, 2014. ISSN 0036-8075. 20

[111] Douglas I Kelley, Ioannis Bistinas, Rhys Whitley, Chantelle Burton, Toby R Marthews, and Ning Dong. How contemporary bioclimatic and human controls change global fire regimes. *Nature Climate Change*, 9(9):690–696, 2019. ISSN 1758-6798. 20, 45, 48, 49, 52, 62, 65, 109, 113

[112] Lahiru S. Wijedasa, Jyrki Jauhiainen, Mari Könönen, Maija Lampela, Harri Vasander, Marie-Claire Leblanc, Stephanie Evers, Thomas E. L. Smith, Catherine M. Yule, Helena Varkkey, Massimo Lupascu, Faizal Parish, Ian Singleton, Gopalasamy R. Clements, Sheema Abdul Aziz, Mark E. Harrison, Susan Cheyne, Gusti Z. Anshari, Erik Meijaard, Jenny E. Goldstein, Susan Waldron, Kristell Hergoualc'h, Rene Dommain, Steve Frolking, Christopher D. Evans, Mary Rose C. Posa, Paul H. Glaser, Nyoman Suryadiputra, Reza Lubis, Truly Santika, Rory Padfield, Sofyan Kurnianto, Panut Hadisiswoyo, Teck Wyn Lim, Susan E. Page, Vincent Gauci, Peter J. Van Der Meer, Helen Buckland, Fabien Garnier, Marshall K. Samuel, Liza Nuriati Lim Kim Choo, Patrick O'Reilly, Matthew Warren, Surin Suksuwan, Elham Sumarga, Anuj Jain, William F. Laurance, John Couwenberg, Hans Joosten, Ronald

Vernimmen, Aljosja Hooijer, Chris Malins, Mark A. Cochrane, Balu Perumal, Florian Siegert, Kelvin S.-H. Peh, Louis-Pierre Comeau, Louis Verchot, Charles F. Harvey, Alex Cobb, Zeehan Jaafar, Henk Wösten, Solichin Manuri, Moritz Müller, Wim Giesen, Jacob Phelps, Ding Li Yong, Marcel Silvius, Béatrice M. M. Wedeux, Alison Hoyt, Mitsuru Osaki, Takashi Hirano, Hidenori Takahashi, Takashi S. Kohyama, Akira Haraguchi, Nunung P. Nugroho, David A. Coomes, Le Phat Quoi, Alue Dohong, Haris Gunawan, David L. A. Gaveau, Andreas Langner, Felix K. S. Lim, David P. Edwards, Xingli Giam, Guido Van Der Werf, Rachel Carmenta, Caspar C. Verwer, Luke Gibson, Laure Gandois, Laura Linda Bozena Graham, Jhanson Regalino, Serge A. Wich, Jack Rieley, Nicholas Kettridge, Chloe Brown, Romain Pirard, Sam Moore, B. Ripoll Capilla, Uwe Ballhorn, Hua Chew Ho, Agata Hoscilo, Sandra Lohberger, Theodore A. Evans, Nina Yulianti, Grace Blackham, Onrizal, Simon Husson, Daniel Murdiyarso, Sunita Pangala, Lydia E. S. Cole, Luca Tacconi, Hendrik Segah, Prayoto Tonoto, Janice S. H. Lee, Gerald Schmilewski, Stephan Wulffraat, Erianto Indra Putra, Megan E. Cattau, R. S. Clymo, Ross Morrison, Aazani Mujahid, Jukka Miettinen, Soo Chin Liew, Samu Valpola, David Wilson, Laura D'Arcy, Michiel Gerding, Siti Sundari, Sara A. Thornton, Barbara Kalisz, Stephen J. Chapman, Ahmad Suhaizi Mat Su, Imam Basuki, Masayuki Itoh, Carl Traeholt, Sean Sloan, Alexander K. Sayok, and Roxane Andersen. Denial of long-term issues with agriculture on tropical peatlands will have devastating consequences. *Global Change Biology*, 23(3):977–982, 2017. ISSN 13541013. doi: 10.1111/gcb.13516. 20

[113] William S. Symes, David P. Edwards, Jukka Miettinen, Frank E. Rheindt, and L. Roman Carrasco. Combined impacts of deforestation and wildlife trade on tropical biodiversity are severely underestimated. *Nature Communications*, 9(1):4052, 2018. ISSN 2041-1723. doi: 10.1038/s41467-018-06579-2. 20

[114] Xiaohua Pan, Charles Ichoku, Mian Chin, Huisheng Bian, Anton Darmenov, Peter Colarco, Luke Ellison, Tom Kucsera, Arlindo da Silva, Jun Wang, Tomohiro Oda, and Ge Cui. Six global biomass burning emission datasets: Intercomparison and application in one global aerosol model. *Atmospheric Chemistry and Physics*, 20(2):969–994, 2020. ISSN 1680-7316. doi: 10.5194/acp-20-969-2020. 21, 49, 64

[115] Ruben Ramo, Ekhi Roteta, Ioannis Bistinas, Dave van Wees, Aitor Bastarrika, Emilio Chuvieco, and Guido R. van der Werf. African burned area and fire carbon emissions are strongly impacted by small fires undetected by coarse resolution satellite data. *Proceedings of the National Academy of Sciences*, 118(9):e2011160118, 2021. ISSN 0027-8424, 1091-6490. doi: 10.1073/pnas.2011160118. 21, 64

[116] Christopher J Dunn, Christopher D O'Connor, Jesse Abrams, Matthew P Thompson, Dave E Calkin, James D Johnston, Rick Stratton, and Julie

Gilbertson-Day. Wildfire risk science facilitates adaptation of fire-prone social-ecological systems to the new fire reality. *Environmental Research Letters*, 15(2):025001, 2020. ISSN 1748-9326. 22, 70

[117] Shane R Coffield, Casey A Graff, Yang Chen, Padhraic Smyth, Efi Foufoula-Georgiou, and James T Randerson. Machine learning to predict final fire size at the time of ignition. *International journal of wildland fire*, 28(11):861–873, 2019. ISSN 1448-5516. 22

[118] Max A Little and Reham Badawy. Causal bootstrapping. *arXiv preprint arXiv:1910.09648*, 2019. 28

[119] Huajun Liu, Mingyu Lei, Naixin Zhang, and Guangjie Du. The causal nexus between energy consumption, carbon emissions and economic growth: New evidence from China, India and G7 countries using convergent cross mapping. *PloS one*, 14(5):e0217319, 2019. ISSN 1932-6203. 29

[120] Stefanie Muff, Leonhard Held, and Lukas F Keller. Marginal or conditional regression models for correlated non-normal data? *Methods in Ecology and Evolution*, 7(12):1514–1524, 2016. ISSN 2041-210X. 29

[121] Judea Pearl. Theoretical impediments to machine learning with seven sparks from the causal revolution. *arXiv preprint arXiv:1801.04016*, 2018. 29

[122] Christoph Molnar, Giuseppe Casalicchio, and Bernd Bischl. Interpretable machine learning–a brief history, state-of-the-art and challenges. In *Joint European Conference on Machine Learning and Knowledge Discovery in Databases*, pages 417–431. Springer, 2020. 29, 37

[123] GB Arhonditsis, CA Stow, LJ Steinberg, MA Kenney, RC Lathrop, SJ McBride, and KH Reckhow. Exploring ecological patterns with structural equation modeling and Bayesian analysis. *Ecological Modelling*, 192 (3-4):385–409, 2006. 30, 83

[124] Arif Masrur, Manzhu Yu, Prasenjit Mitra, Donna Peuquet, and Alan Taylor. Interpretable machine learning for analysing heterogeneous drivers of geographic events in space-time. *International Journal of Geographical Information Science*, 36(4):692–719, 2022. ISSN 1365-8816. 30

[125] Andreas C Müller and Sarah Guido. *Introduction to Machine Learning with Python: A Guide for Data Scientists*. " O'Reilly Media, Inc.", 2016. ISBN 1-4493-6990-1. 31

[126] J. T. Randerson, Y. Chen, G. R. van der Werf, B. M. Rogers, and D. C. Morton. Global burned area and biomass burning emissions from small fires. *Journal of Geophysical Research: Biogeosciences*, 117(G4), 2012. ISSN 2156-2202. doi: 10.1029/2012JG002128. 33

[127] Louis Giglio, James T. Randerson, and Guido R. van der Werf. Analysis of daily, monthly, and annual burned area using the fourth-generation global fire emissions database (GFED4). *Journal of Geophysical Research: Biogeosciences*, 118(1):317–328, 2013. ISSN 2169-8961. doi: 10.1002/jgrg.20042. 33, 49

[128] A Huete, K Didan, T Miura, E.P Rodriguez, X Gao, and L.G Ferreira. Overview of the radiometric and biophysical performance of the MODIS vegetation indices. *Remote Sensing of Environment*, 83(1-2):195–213, 2002. ISSN 00344257. doi: 10.1016/S0034-4257(02)00096-2. 33

[129] Guolin Ke, Qi Meng, Thomas Finley, Taifeng Wang, Wei Chen, Weidong Ma, Qiwei Ye, and Tie-Yan Liu. LightGBM: A highly efficient gradient boosting decision tree. In *Advances in Neural Information Processing Systems*, volume 30. Curran Associates, Inc., 2017. 33, 39, 52

[130] Arie Staal, Egbert H van Nes, Stijn Hantson, Milena Holmgren, Stefan C Dekker, Salvador Pueyo, Chi Xu, and Marten Scheffer. Resilience of tropical tree cover: The roles of climate, fire, and herbivory. *Global Change Biology*, 24(11):5096–5109, 2018. ISSN 1354-1013. 33, 79, 110

[131] Adam Thomas Clark, Hao Ye, Forest Isbell, Ethan R. Deyle, Jane Cowles, G. David Tilman, and George Sugihara. Spatial convergent cross mapping to detect causal relationships from short time series. *Ecology*, 96(5):1174–1181, 2015. ISSN 1939-9170. doi: 10.1890/14-1479.1. 35, 52

[132] Adam Clark. multispatialCCM: Multispatial Convergent Cross Mapping, 2014. 35, 39, 52

[133] David M. Olson, Eric Dinerstein, Eric D. Wikramanayake, Neil D. Burgess, George V. N. Powell, Emma C. Underwood, Jennifer A. D'amico, Illanga Itoua, Holly E. Strand, John C. Morrison, Colby J. Loucks, Thomas F. Allnutt, Taylor H. Ricketts, Yumiko Kura, John F. Lamoreux, Wesley W. Wettengel, Prashant Hedao, and Kenneth R. Kassem. Terrestrial ecoregions of the world: A new map of life on earth. *BioScience*, 51(11):933, 2001. ISSN 0006-3568. doi: 10.1641/0006-3568(2001)051[0933:TEOTWA]2.0.CO;2. 35, 52, 63, 79, 113

[134] Gavin C Cawley and Nicola L C Talbot. On over-fitting in model selection and subsequent selection bias in performance evaluation. *Journal of Machine Learning Research*, 11:2079–2107, 2010. 37

[135] Scott M. Lundberg, Gabriel Erion, Hugh Chen, Alex DeGrave, Jordan M. Prutkin, Bala Nair, Ronit Katz, Jonathan Himmelfarb, Nisha Bansal, and Su-In Lee. From local explanations to global understanding with explainable AI for trees. *Nature Machine Intelligence*, 2(1):56–67, 2020. ISSN 2522-5839. doi: 10.1038/s42256-019-0138-9. 37, 39, 52

[136] Zhenyue Zhang and Hongyuan Zha. Principal manifolds and nonlinear dimensionality reduction via tangent space alignment. *SIAM journal on scientific computing*, 26(1):313–338, 2004. ISSN 1064-8275. 38

[137] Markus Ringnér. What is principal component analysis? *Nature biotechnology*, 26(3):303–304, 2008. ISSN 1546-1696.

[138] Alexander N Gorban, Balázs Kégl, Donald C Wunsch, and Andrei Y Zinovyev. *Principal Manifolds for Data Visualization and Dimension Reduction*, volume 58. Springer, 2008. 38

[139] Benson Mwangi, Tian Siva Tian, and Jair C Soares. A review of feature reduction techniques in neuroimaging. *Neuroinformatics*, 12(2):229–244, 2014. ISSN 1559-0089. 38

[140] Michel Verleysen and Damien François. The curse of dimensionality in data mining and time series prediction. In *International Work-Conference on Artificial Neural Networks*, pages 758–770. Springer, 2005. 38

[141] R Core Team. R: A Language and Environment for Statistical Computing, 2021. 39, 52

[142] Fabian Pedregosa, Gael Varoquaux, Alexandre Gramfort, Vincent Michel, Bertrand Thirion, Olivier Grisel, Mathieu Blondel, Peter Prettenhofer, Ron Weiss, Vincent Dubourg, Jake Vanderplas, Alexandre Passos, and David Cournapeau. Scikit-learn: Machine Learning in Python. *Journal of Machine Learning Research*, 12:2825–2830, 2011. 39, 52

[143] Van Rossum Guido and Drake L., Fred. *Python 3 Reference Manual*. CreateSpace, 2009. ISBN 1-4414-1269-7. 39, 52

[144] Paul J Ferraro and Merlin M Hanauer. Advances in measuring the environmental and social impacts of environmental programs. *Annual review of environment and resources*, 39(1):495–517, 2014. 44

[145] Chao Wu, Sergey Venevsky, Stephen Sitch, Lina M Mercado, Chris Huntingford, and A Carla Staver. Historical and future global burned area with changing climate and human demography. *One Earth*, 4(4):517–530, 2021. 45, 62, 64

[146] Carl Folke, Steve Carpenter, Brian Walker, Marten Scheffer, Thomas Elmqvist, Lance Gunderson, and Crawford Stanley Holling. Regime shifts, resilience, and biodiversity in ecosystem management. *Annual Review of Ecology, Evolution, and Systematics*, 35:557–581, 2004. 46, 70, 79, 82, 84, 98

[147] Zsigmond Benkő, Adám Zlatniczki, Marcell Stippinger, Dániel Fabó, András Sólyom, Loránd Erőss, András Telcs, and Zoltán Somogyvári. Complete inference of causal relations between dynamical systems. *arXiv preprint arXiv:1808.10806*, 2018. 46

[148] Edward De Brouwer, Adam Arany, Jaak Simm, and Yves Moreau. Latent convergent cross mapping. In *International Conference on Learning Representations*, 2021. 46

[149] Gareth P Hempson, Sally Archibald, and William J Bond. The consequences of replacing wildlife with livestock in Africa. *Scientific Reports*, 7(1):1–10, 2017. ISSN 2045-2322. 48

[150] Adam F. A. Pellegrini, Anders Ahlström, Sarah E. Hobbie, Peter B. Reich, Lars P. Nieradzik, A. Carla Staver, Bryant C. Scharenbroch, Ari Jumpponen, William R. L. Anderegg, James T. Randerson, and Robert B. Jackson. Fire frequency drives decadal changes in soil carbon and nitrogen and ecosystem productivity. *Nature*, 553(7687):194–198, 2018. ISSN 0028-0836, 1476-4687. doi: 10.1038/nature24668. 48

[151] Xanthe J Walker, Brendan M Rogers, Jennifer L Baltzer, Steven G Cumming, Nicola J Day, Scott J Goetz, Jill F Johnstone, Edward AG Schuur, Merritt R Turetsky, and Michelle C Mack. Cross-scale controls on carbon emissions from boreal forest megafires. *Global Change Biology*, 24(9):4251–4265, 2018. ISSN 1354-1013. 49

[152] L Giglio. Global estimation of burned area using MODIS active fire observations. *Atmos. Chem. Phys.*, page 18, 2006. 49, 101, 113

[153] Kimberly M. Carlson, Robert Heilmayr, Holly K. Gibbs, Praveen Noojipady, David N. Burns, Douglas C. Morton, Nathalie F. Walker, Gary D. Paoli, and Claire Kremen. Effect of oil palm sustainability certification on deforestation and fire in Indonesia. *Proceedings of the National Academy of Sciences*, 115(1):121–126, 2018. ISSN 0027-8424, 1091-6490. doi: 10.1073/pnas.1704728114. 49

[154] Andreas Muhlbauer, Peter Spichtinger, and Ulrike Lohmann. Application and comparison of robust linear regression methods for trend estimation. *Journal of Applied Meteorology and Climatology*, 48(9):1961–1970, 2009. ISSN 1558-8432. 51

[155] Peter J Huber. Robust estimation of a location parameter. In *Breakthroughs in Statistics*, pages 492–518. Springer, 1992. 51

[156] Eric R Ziegel. Modern applied statistics with S. *Technometrics*, 45(1):111, 2003. ISSN 0040-1706. 52

[157] Martin Maechler. Sfsmisc: Utilities from 'Seminar fuer Statistik' ETH Zurich, 2020. 52

[158] Jean Marchal, Steven G Cumming, and Eliot JB McIntire. Turning down the heat: Vegetation feedbacks limit fire regime responses to global warming. *Ecosystems*, 23(1):204–216, 2020. ISSN 1435-0629. 62

[159] Hiren Jethva, Omar Torres, Robert D Field, Alexei Lyapustin, Ritesh Gautam, and Vinay Kayetha. Connecting crop productivity, residue fires, and air quality over northern India. *Scientific Reports*, 9(1):1–11, 2019. ISSN 2045-2322. 63

[160] Carlos A Nobre, Gilvan Sampaio, Laura S Borma, Juan Carlos Castilla-Rubio, José S Silva, and Manoel Cardoso. Land-use and climate change risks in the Amazon and the need of a novel sustainable development paradigm. *Proceedings of the National Academy of Sciences*, 113(39):10759–10768, 2016. ISSN 0027-8424. 63, 64, 66, 70, 106

[161] R Libonati, JMC Pereira, CC Da Camara, LF Peres, D Oom, JA Rodrigues, FLM Santos, RM Trigo, CMP Gouveia, and F Machado-Silva. Twenty-first century droughts have not increasingly exacerbated fire season severity in the Brazilian Amazon. *Scientific Reports*, 11(1):1–13, 2021. ISSN 2045-2322. 63, 106

[162] G. R. van der Werf, J. T. Randerson, L. Giglio, G. J. Collatz, P. S. Kasibhatla, and A. F. Arellano. Interannual variability in global biomass burning emissions from 1997 to 2004. *Atmospheric Chemistry and Physics*, 6(11): 3423–3441, 2006. ISSN 1680-7324. doi: 10.5194/acp-6-3423-2006. 63, 113

[163] Viacheslav I Kharuk, Evgenii I Ponomarev, Galina A Ivanova, Maria L Dvinskaya, Sean CP Coogan, and Mike D Flannigan. Wildfires in the Siberian taiga. *Ambio*, 50(11):1953–1974, 2021. ISSN 1654-7209. 63

[164] Sujay Kumar, Augusto Getirana, Renata Libonati, Christopher Hain, Sarith Mahanama, and Niels Andela. Changes in land use enhance the sensitivity of tropical ecosystems to fire-climate extremes. *Scientific Reports*, 12(1):1–11, 2022. ISSN 2045-2322. 64

[165] Michael L Humber, Luigi Boschetti, Louis Giglio, and Christopher O Justice. Spatial and temporal intercomparison of four global burned area products. *International Journal of Digital Earth*, 12(4):460–484, 2019. ISSN 1753-8947. 64

[166] Kees Klein Goldewijk, Arthur Beusen, Gerard Van Drecht, and Martine De Vos. The HYDE 3.1 spatially explicit database of human-induced global land-use change over the past 12,000 years. *Global Ecology and Biogeography*, 20(1):73–86, 2011. ISSN 1466-822X. 65

[167] Yuqi Hu, Nieves Fernandez-Anez, Thomas EL Smith, and Guillermo Rein. Review of emissions from smouldering peat fires and their contribution to regional haze episodes. *International Journal of Wildland Fire*, 27(5):293–312, 2018. ISSN 1448-5516. 65

[168] Nathan C Dadap, Alexander R Cobb, Alison M Hoyt, Charles F Harvey, and Alexandra G Konings. Satellite soil moisture observations predict burned area in Southeast Asian peatlands. *Environmental Research Letters*, 14(9): 094014, 2019. ISSN 1748-9326. doi: 10.1088/1748-9326/ab3891. 65

[169] Bert Wuyts, Alan R Champneys, and Joanna I House. Amazonian forest-savanna bistability and human impact. *Nature Communications*, 8(1):1–12, 2017. ISSN 2041-1723. 66, 70, 101, 106

[170] Xiyan Xu, Gensuo Jia, Xiaoyan Zhang, William J Riley, and Ying Xue. Climate regime shift and forest loss amplify fire in Amazonian forests. *Global change biology*, 26(10):5874–5885, 2020. ISSN 1354-1013. 70

[171] G. R. van der Werf, J. Dempewolf, S. N. Trigg, J. T. Randerson, P. S. Kasibhatla, L. Giglio, D. Murdiyarso, W. Peters, D. C. Morton, G. J. Collatz, A. J. Dolman, and R. S. DeFries. Climate regulation of fire emissions and deforestation in equatorial Asia. *Proceedings of the National Academy of Sciences*, 105(51):20350–20355, 2008. ISSN 0027-8424, 1091-6490. doi: 10.1073/pnas.0803375105. 70, 78

[172] Kiunnei Kirillina, Evgeny G Shvetsov, Viktoriya V Protopopova, Lynn Thiesmeyer, and Wanglin Yan. Consideration of anthropogenic factors in boreal forest fire regime changes during rapid socio-economic development: Case study of forestry districts with increasing burnt area in the Sakha Republic, Russia. *Environmental Research Letters*, 15(3):035009, 2020. ISSN 1748-9326. 70

[173] John J. Battles, Timothy Robards, Adrian Das, Kristen Waring, J. Keith Gilless, Gregory Biging, and Frieder Schurr. Climate change impacts on forest growth and tree mortality: A data-driven modeling study in the mixed-conifer forest of the Sierra Nevada, California. *Climatic Change*, 87(1):193–213, 2008. ISSN 1573-1480. doi: 10.1007/s10584-007-9358-9. 70, 78

[174] Alan J Tepley, Enrique Thomann, Thomas T Veblen, George LW Perry, Andrés Holz, Juan Paritsis, Thomas Kitzberger, and Kristina J Anderson-Teixeira. Influences of fire–vegetation feedbacks and post-fire recovery rates on forest landscape vulnerability to altered fire regimes. *Journal of Ecology*, 106(5):1925–1940, 2018. ISSN 0022-0477. 70

[175] Brian J Harvey, Daniel C Donato, and Monica G Turner. Burn me twice, shame on who? Interactions between successive forest fires across a temperate mountain region. *Ecology*, 97(9):2272–2282, 2016. ISSN 0012-9658. 70

[176] Robert M May. Simple mathematical models with very complicated dynamics. In *The Theory of Chaotic Attractors*, pages 85–93. Springer, 2004. 70, 71

[177] Timothy FH Allen and Thomas W Hoekstra. *Toward a Unified Ecology*. Columbia University Press, 2015. 71, 84

[178] Stephen R Carpenter, Kenneth J Arrow, Scott Barrett, Reinette Biggs, William A Brock, Anne-Sophie Crépin, Gustav Engström, Carl Folke, Terry P Hughes, Nils Kautsky, et al. General resilience to cope with extreme events. *Sustainability*, 4(12):3248–3259, 2012. 71, 83, 98

[179] E. Schertzer, A. C. Staver, and S. A. Levin. Implications of the spatial dynamics of fire spread for the bistability of savanna and forest. *Journal of Mathematical Biology*, 70(1-2):329–341, 2015. ISSN 0303-6812, 1432-1416. doi: 10.1007/s00285-014-0757-z. 71, 72, 73, 74

[180] Robert M May. Thresholds and breakpoints in ecosystems with a multiplicity of stable states. *Nature*, 269(5628):471, 1977. 71, 83, 98

[181] Jonathan David Touboul, Ann Carla Staver, and Simon Asher Levin. On the complex dynamics of savanna landscapes. *Proceedings of the National Academy of Sciences*, 115(7), 2018. ISSN 0027-8424, 1091-6490. doi: 10.1073/pnas.1712356115. 71, 72, 73, 74

[182] A Carla Staver, Sally Archibald, and Simon Levin. Tree cover in sub-saharan africa: rainfall and fire constrain forest and savanna as alternative stable states. *Ecology*, 92(5):1063–1072, 2011. 72

[183] William J. Bond and Jon E. Keeley. Fire as a global 'herbivore': the ecology and evolution of flammable ecosystems. *Trends in Ecology & Evolution*, 20(7):387–394, 2005. ISSN 0169-5347. doi: https://doi.org/10.1016/j.tree.2005.04.025. URL `https://www.sciencedirect.com/science/article/pii/S0169534705001321`. 73, 79

[184] Pauli Virtanen, Ralf Gommers, Travis E. Oliphant, Matt Haberland, Tyler Reddy, David Cournapeau, Evgeni Burovski, Pearu Peterson, Warren Weckesser, Jonathan Bright, Stéfan J. van der Walt, Matthew Brett, Joshua Wilson, K. Jarrod Millman, Nikolay Mayorov, Andrew R. J. Nelson, Eric Jones, Robert Kern, Eric Larson, C J Carey, İlhan Polat, Yu Feng, Eric W. Moore, Jake VanderPlas, Denis Laxalde, Josef Perktold, Robert Cimrman, Ian Henriksen, E. A. Quintero, Charles R. Harris, Anne M. Archibald, Antônio H. Ribeiro, Fabian Pedregosa, Paul van Mulbregt, and SciPy 1.0 Contributors. SciPy 1.0: Fundamental Algorithms for Scientific Computing in Python. *Nature Methods*, 17:261–272, 2020. doi: 10.1038/s41592-019-0686-2. 75, 76

[185] Frank Van Langevelde, Claudius ADM Van De Vijver, Lalit Kumar, Johan Van De Koppel, Nico De Ridder, Jelte Van Andel, Andrew K Skidmore, John W Hearne, Leo Stroosnijder, William J Bond, et al. Effects of fire and herbivory on the stability of savanna ecosystems. *Ecology*, 84(2):337–350, 2003. 79

[186] Mahesh Sankaran, Niall P Hanan, Robert J Scholes, Jayashree Ratnam, David J Augustine, Brian S Cade, Jacques Gignoux, Steven I Higgins, Xavier Le Roux, Fulco Ludwig, et al. Determinants of woody cover in african savannas. *Nature*, 438(7069):846–849, 2005.

[187] Arie Staal, Stefan C Dekker, Chi Xu, and Egbert H van Nes. Bistability, spatial interaction, and the distribution of tropical forests and savannas. *Ecosystems*, 19:1080–1091, 2016. 79

[188] Zak Ratajczak, Paolo D'odorico, Scott L Collins, Brandon T Bestelmeyer, Forest I Isbell, and Jesse B Nippert. The interactive effects of press/pulse intensity and duration on regime shifts at multiple scales. *Ecological Monographs*, 87(2):198–218, 2017. 79, 83, 84, 85, 91

[189] David J Beerling and Colin P Osborne. The origin of the savanna biome. *Global change biology*, 12(11):2023–2031, 2006. 79

[190] Donald L DeAngelis and Simeon Yurek. Spatially explicit modeling in ecology: a review. *Ecosystems*, 20(2):284–300, 2017. 79

[191] Zak Ratajczak, Stephen R Carpenter, Anthony R Ives, Christopher J Kucharik, Tanjona Ramiadantsoa, M Allison Stegner, John W Williams, Jien Zhang, and Monica G Turner. Abrupt change in ecological systems: Inference and diagnosis. *Trends in Ecology & Evolution*, 2018. 82, 85, 98

[192] Carl Folke, Stephen R Carpenter, Brian Walker, Marten Scheffer, Terry Chapin, and Johan Rockström. Resilience thinking: Integrating resilience, adaptability and transformability. *Ecology and Society*, 15(4), 2010. 82

[193] Stephen R Carpenter, Donald Ludwig, and William A Brock. Management of eutrophication for lakes subject to potentially irreversible change. *Ecological Applications*, 9(3):751–771, 1999. 82, 86, 89

[194] Alex CY Yeung and John S Richardson. Some conceptual and operational considerations when measuring 'resilience': A response to Hodgson et al. *Trends in Ecology & Evolution*, 31(1):2–3, 2016. 82, 83

[195] Brian Walker, Stephen Carpenter, John Anderies, Nick Abel, Graeme Cumming, Marco Janssen, Louis Lebel, Jon Norberg, Garry D Peterson, and Rusty Pritchard. Resilience management in social-ecological systems: A working hypothesis for a participatory approach. *Conservation Ecology*, 6 (1), 2002.

[196] Tom Andersen, Jacob Carstensen, Emilio Hernandez-Garcia, and Carlos M Duarte. Ecological thresholds and regime shifts: Approaches to identification. *Trends in Ecology & Evolution*, 24(1):49–57, 2009. 82

[197] Graeme S Cumming and Stephan von Cramon-Taubadel. Linking economic growth pathways and environmental sustainability by understanding development as alternate social–ecological regimes. *Proceedings of the National Academy of Sciences*, 115(38):9533–9538, 2018. 82, 83

[198] Will Steffen, Katherine Richardson, Johan Rockström, Sarah E Cornell, Ingo Fetzer, Elena M Bennett, Reinette Biggs, Stephen R Carpenter, Wim De Vries, Cynthia A De Wit, et al. Planetary boundaries: Guiding human development on a changing planet. *Science (New York, N.Y.)*, 347(6223): 1259855, 2015. 82, 83, 99

[199] Thomas Elmqvist, Carl Folke, Magnus Nyström, Garry Peterson, Jan Bengtsson, Brian Walker, and Jon Norberg. Response diversity, ecosystem change, and resilience. *Frontiers in Ecology and the Environment*, 1(9):488–494, 2003. 82

[200] Samantha K Oliver, Sarah M Collins, Patricia A Soranno, Tyler Wagner, Emily H Stanley, John R Jones, Craig A Stow, and Noah R Lottig. Unexpected stasis in a changing world: Lake nutrient and chlorophyll trends since 1990. *Global Change Biology*, 23(12):5455–5467, 2017. 83

[201] Crawford S Holling. Resilience and stability of ecological systems. *Annual review of ecology and systematics*, 4(1):1–23, 1973. 83, 84

[202] Bas W Ibelings, Rob Portielje, Eddy HRR Lammens, Ruurd Noordhuis, Marcel S van den Berg, Willemien Joosse, and Marie Louise Meijer. Resilience of alternative stable states during the recovery of shallow lakes from eutrophication: Lake Veluwe as a case study. *Ecosystems (New York, N.Y.)*, 10(1): 4–16, 2007. 83, 98, 99

[203] Marten Scheffer, Stephen R Carpenter, Vasilis Dakos, and Egbert H van Nes. Generic indicators of ecological resilience: Inferring the chance of a critical transition. *Annual Review of Ecology, Evolution, and Systematics*, 46:145–167, 2015. 83

[204] Steve Carpenter, Brian Walker, J Marty Anderies, and Nick Abel. From metaphor to measurement: Resilience of what to what? *Ecosystems (New York, N.Y.)*, 4(8):765–781, 2001. 83

[205] Charles Rougé, Jean-Denis Mathias, and Guillaume Deffuant. Extending the viability theory framework of resilience to uncertain dynamics, and application to lake eutrophication. *Ecological Indicators*, 29:420–433, 2013. 83, 99

[206] Zeinab Hazbavi, Jantiene EM Baartman, João P Nunes, Saskia D Keesstra, and Seyed Hamidreza Sadeghi. Changeability of reliability, resilience and vulnerability indicators with respect to drought patterns. *Ecological Indicators*, 87:196–208, 2018. 83

[207] Zhen Wu, Yong Liu, Zhongyao Liang, Sifeng Wu, and Huaicheng Guo. Internal cycling, not external loading, decides the nutrient limitation in eutrophic lake: A dynamic model with temporal Bayesian hierarchical inference. *Water Research*, 116:231–240, 2017. 83, 84, 100

[208] Zhongyao Liang, Sifeng Wu, Huili Chen, Yanhong Yu, and Yong Liu. A probabilistic method to enhance understanding of nutrient limitation dynamics of phytoplankton. *Ecological Modelling*, 368:404–410, 2018. 83

[209] Robert M Dorazio and Fred A Johnson. Bayesian inference and decision theory—a framework for decision making in natural resource management. *Ecological Applications*, 13(2):556–563, 2003. 84

[210] Michael A McCarthy and Hugh P Possingham. Active adaptive management for conservation. *Conservation Biology*, 21(4):956–963, 2007. 84

[211] Motomi Genkai-Kato and Stephen R Carpenter. Eutrophication due to phosphorus recycling in relation to lake morphometry, temperature, and macrophytes. *Ecology*, 86(1):210–219, 2005. 84

[212] Tom H Oliver, Matthew S Heard, Nick JB Isaac, David B Roy, Deborah Procter, Felix Eigenbrod, Rob Freckleton, Andy Hector, C David L Orme, Owen L Petchey, et al. Biodiversity and resilience of ecosystem functions. *Trends in Ecology & Evolution*, 30(11):673–684, 2015. 84, 98

[213] Annette BG Janssen, Victor CL De Jager, Jan H Janse, Xiangzhen Kong, Sien Liu, Qinghua Ye, and Wolf M Mooij. Spatial identification of critical nutrient loads of large shallow lakes: Implications for Lake Taihu (China). *Water Research*, 119:276–287, 2017. 84, 99

[214] F Stuart Chapin, Stephen R Carpenter, Gary P Kofinas, Carl Folke, Nick Abel, William C Clark, Per Olsson, D Mark Stafford Smith, Brian Walker, Oran R Young, et al. Ecosystem stewardship: Sustainability strategies for a rapidly changing planet. *Trends in Ecology & Evolution*, 25(4):241–249, 2010. 84

[215] Sonia Kéfi, Max Rietkerk, Manojit Roy, Alain Franc, Peter C De Ruiter, and Mercedes Pascual. Robust scaling in ecosystems and the meltdown of patch size distributions before extinction. *Ecology Letters*, 14(1):29–35, 2011. 84

[216] David Tilman, Robert M May, Clarence L Lehman, and Martin A Nowak. Habitat destruction and the extinction debt. *Nature*, 371(6492):65–66, 1994. 84

[217] David G Angeler and Craig R Allen. Quantifying resilience. *Journal of Applied Ecology*, 53(3):617–624, 2016. 84

[218] Stephen R Carpenter and William A Brock. Rising variance: A leading indicator of ecological transition. *Ecology Letters*, 9(3):311–318, 2006. 85, 89, 91, 98

[219] Saskia Keesstra, Joao Nunes, Agata Novara, David Finger, David Avelar, Zahra Kalantari, and Artemi Cerdà. The superior effect of nature based solutions in land management for enhancing ecosystem services. *Science of the Total Environment*, 610:997–1009, 2018. 85

[220] E Cohen-Shacham, G Walters, C Janzen, and S Maginnis. Nature-based solutions to address global societal challenges. *IUCN, Gland, Switzerland*, 97, 2016.

[221] Takehiro Sasaki, Takuya Furukawa, Yuichi Iwasaki, Mayumi Seto, and Akira S Mori. Perspectives for ecosystem management based on ecosystem resilience and ecological thresholds against multiple and stochastic disturbances. *Ecological Indicators*, 57:395–408, 2015. 85

[222] F Hartig, F Minunno, and S Paul. BayesianTools: General-purpose MCMC and SMC samplers and tools for Bayesian statistics, 2017. 88, 89, 92

[223] Song S Qian, Craig A Stow, and Mark E Borsuk. On monte carlo methods for Bayesian inference. *Ecological Modelling*, 159(2-3):269–277, 2003. 89

[224] Andrew Gelman, Jessica Hwang, and Aki Vehtari. Understanding predictive information criteria for Bayesian models. *Statistics and Computing*, 24(6): 997–1016, 2014. 89

[225] Stephen R Carpenter. Eutrophication of aquatic ecosystems: Bistability and soil phosphorus. *Proceedings of the National Academy of Sciences*, 102(29): 10002–10005, 2005. 91

[226] R Core Team. *R: A Language and Environment for Statistical Computing*. R Foundation for Statistical Computing, Vienna, Austria, 2017. 92

[227] Egbert H van Nes, Babak MS Arani, Arie Staal, Bregje van der Bolt, Bernardo M Flores, Sebastian Bathiany, and Marten Scheffer. What do you mean, 'tipping point'? *Trends in Ecology & Evolution*, 31(12):902–904, 2016. 98

[228] Axel G Rossberg, Laura Uusitalo, Torsten Berg, Anastasija Zaiko, Anne Chenuil, María C Uyarra, Angel Borja, and Christopher P Lynam. Quantitative criteria for choosing targets and indicators for sustainable use of ecosystems. *Ecological Indicators*, 72:215–224, 2017. 99

[229] Kaitlyn M Gaynor, Joel S Brown, Arthur D Middleton, Mary E Power, and Justin S Brashares. Landscapes of fear: Spatial patterns of risk perception and response. *Trends in Ecology & Evolution*, 2019. 99

[230] Oliver R Wearn, Daniel C Reuman, and Robert M Ewers. Extinction debt and windows of conservation opportunity in the Brazilian Amazon. *Science (New York, N.Y.)*, 337(6091):228–232, 2012. 99

[231] Maurizio Bagnara, Ramiro Silveyra Gonzalez, Stefan Reifenberg, Jörg Steinkamp, Thomas Hickler, Christian Werner, Carsten F Dormann, and Florian Hartig. An R package facilitating sensitivity analysis, calibration and forward simulations with the LPJ-GUESS dynamic vegetation model. *Environmental Modelling & Software*, 111:55–60, 2019. 100

[232] Kamel Didan. MOD13Q1 MODIS/Terra Vegetation Indices 16-Day L3 Global 250m SIN Grid V006 [Data set], 2015. 101, 109

[233] Ype van der Velde, Arnaud JAM Temme, Jelmer J Nijp, Maarten C Braakhekke, George AK van Voorn, Stefan C Dekker, A Johannes Dolman, Jakob Wallinga, Kevin J Devito, and Nicholas Kettridge. Emerging forest–peatland bistability and resilience of European peatland carbon stores. *Proceedings of the National Academy of Sciences*, 118(38):e2101742118, 2021. ISSN 0027-8424. 107

[234] Noel Gorelick, Matt Hancher, Mike Dixon, Simon Ilyushchenko, David Thau, and Rebecca Moore. Google Earth Engine: Planetary-scale geospatial analysis for everyone. *Remote Sensing of Environment*, 202:18–27, 2017. ISSN 00344257. doi: 10.1016/j.rse.2017.06.031. 109

[235] Amanda M Schwantes and Chase Nuñez. geeDataExtract, 2019. 109

[236] John T. Abatzoglou, Solomon Z. Dobrowski, Sean A. Parks, and Katherine C. Hegewisch. TerraClimate, a high-resolution global dataset of monthly climate and climatic water balance from 1958–2015. *Scientific Data*, 5(1):170191, 2018. ISSN 2052-4463. doi: 10.1038/sdata.2017.191. 109